ENCLOSURE 4

WATTS BAR NUCLEAR PLANT UNIT 1
STEAM GENERATOR ALTERNATE REPAIR CRITERIA
OUTSIDE DIAMETER STRESS CORROSION CRACKING (ODSCC)
EPRI FINAL REPORT 1001441

EPRI

Effect of Pressurization Rate on Degraded Steam Generator Tubing Burst Pressure

Technical Report

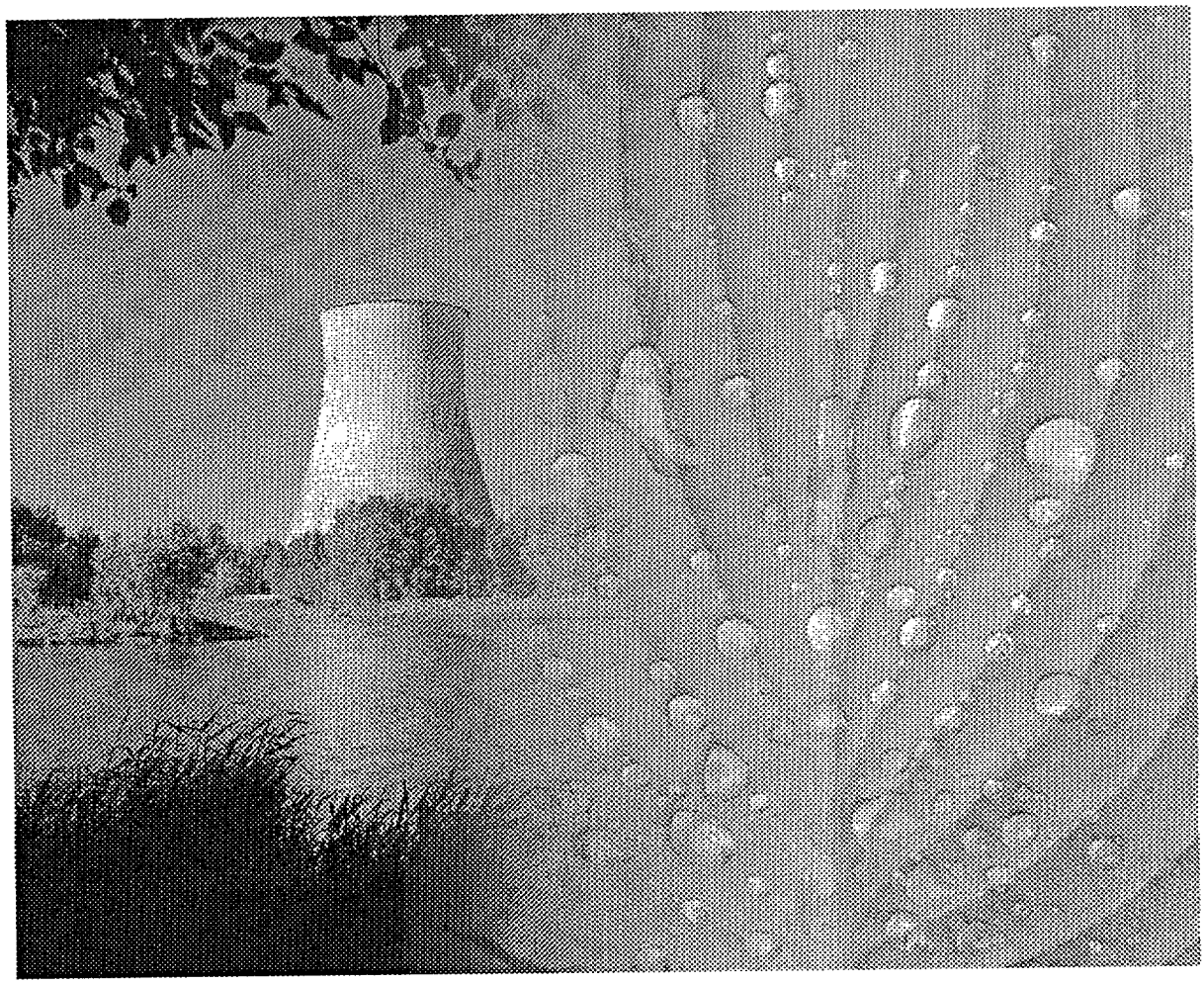

Effect of Pressurization Rate on Degraded Steam Generator Tubing Burst Pressure

1001441

Final Report, April 2001

EPRI Project Manager
M. Merilo

EPRI • 3412 Hillview Avenue, Palo Alto, California 94304 • PO Box 10412, Palo Alto, California 94303 • USA
800.313.3774 • 650.855.2121 • askepri@epri.com • www.epri.com

DISCLAIMER OF WARRANTIES AND LIMITATION OF LIABILITIES

ORGANIZATION(S) THAT PREPARED THIS DOCUMENT

Westinghouse Electric Company
E-Mech Technology, Inc.

ORDERING INFORMATION

Requests for copies of this report should be directed to the EPRI Distribution Center, 1355 Willow Way, Suite 2478, Concord, CA 94520, (800) 313-3774.

CITATIONS

This report was prepared by

Westinghouse Electric Company
Nuclear Services Division
P. O. Box 158
Madison, PA 15663-0158

Principal Investigator
R. F. Keating

E-Mech Technology, Inc.
295 W. Steuben Street
Pittsburgh, PA 15205

Principal Investigator
J. A. Begley

This report describes research sponsored by EPRI.

The report is a corporate document that should be cited in the literature in the following manner:

Effect of Pressurization Rate on Degraded Steam Generator Tubing Burst Pressure, EPRI, Palo Alto, CA: 2001. 1001441.

REPORT SUMMARY

A recent in situ pressure test of a degraded steam generator tube at a nuclear power plant suggested that the measured burst pressure of the specimens could be influenced by the rate at which the pressurization of the specimens takes place. This report reviews industry steam generator tube burst testing procedures and assesses recent data on the effect of pressurization rate on the measured burst pressure of flawed tubing.

Background

Damage to steam generator tubing can impair its ability to adequately perform required safety functions in terms of structural stability and leakage. Therefore, assessment of tube integrity is an important component of a steam generator program that is required by NEI 97-06. To perform an integrity assessment it is necessary to determine the strength of degraded steam generator tubing. Recent test results have suggested that the test pressurization rate may, under certain conditions, have an effect on the measured burst pressure. The current research was undertaken to determine the existence and possible implications of this effect.

Objectives

- To develop an understanding of the recent test data implying a possible pressurization rate effect
- To determine the conditions under which such an effect would be present
- To assess the impact of the pressurization rate effect on the existing burst test database and industry integrity assessment evaluation models.

Approach

The investigators documented, verified, and reassessed the recent burst testing program in which the pressurization rate effect was first observed to ensure that the observations were correct. They then surveyed industry laboratory practices to determine commonly used pressurization rates and test procedures. Subsequently, they performed room temperature tensile tests to determine whether material property effects could explain the observed results. Finally, the investigators examined the industry burst pressure database and evaluation methods to determine whether these needed to be modified for steam generator tube integrity assessment.

Results

The results indicate that rate dependent deformation and burst phenomena do exist; but their significance is limited to planar, part-throughwall cracks that are both long and very deep. These effects are due both to the material properties of the tube and geometries of the flaws.

Examination of the very extensive database of previous burst test results did not suggest that a loading or hold time effect is present. The industry evaluation models were found to be sufficiently conservative to be used for condition monitoring and operational assessment. However, the application of these models to deep coplanar cracks needs to be modified.

EPRI Perspective

As a result of this work interim guidance has been provided to industry regarding in-situ pressure testing, specifically requiring the use of minimum hold times at a number of pressures and limiting the pressurization rate. This revised guidance will be included in the next revision of the Steam Generator In Situ Pressure Test Guidelines (EPRI report TR-107620-R1).

Keywords

Nuclear Steam Generators
Condition Monitoring
Operational Assessment
Integrity Assessment

ABSTRACT

During the performance of an in situ pressure test of a degraded steam generator (SG) tube at a nuclear power plant, the maximum pressure attained during the test was less than three times the normal operating differential pressure for the plant. Although the flaw was leak tight up to a pressure greater than 3000 psi, the 100% throughwall dimension of the flaw at the maximum pressure was too large for the test equipment to continue to supply enough water to increase the pressure further. The pressure test was performed as a whole tube test, as contrasted to use of a localized test employing a sealing bladder. In such cases, the maximum pressure that can be attained during the test is limited by the flow capacity of the testing equipment. Subsequent testing of tube specimens fabricated to simulate the eddy current estimated profile of the flaw demonstrated that the measured burst pressure of the specimens was influenced by the rate at which the pressurization of the specimens took place. This observation led to concern that, although the tested flaw was axial and planar in nature, the test data for other types of degradation might be biased by the rate at which the testing was performed. An evaluation was performed to investigate this possibility and to develop recommendations relative to future laboratory and in situ pressure testing and relative to the analytical models used to evaluate the strength of degraded SG tubes. The conclusions of the evaluation are that it is unlikely that the pressurization rate has an affect on the results of testing of most types of SG tube degradation. However, recommendations are made for some modification of the testing procedures relative to pressurization rates and hold times, and for the analysis of individual crack-like defects when the maximum depth of the crack is greater than 90% of the thickness of the tube wall. No information has been developed to suggest that the pressurization rate has had any meaningful influence on the models developed to deal with ODSCC or PWSCC alternate repair criteria, thinning type degradation, circumferential cracking, pitting, or the statistical nature of individual cracks. Hence, there are no recommendations made to change the manner in which such degradation morphologies are currently analyzed or in which the results of such analyses are used to estimate the influence of the degradation on the future operation of the plant.

CONTENTS

LIST OF FIGURES

LIST OF TABLES

1
INTRODUCTION

During the inspection of the steam generator (SG) tubes at the Arkansas Nuclear One Unit 2 (ANO 2) nuclear power plant in November 1999, the tube located in row 72 and column 72 (R72C72) in steam generator (SG) B was pressure tested in situ to evaluate the burst resistance and leakage potential of an axial indication found by eddy current inspection (ECT) at the elevation of the second egg-crate tube support on the hot leg side of the SG. The maximum pressure attained during the test was 4147 psi when adjusted to account for the pressure drop due to pressurization fluid flow and for instrument error [1, 2]. At that pressure, the 100% throughwall dimension of the flaw in the tube was of such a size that the test equipment could not supply enough water to maintain the pressure. The pressure test was performed as a whole tube test, as contrasted to use of a localized test employing a sealing bladder. In such cases, the maximum pressure that can be attained during the test is limited by the flow capacity of the testing equipment.

One of the objectives of performing a pressurization test is to determine if the burst resistance of the tube with the indication meets a performance criterion value of three times the normal operation primary-to-secondary pressure difference (3ΔP). The criterion value for the ANO 2 SG tubes is greater than the pressure achieved during the test. The results from the pressure test were considered to be inconclusive because the information available from the test is not sufficient to demonstrate that the burst pressure of the tube had been reached even though a pressure of 3ΔP had not been reached. To further evaluate whether or not the R72C72 tube burst pressure was greater than or equal to 3ΔP, a series of surrogate specimens were fabricated and pressure tested. The flaws in the test specimens were made using EDM techniques to simulate the single, eddy current (ECT) estimated crack profile of the R72C72 indication. Separate series of pressure tests were conducted to identify both the leak (ligament tearing) and burst resisting capability of the flawed tube.

Information was presented by ANO 2 personnel to the NRC staff on June 8, 2000, which compared burst pressures obtained following ligament tearing with standard burst pressure test results obtained using a foil reinforced bladder with pressurization rates on the order of 2000 psi/s (in accord with industry guidelines). The results from the ligament tearing and burst pressure testing were as follows:

1. Ligament tearing pressure tests of the EDM specimens demonstrated ligament tearing pressures significantly below the value of 3ΔP for the ANO 2 plant SGs. Ligament tearing tests were performed using very slow pressurization rates (on the order of several psi per minute) in order to achieve tearing of a portion of the crack without opening the whole crack.

2. Burst pressure tests performed on specimens that had been previously pressurized to ligament tearing did not result in demonstrating a burst pressure in excess of the ligament tearing

pressure. The burst pressures following ligament tearing were found to be less than the burst pressures obtained using the industry standard burst pressure test techniques. These tests were performed per EPRI guidelines [3] using a foil reinforced plastic liner to prevent loss of pressure through the simulated flaw opening.

3. Burst pressure tests performed on non-previously tested specimens exhibited burst pressures significantly in excess of the ligament tearing pressures. Burst pressures in excess of three times the normal operating pressure differential, 3ΔP, for the ANO 2 plant SGs were measured for several of the specimens. The burst pressure tests were performed using a pressurization rate of about 2000 psi/s. The specimens were also lined with a flexible bladder which was reinforced in the immediate vicinity of the flaw with a lubricated brass foil patch prior to testing.

4. At the time, subsequent fractography, material testing and flaw depth profiling had not been performed on the EDM specimens to determine if the results are truly indicative of a previously unknown effect of the pressurization rate on the fracture.

The ANO 2, R72C72 indication was about 1.4 inches long (based on the NDE performed before the in situ testing) with two deep sections separated by a shallower ligament, such that when that ligament tore, the resulting throughwall length did not permit a higher burst pressure than the ligament tearing pressure. It was postulated that if these test results were confirmed to indicate a pressurization rate and/or hold-time influence on burst pressures, only long and near-throughwall cracks (likely longer than an acceptable length for a throughwall flaw such as about 0.7 inch) with their attendant irregular crack shapes, would be expected to be affected. It has also been noted that testing performed by the Combustion Engineering Owner's Group (CEOG) of laboratory environmentally generated, long deep flaws did not produce results similar to those from the ANO test program [4]. Some of those flaw samples from the CEOG program, e.g., FS-106, FS-108, FS-111, had profiles with long, deep multiple sections.

During a SGTF telephone conference on June 20, 2000 [6], the NRC staff expressed the opinion that the results indicate that if the pressure were raised slowly, and if hold times were included in the pressurization process, the tubes would have failed at pressures significantly lower than 3ΔP. The NRC staff also opined that the rapid increase in pressure used for the burst tests did not allow time for ligament failures to occur, thus artificially elevating the measured burst pressure of the surrogate specimens. The industry position was that the cause of the apparent anomaly was not fully understood and that a significant number of laboratory and field in situ test results were available that did not exhibit a similar pressure ramp rate dependence. Moreover, in situ pressurization rates are quite slow owing to the small diameter and long length of the hydraulic lines used to pressurize the tubes. During that same SGTF telephone conference, the NRC staff indicated that this issue may have safety concerns as it raises questions about the adequacy of analytical burst models and of the results of similar laboratory tests that were used as a basis for several voltage based alternate repair criteria. If the laboratory tests are flawed, i.e., if a pressure ramp rate dependency has been overlooked, the validity of the data used to support the ARCs could be questioned and so could the operability of the steam generators at plants that have implemented the ARCs. The staff noted that they thought this could affect eight to ten plants.

In summary, the pressurization rate associated with the use of industry standard procedures for burst testing was thought to not significantly affect the test result. However, the results from the

testing program conducted using the R72C72 surrogate specimens indicated that the standard test pressurization rates may lead to higher burst pressure results than would be obtained from tests conducted in a quasi-static manner. This raised the following issues:

1. Is the burst pressure of degraded tubing a function of the pressurization rate, including the consideration that a hold-time is a zero pressurization rate, used to test the tubing?

2. Should changes be made to industry test procedures to account for the potential dependence of the burst pressure on the pressurization rate?

3. Are there industry evaluation models that were empirically derived or qualified using data which might be pressurization rate dependent, e.g., data used for the ODSCC ARC?

4. Do the industry evaluation models need to be modified to account for the potential dependence of the burst pressure on the pressurization rate, i.e., to account for the potential for ligaments to tear prior to burst, thus reducing the burst pressure?

It is industry's current position that there is enough other information regarding testing ramp rates to demonstrate that a significant concern relative to the suitability of the data developed to support industry developed burst correlations and/or models should not exist. In early July of 2000, industry representatives proceeded with a systematic approach aimed at developing an understanding of the ANO test program results and their implications relative to the results from other test programs.

The results of that investigation support the initial supposition that a material strength issue, i.e., strain-rate, was not responsible for the observations, and that the industry database remains valid. The following sections provide information on the ANO burst testing program, burst testing procedures, material property considerations, tube integrity evaluation methods and models, and in situ testing results. A detailed analysis and discussion is included as Section 7 of this report. The discussion provides and explanation for the observed rate effects, explains why the strain-rate was not the cause of the test result differences, and explains why the morphology of degradation likely to be affected by the pressurization rate is limited. However, recommendations have been developed for changes to be made to in situ and laboratory testing procedures, and for limitations regarding the application of calculation models. These recommendations are summarized in Section 8 of this report.

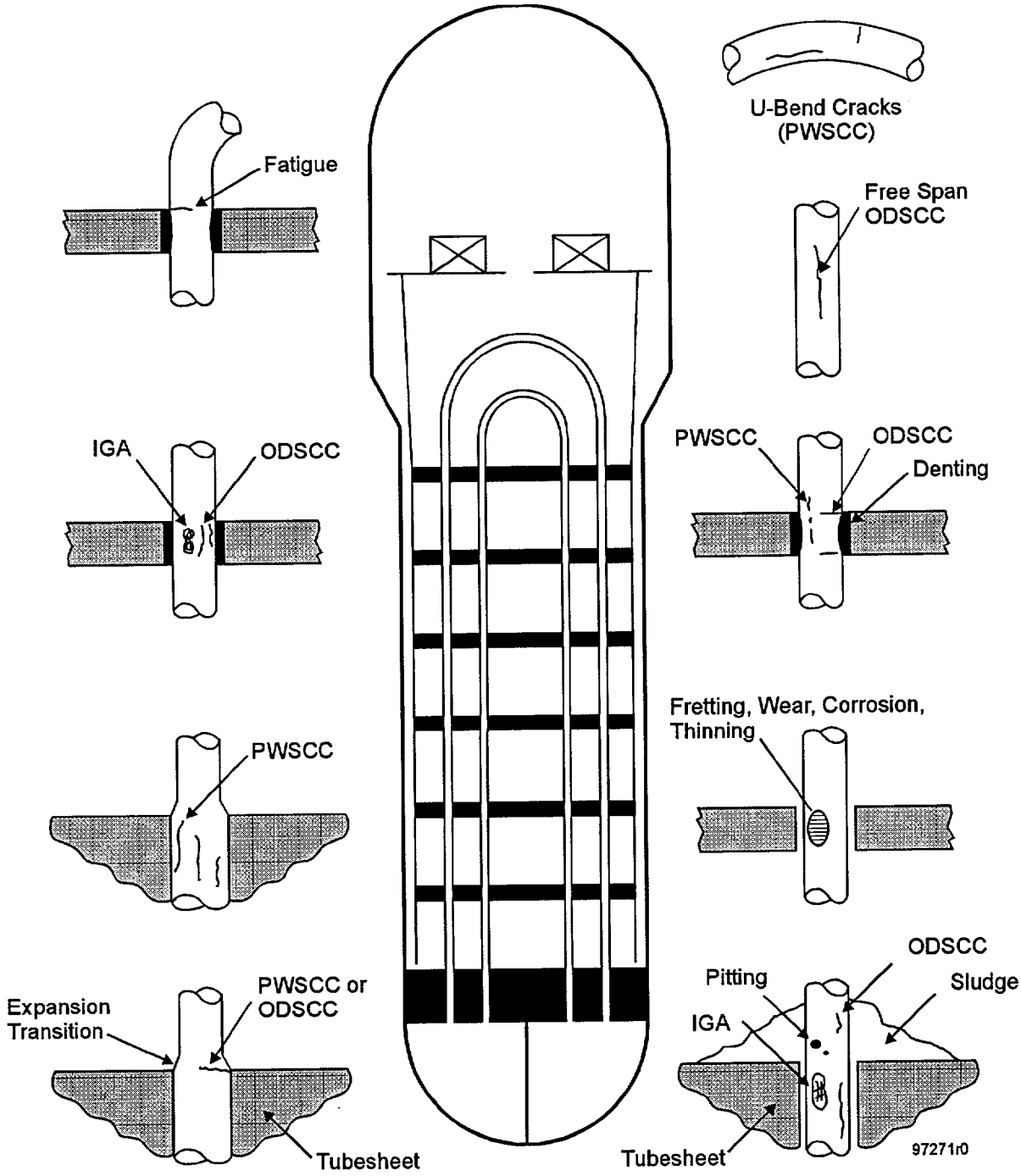

Figure 1-1
Typical locations of SG degradation

2
REVIEW OF THE ANO BURST TESTING PROGRAM

2.1 Test Procedures and Conduct

The ANO test program was performed in accordance with a test procedure prepared specifically for testing of the ANO 2 surrogate specimens [7]. The test matrix consisted of a total of ninety-six (96) tube specimens which were electrical discharge machined (EDM) with various flaw profile configurations as described in the following paragraphs. The intent of the program was to investigate and verify the strength of a degraded portion of the tube at R72C72 in SG B. It is noted that not all of the specimens fabricated were used since the results of the completed tests influenced how the remaining specimen configurations were utilized in the testing program.

All of the test specimens were prepared by cutting certified Alloy 600 tubing into approximately eight-inch long sections. The specimens were cut to length, de-burred, cleaned and identified by serial number per the test matrix. The dimensions of all of the specimens and the test results were recorded on test data sheets. Tube specimens were non-destructively examined using both bobbin and rotating pancake coil (RPC) inspection probes prior to machining to document any initially existing flaws.

Test material used during this program was obtained from known material heats where the material and chemical properties of the tubing were documented. Material released for this test program was supplied by Westinghouse (Windsor) through Entergy and documented in certified material test reports. The material heat numbers involved in this testing were identified either as 752677 (manufactured by Sandvik) or NX 8520-K. All of the specimens for which the results are of particular interest to this study were from the latter heat.

The initial scoping test matrix was divided into three specific EDM notch types where the specimens were prepared to simulate a specific crack application. The intent of this scoping test matrix was to permit the test program to establish a set of initial flaw parameters which would best simulate the ANO 2 R72C72 tube and allow the program to develop similar test specimens which would characterize the ANO tube indication. Dimensional, EDM flaw profiles, burst strength and eddy current test (ECT) results were collected and recorded for each specimen.

Additional EDM notch types were added to the test matrix to better simulate the characteristics of the R72C72 tube indications as seen from the leak rates and burst pressures during the tube failure. The ECT profile of the R72C72 crack is illustrated on Figure 2-1 and the final simulant profile design, designated as Type 14, is illustrated on Figure 2-2. The EDM notches were positioned at approximately mid-span of the specimen. The slits had an axial length of 1.42 inches and widths of 0.004 to 0.006 inches. The slit depths ranged from about 60% to 95% of the total wall thickness. The test matrix allowed for replicate specimens of depth combinations of

each size to provide an averaging basis for the potential tube property variations. The design of the EDM slot depth versus length profiles of all of the types of test specimens in the test program are presented in Appendix A.

Tube dimensional data for each EDM specimen profile type were measured and documented by the machine shop quality control inspector. The data were subsequently factored into the burst calculations. After the EDM machining process was performed, each specimen was RPC (pancake and plus point) inspected to determine the effect of the EDM notch indication on the voltage signal for that specific tube. The data were collected and stored on an optical disk provided from previously performed steps after the EDM notch machining operation. The data were then entered into a portable computer spreadsheet program matrix for future evaluation

Several types of pressurization procedures were followed for the Type 14 specimens. Burst tests were performed by following the EPRI burst testing guidelines and by using conventional laboratory burst testing equipment. A plastic sealing bladder was typically used with a 0.006 inch thick brass foil reinforcement, although some tests were performed without the use of the reinforcing foil. In addition, some of the tests were performed without a sealing bladder. Most of the tests were performed at a pressurization rate near 2000 psi/s. Five specimens were tested using the laboratory test system with the pressurization rate restricted to about 70 psi/s in an attempt to determine the onset of throughwall crack tearing. i.e., tearing of the remaining radial ligament of material, and leakage. These latter tests were terminated as soon as leakage was detected. A plastic bladder with a foil reinforcement was then inserted and a retest at the 2000 psi/s pressurization rate was performed. The results from the leakage onset, i.e., ligament tearing tests and the burst tests are listed in Table 2-1. Maximum test pressures and times to maximum pressure are listed.

Pressurization tests at very slow rates were also performed using an in situ test system. The objective of this series of tests was to determine the onset of throughwall crack tearing and leakage. Test times ranged from 1.5 minutes to 5 hours. Most tests were in the range of 10 to 30 minutes in duration. Pressure and leak rate versus time plots for tests with the in situ system are presented in Appendix B from the computerized data acquisition system. Typically after slow pressurization testing to some degree of leakage, the test specimen was removed from the in situ apparatus, a bladder and foil reinforcement was inserted and a retest was conducted at a fast pressurization rate. This retest was performed at a rate on the order of 2000 psi/s in the conventional laboratory burst test set up.

2.2 Test Data

Test results are presented in Table 2-1. After the specimen number, the profile type is listed. Appendix A illustrates all the profiles specified in the design drawings. As discussed below, actual depths seem to be somewhat larger than those specified. The total length of the EDM slot is entered next, followed by the maximum specified depth along the profile. For specimens subjected to leak tests, the pressure at the onset of leakage is provided with the next column giving the maximum pressure reached in the leak test. The total duration of the leak test is listed followed by 3 post leak test parameters, the maximum torn throughwall length observed in the leak test, the maximum pressure observed at a leak rate of 2.5 gpm and the maximum leak rate observed. The 3 columns before the final comment column provide burst test results. The

thickness of the reinforcing foil is listed, then the burst test pressure and the time to reach maximum pressure in the burst test. Note that some specimens were burst tested without any prior leak rate test. The comment column describes the condition of the ends of the EDM slot after burst testing. Tearing of the full thickness material at the ends of the EDM slot confirms that the full pressure bearing capacity has been exceeded and the final condition can be termed a tube burst.

2.3 Post-test Specimen Examination Results

After testing, all test specimens were photographed to record the extent of the burst or leak openings. The specimens of greatest interest are the Type 14 specimens. The most definitive series of both slow and relatively fast pressurization tests were performed on Type 14 specimens. As discussed below, measured burst pressures for these specimens seemed dependent on the pressurization rate. The EDM profiles of these specimens were measured in a scanning electron microscope after testing. Post test general specimen appearance and destructive examination results for Type 14 specimen EDM profiles are discussed in the following paragraphs.

2.3.1 Specimen Appearance

The range of post-test specimen appearance is illustrated by Figures 2-3 through 2-6. Figure 2.3 shows a small amount of throughwall tearing which occurred during a slow pressurization rate leak test. Figure 2-4 shows a relatively large opening generated in the same type of test. Crack tearing into the full thickness material at the end of an EDM slot during a burst test is shown in Figure 2-5. This is unequivocal evidence that the pressure bearing capacity of the degraded tube has been exceeded and a true tube burst has developed. Figure 2-6 shows a large opening created in another burst test with the same nominal EDM profile. No tearing beyond the EDM profile is evident for this specimen. However, the pressure attained in this was higher than the burst pressure of a nominally identical specimen. Thus, large crack mouth openings, without tearing beyond the EDM profile, are still indicative of essentially reaching a pressure plateau very close to the onset of tearing.

2.3.2 As-Built Dimensions & Fractography Results

Post-test destructive examination using a scanning electron microscope (SEM) allowed measurements of the EDM depth versus length profiles. Appendix C illustrates all of the measured Type 14 specimen EDM profiles. Generally, the measured profiles were deeper than the target machine drawing profiles by about 5 to 10% TW. Figure 2-7 shows a typical measured profile. The dotted line is the target or specified profile. Figure 2-8 shows that some profiles were excellent matches to the machining drawing. Figure 2-9 illustrates the worst discrepancy between the specified and actual measured EDM profiles. The measured EDM profiles were used in all calculations of the ligament tearing and burst pressures.

2.4 Calculation Models

There are different calculation models used for predicting the burst pressure of degraded SG tubes depending on the severity of the degradation. Of interest in the evaluation of the data from the ANO 2 test program are models for predicting the ligament tearing and burst pressures of part-throughwall cracks, and the burst pressure of throughwall cracks. The calculation models treat the crack as having an idealized rectangular profile characterized only by the length, L, and depth, d, or relative depth, h, i.e., the depth-to-thickness ratio. The ligament may tear for a very deep and short crack, but the resulting throughwall crack may resist burst at a pressure higher than that required to tear the ligament. Hence, ligament tearing does not always lead to burst. However, the ligament tearing model may be assumed to predict a lower bound for the burst pressure and may be used as the primary prediction model. The model specified in the EPRI Flaw Handbook [15] for estimating the ligament tearing pressure of part-throughwall cracks was originally presented by Cochet in Reference 16. The ligament tearing pressure, P_t, is given as a function of the non-degraded tube burst pressure, P_0, as,

$$P_t = P_0\left[1 - \frac{L}{L + 2t}h\right], \qquad \textbf{Equation 2-1}$$

where L is the length of the crack, t is the thickness of the tube, and h is the relative depth of the crack. Based on pulled tube burst tests, the average or nominal estimate of the burst pressure of steam generator tubes with service induced axial stress corrosion cracking is obtained by replacing the "1" in the above equation by "1.104". The value of "1" is appropriate for specimens with machined (EDM or laser) slots or as an approximate lower bound for service induced axial cracking. Cochet [16] originally referred to the predictions from the above equation as being ligament tearing and burst predictions without delineating a difference. The non-degraded tube burst pressure may be calculated as,

$$P_0 = 0.598\left(S_y + S_u\right)\frac{t}{R_m}, \qquad \textbf{Equation 2-2}$$

where S_y and S_u are the yield and ultimate strengths of the material respectively, and R_m is the mean radius of the tube [12]. Alternatively, P_0 may be equivalently (nearly) expressed in terms of the elastic hoop stress in the tube by replacing the constant with 0.58 and the denominator in the fraction with the inside radius of the tube, R_i. This second form corresponds exactly to the model specified in the EPRI Flaw Handbook. When the model was originally developed, for ligament tearing, it was intended to be used for indications ranging from 20 to 85% deep [16]. Two other models were also presented to cover the range for 0 to 20% deep and from 85% to 100% deep. However, it was also noted during the original development that the coefficient in the equation could be slightly different for different tube sizes. Experience has demonstrated that Equation 2-1 is a good practical model for predicting burst pressures regardless of the depth of the degradation.

The model for the burst pressure of throughwall cracks is [12],

$$P_B = \left(0.061319 + 0.53648e^{-0.2778\frac{L}{\sqrt{R_m t}}} \right) \left(S_y + S_u\right)\frac{t}{R_m}. \qquad \textbf{Equation 2-3}$$

An outcome of the development, presentation and subsequent discussion of the ANO burst test data has been a heightened sensitivity to the need to distinguish between ligament tearing and burst when the structural integrity of degraded tubes is being modeled and evaluated. It is intended that the discussions in this report identify which model is being considered in order to avoid confusion. For example, if equation 2-1 is used as-is, it is the ligament tearing pressure that is being calculated, but the context of the use of the result may be as a lower bound to the estimate of the burst pressure.

2.5 Discussion

A review of the post test specimen appearance from all burst tests and maximum pressure values of nominally identical specimens shows that either the pressures reached in burst tests, or sometimes higher pressures attained in preceding leak tests are truly indicative of the burst pressure of the tested geometry. Hence, in Table 2-1, the higher of the pressures in the "All Ligament Torn" or "Burst Test" columns is a very good indicator of the burst pressure even if the "Comments" column denotes no tearing occurred.

Comparing the maximum pressures in the leak rate tests with those in subsequent burst tests shows that there were very few instances where a higher pressure was attained in the burst test compared to the maximum pressure in the leak test. This is because the leak tests led to throughwall tearing with relatively long throughwall cracks. Figure 2-10 shows a plot of the maximum pressure in leak tests versus the length of throughwall cracks generated by the leak tests. The solid line is the best estimate burst pressure for a throughwall crack using Equation 2-1 (the industry standard model for predicting the burst pressure of tubes with axial, part-throughwall cracks). Points plotted above the line obviously are not expected to exhibit a higher burst pressure in a subsequent burst test. In fact, the points above the line are expected to fall back to the throughwall structural limit curve in a subsequent burst test. Thus, it is expected for some burst tests to exhibit lower burst pressures than the maximum pressure reached in a previous leak test. This occurs when pressurization during the leak test results in throughwall crack tearing of significant length.

On Figure 2-10 the two points farthest from the throughwall burst curve (with a length of 0.5") did show an increase in maximum pressure in a burst test subsequent to the leak rate test. However, the burst tests did not reach a pressure of about 5000 psi indicated for 0.50 inch long throughwall cracks. This is because the ends of throughwall tearing did not reside in full thickness material, as assumed for application of the throughwall burst equation. The retest burst pressure was about 3300 psi. The tips of the torn 0.50 inch long throughwall cracks ended at a position along the EDM profile where the slot depth was about 80%TW or greater. Thus a reduction in burst pressure, compared to that of the same length of throughwall crack in full thickness material, is expected. This is a key point. The stability of throughwall tearing, as a function of pressure, in a long crack profile is an underdeveloped area in steam generator tubing

structural integrity evaluations. This concept is discussed further in Sections 5 and 7 and in the recommendations of Section 8.

From the above discussion, it is clear that points close to, but below the structural limit burst curve in Figure 2-10 are not expected to develop higher pressures in a subsequent burst test. The tips of the throughwall cracks develop in the leak test do not reside in material thick enough to realize the full thickness throughwall burst strength curve. One additional retest consideration is that it is more difficult to effectively seal a throughwall crack if a significant opening is present at the start of the burst test. Premature seal release is another factor in retest burst pressures being less than the maximum pressure reached in previous leak tests. Retest burst pressures being less than the maximum pressure reached in previous leak tests is not an unexpected or unexplained phenomenon. It is equally clear that there is a broad range of EDM slot or crack profiles where retest burst pressures will be much higher than any maximum pressure reached in a leak test. Consider a very deep bathtub shaped crack with total length of about 0.4 inches and a uniform depth of about 99% TW. A small pressure in a leak test will generate a 0.4 inch long throughwall crack and a substantial leak rate. However burst will not occur until a pressure in excess of typical $3\Delta P$ levels is reached because the ends of the crack terminate in full thickness material.

Most replicate tests were performed on Type 14 EDM profile specimens since these were the best match to ANO tube R72C72. Ten slow rate pressurization leak tests were performed. Three of these leak tests were followed by retest burst tests. In these three instances the retest burst pressures were not higher than the maximum pressure reached in the leak tests. Based on the post leak test specimen appearance it is judged that the length of throughwall cracks generated in the seven leak tests not followed up with subsequent burst tests are sufficient to infer that the maximum pressure reached in these leak tests is a good indicator of the actual pressure bearing capacity of this degraded tube geometry. Hence, to a good approximation, there are ten slow rate burst pressures for Type 14 specimens. There are ten additional burst pressures on Type 14 specimens from conventional burst tests (this includes a test performed at a separate facility). A summary of the pertinent test results from the Type 14 specimens is provided in Table 2-2. Here, no prior leak tests were performed. Pressurization to burst occurred in about 2 seconds. In the ten leak tests, the test duration ranged from minutes to hours.

Figure 2-11 shows the cumulative distributions of the slow rate and fast rate burst pressures for Type 14 specimens (the data from Table 2-2). The mean of the slow rate tests is 3998 psi with a standard deviation of 425 psi while the mean of the fast rate tests is 5190 psi with a standard deviation of 394 psi. The statistics obtained from comparing the results from the different pressurization rate tests is provided at the bottom of Table 2-2. A one-tailed F-test was used to compare the variances of the maximum pressures from the separate data sets. The results indicate that the probability that the variances of the parent populations from which the data were obtained are equal is 83%. This result is not necessarily significant in itself regarding physical comparisons between the processes, but is used to determine the type of test used to compare the means of the two data sets. A subsequent two-tailed t-test, assuming equal variances, indicates that the probability that the means of the parent populations of the data sets are equal is about $4 \cdot 10^{-6}$. If the variances are assumed to be different, the resulting probability is not changed significantly for these data. One of the test results from the fast rate testing, that for specimen 070, was reported as corresponding to no tearing at the ends of the EDM slot. The inclusion of the result from this specimen in the fast rate burst pressure data set is conservative in that it increases the probability obtained from the t-test of the difference of the means of the data sets.

In conclusion, there is a clear statistical difference between maximum pressures obtained from the slow rate and fast rate results.

The difference in the maximum pressures obtained from the two testing rates could be due to a variety of factors. Four potential contributors identified and considered were as follows:

1. Systematic differences in actual depth profiles — Measurements of EDM profiles in the scanning electron microscope rule out the first factor. The difference in actual profiles from the specified drawing appear to be random. This contributes to the scatter in burst test results, but does not account for a systematic difference between slow and fast test results.

2. The assumption that the maximum pressure in the leak rate test is a good indicator of the burst pressure — Burst retests of three leak rate specimens together with the throughwall crack lengths in the other seven leak rate specimens support the judgment than leak test (slow rate) maximum pressures are good indicators of burst pressure.

3. Strengthening effects of using metal foil to reinforce the bladder used in fast rate tests but not the slow rate tests — Tests of Type 1 and Type 2 specimens with and without foil reinforcement show that any foil strengthening effects are small. However, Type 1 and Type 2 geometries have maximum depths of about 83%. There may be foil strengthening effects for the 95% TW EDM slots in the Type 14 specimens. A 0.006 inch thick foil with a 0.008 inch thick remaining ligament in the Type 1 and Type 2 specimens may not be significant. A 0.0024 inch thick ligament in the Type 14 specimens may experience some degree of strengthening from use of the 0.006 inch thick reinforcing foil. Sealing of throughwall cracks with a 0.006 reinforcing foil can lead to about a 5% strengthening effect relative to tests without the foil (although the French experience with lubricated foils indicates that there is not a significant effect [16]). It is difficult to argue for a larger foil strengthening effect with a 95% TW ligament than for no ligament at all. However, useful data could be obtained from running fast rate burst tests of Type 14 specimens without any sealing bladder or foil. This testing should be conducted as a high priority item as recommended in Section 8.

4. Pressurization rate effect on burst pressure for this degradation geometry — The data from the Type 14 specimen tests exhibit higher burst pressures under rates of pressurization in the range of 2000 psi/s than for the slow pressurization rate tests. The magnitude of this increase is about 25% compared to slow rate tests. This rate effect hasn't been observed in years of previous testing.

The following sections of this report deal with the evaluation of the causes and relevance of the conclusion that a pressurization rate effect has been observed. Discussions have also involved consideration of hold-time effects. There is no difference from a practical standpoint because a hold-time is simply a zero pressurization rate. There is no pressurization rate strain-hardening effect on the ligament material which would materially increase the subsequent burst pressure. Thus, the entire consider of pressurization rate is as an integrated effect. The pressurization rate could be infinite between hold-times. If burst does not immediately occur following a pressure increase, regardless of the ramp rate, then the ramp rate had no effect on the measured burst pressure. However, if burst ensues during the subsequent hold period, then the ramp rate could have had an effect, but it would be of unknown magnitude. It is for this reason that recommendations were developed, and delineated in Section 8, for pressure testing. It is worth

noting that calculations of burst pressures using a standard industry approach, e.g., the methods presented in the EPRI Flaw Handbook [15], and known EDM profiles and tensile properties do agree with the slow rate pressurization test results. That is, none of the test data discussed in this report, including that from the Type 14 specimens, is in disagreement with standard industry calculation approaches of Reference 15. A conservative element of the current approach is the use of a model which was developed to predict ligament tearing pressure for the prediction burst pressures. This point is discussed in detail in Sections 5 and 7.

Table 2-1
ANO Burst Testing—Burst Test Data

	EDM Notches		Structural Characteristics									
						Post Leak Test						
Specimen No.	Type	Length	Depth	Leakage Onset	All Ligament Torn	Test Duration	TW Length	Max ΔP at 2.5 GPM	Leak Rate (GPM)	Foil Used	Burst Test	Test Duration	Comments
ANO-00-001	1	0.75	83.0%	3.920 ksi		1.90 sec				0.004	2.750 ksi	1.35 sec	No Tearing [1]
ANO-00-002	1	0.75	83.0%	4.240 ksi		1.95 sec					4.240 ksi	1.95 sec	No Tearing [1]
ANO-00-003	1	0.75	83.0%							0.004	3.600 ksi	1.85 sec	No Tearing [1]
ANO-00-004	1	0.75	83.0%							0.004	4.000 ksi	2.03 sec	No Tearing [1]
ANO-00-005	1	0.75	83.0%							0.006	4.060 ksi	2.20 sec	No Tearing [1]
ANO-00-021	1	0.75	83.0%							0.006	4.050 ksi	2.07 sec	No Tearing [1]
ANO-00-022	1	0.75	83.0%							0.006	3.900 ksi	1.97 sec	No Tearing [1]
ANO-00-023	1	0.75	83.0%	Not Used									
ANO-00-006	2	1.42	Variable	3.100 ksi		1.47 sec					3.100 ksi	1.47 sec	No Tearing [2]
ANO-00-007	2	1.42	Variable	4.200 ksi		2.10 sec				0.010	3.400 ksi	1.78 sec	No Tearing [2]
ANO-00-008	2	1.42	Variable	N/A					N/A	0.006	3.360 ksi	1.65 sec	Burst [2]
ANO-00-009	2	1.42	Variable	N/A					N/A	0.006	4.100 ksi	1.95 sec	Burst [2]
ANO-00-010	2	1.42	Variable	Not Used									
ANO-00-011	2	1.42	Variable	Not Used									
ANO-00-012	2	1.42	Variable	Not Used									
ANO-00-013	2	1.42	Variable	Not Used									
ANO-00-014	2	1.42	Variable	Not Used									
ANO-00-015	2	1.42	Variable	Not Used									
ANO-00-024	2	1.42	Variable	Not Used									
ANO-00-025	2	1.42	Variable	Not Used									
ANO-00-026	2	1.42	Variable	Not Used									

Table 2-1 (Cont.)
ANO Burst Testing—Burst Test Data

		EDM Notches		Structural Characteristics									
							Post Leak test						
Specimen No.	Type	Length	Depth	Leakage Onset	All Ligament Torn	Test Duration	TW Length	Max ΔP at 2.5 GPM	Leak Rate (GPM)	Foil Used	Burst Test	Test Duration	Comments
ANO-00-016	3.X[3.]	1.42	Variable	N/A					N/A	0.006	5.140 ksi	2.60 sec	No Tearing
ANO-00-017	3.X[3.]	1.42	Variable	N/A					N/A	0.006	5.060 ksi	2.55 sec	
ANO-00-018	3.X[3.]	1.42	Variable	4.500 ksi		61.0 sec				0.006	5.400 ksi	2.55 sec	No Tearing
ANO-00-019	3.X[3.]	1.42	Variable	5.380 ksi		57.0 sec				0.006	5.600 ksi	2.81 sec	No Tearing
ANO-00-020	3.X[3.]	1.42	Variable	4.540 ksi		72.0 sec			1.40	0.006	5.300 ksi	2.73 sec	No Tearing
ANO-00-027	3.X[3.]	1.42	Variable	4.220 ksi		59.0 sec			0.93	0.006	5.300 ksi	2.73 sec	No Tearing
ANO-00-028	3.X[3.]	1.42	Variable	4.060 ksi		58.0 sec			0.13	0.006	5.200 ksi	2.65 sec	No Tearing
ANO-00-029	3.X[3.]	1.42	Variable	3.800 ksi					0.37				No tearing at 8 GPM/4.000 ksi
ANO-00-030	3	1.42	Variable	2.900 ksi		1.45 sec				Bladder	2.660 ksi	0.97 sec	No Tearing
ANO-00-031	3	1.42	Variable	2.700 ksi		1.15 sec				Bladder	2.700 ksi	1.15 sec	No Tearing
ANO-00-032	3	1.42	Variable	3.226 ksi	3.226 ksi	6.05 min	0.900	1.300 ksi	0.0001	0.006	3.200 ksi	1.50 sec	No Tearing
ANO-00-033	3	1.42	Variable	3.319 ksi	3.319 ksi	3.55 min	0.700	2.400 ksi	0.00545	0.006	3.350 ksi	1.67 sec	No Tearing
ANO-00-034	3	1.42	Variable	2.294 ksi	2.294 ksi	4.08 min	0.500		0.00033	0.006	3.300 ksi	1.65 sec	No Tearing
ANO-00-035	3	1.42	Variable	2.250 ksi	2.323 ksi	3.10 min	0.500		0.00018	0.006	3.300 ksi	1.65 sec	Burst Tearing (1/16")
ANO-00-036	3	1.42	Variable	Not Used									Archive Specimen
ANO-00-037	Virgin	0.00	0.0%	N/A					N/A		12.500 ksi	8.70 sec	Virgin Specimen
ANO-00-038	Virgin	0.00	0.0%	N/A					N/A		12.500 ksi	8.70 sec	Virgin Specimen
ANO-00-039	3	1.42	Variable	2.974 ksi	2.974 ksi	7.45 min	0.750	0.325 ksi	2.36	0.006	2.810 ksi	1.30 sec	Burst Tearing
ANO-00-040	3	1.42	Variable	2.778 ksi	2.778 ksi	10.20 min	0.760	0.475 ksi	2.39	0.006	2.720 ksi	1.35 sec	Burst Tearing
ANO-00-041	3	1.42	Variable	Not Used									
ANO-00-042	3	1.42	Variable	Not Used									
ANO-00-043	3	1.42	Variable	Not Used									

Table 2-1 (Cont.)
ANO Burst Testing—Burst Test Data

	EDM Notches		Structural Characteristics									
						Post Leak test						
Specimen No.	Type	Length	Depth	Leakage Onset	All Ligament Torn	Test Duration	TW Length	Max ΔP at 2.5 GPM	Leak Rate (GPM)	Foil Used	Burst Test	Test Duration	Comments
ANO-00-044	3	1.42	Variable	Not Used									
ANO-00-045	3	1.42	Variable	Not Used									
ANO-00-046	3	1.42	Variable	Not Used									
ANO-00-047	3	1.42	Variable	Not Used									
ANO-00-048	3	1.42	Variable	Not Used									
ANO-00-050	4	1.42	Variable	5.024 ksi	5.024 ksi	16.49 min	1.000	0.035 ksi	2.37	0.006	2.720 ksi	1.40 sec	No Tearing
ANO-00-054	4	1.42	Variable	4.351 ksi	4.351 ksi	15.30 min	1.010	0.400 ksi	2.40	0.006	2.710 ksi	1.37 sec	No Tearing
ANO-00-055	4	1.42	Variable	5.073 ksi	5.073 ksi	13.33 min	0.900	0.400 ksi	2.30	0.006	2.790 ksi	1.35 sec	No Tearing
ANO-00-057	4	1.42	Variable	4.746 ksi	4.746 ksi	8.40 min	0.940	0.400 ksi	2.40	0.006	2.530 ksi	1.30 sec	
ANO-00-058	4	1.42	Variable	Not Used									
ANO-00-049	7	1.42	Variable	3.809 ksi	3.809 ksi	8.10 min	1.140	0.040 ksi	2.30	0.006	2.480 ksi	1.65 sec	Tearing occurred (.10 to .15")
ANO-00-056	7	1.42	Variable	3.394 ksi	3.394 ksi	9.07 min	1.040	0.070 ksi	2.40	0.006	2.480 ksi	1.38 sec	No Tearing
ANO-00-059	7	1.42	Variable	3.911 ksi	3.911 ksi	14.55 min	1.040	0.040 ksi	2.30	0.006	2.590 ksi	1.30 sec	No Tearing
ANO-00-051	6	1.42	Variable	4.507 ksi	4.507 ksi	10.56 min	1.100	0.040 ksi	2.40	0.006	2.620 ksi	1.38 sec	Burst Tearing (.08 to .14")
ANO-00-052	6	1.42	Variable	4.409 ksi	4.409 ksi	11.15 min	1.120	0.030 ksi	2.30	0.006	2.390 ksi	1.30 sec	Burst Tearing (.04 to .06")
ANO-00-053	6	1.42	Variable	Not Used									
ANO-00-060	8	1.42	Variable	2.950 ksi	3.452 ksi	56.50 min	0.860		0.003	0.006	2.780 ksi	1.30 sec	Burst Tearing (.04 to .06")
ANO-00-061	8	1.42	Variable	2.500 ksi	3.213 ksi	24.40 min			0.00033	0.006	4.100 ksi	2.00 sec	Burst Tearing (.04 to .06")
ANO-00-062	8	1.42	Variable	N/A					N/A	0.006	4.460 ksi	2.25 sec	Burst Tearing (.04 to .06")

Table 2-1 (Cont.)
ANO Burst Testing—Burst Test Data

	EDM Notches			Structural Characteristics									
							Post Leak test						
Specimen No.	Type	Length	Depth	Leakage Onset	All Ligament Torn	Test Duration	TW Length	Max ΔP at 2.5 GPM	Leak Rate (GPM)	Foil Used	Burst Test	Test Duration	Comments
ANO-00-063	9	1.42	Variable	3.462 ksi	3.462 ksi	27.50 min	0.860		0.0009	0.006	3.300 ksi	1.63 sec	No Tearing
ANO-00-064	9	1.42	Variable	2.300 ksi	2.847 ksi	26.15 min			0.0001	0.006	3.900 ksi	2.03 sec	No Tearing
ANO-00-065	9	1.42	Variable	N/A					N/A	0.006	4.530 ksi	2.25 sec	No Tearing
ANO-00-066	14	1.42	Variable										Sent to FTG for Testing
ANO-00-067	14	1.42	Variable										Sent to FTG for Testing
ANO-00-068	14	1.42	Variable	3.300 ksi	3.433 ksi	31.00 min	0.626	0.650 ksi	0.014	0.006	3.230 ksi		Burst Tearing (.105 to .145")
ANO-00-069	14	1.42	Variable	3.650 ksi	3.755 ksi	25.13 min	0.650	0.075 ksi	0.013	0.006	2.920 ksi	1.37 sec	Burst Tearing (.05 to .150")
ANO-00-070	14	1.42	Variable	N/A					N/A	0.006	4.320 ksi	2.07 sec	No Tearing
ANO-00-074	14	1.42	Variable	4.250 ksi	4.395 ksi	52.15 min			0.20				Leak Only
ANO-00-075	14	1.42	Variable	NA						0.006	5.700 ksi	2.75 sec	Burst Tearing
ANO-00-076	14	1.42	Variable	4.526 ksi	4.526 ksi	29.00 min			0.61				Leak Only
ANO-00-077	14	1.42	Variable	NA						0.006	5.600 ksi	2.67 sec	Burst Tearing
ANO-00-071	12	1.42	Variable	4.653 ksi	4.653 ksi	22.10 min			0.77	0.006	3.980 ksi	1.97 sec	Burst Tearing (.043 to .08")
ANO-00-072	12	1.42	Variable	3.750 ksi	3.882 ksi	30.30 min		0.050 ksi	0.009	0.006	2.910 ksi	1.45 sec	Burst Tearing (.170 to .175")
ANO-00-073	12	1.42	Variable	N/A					N/A	0.006	4.800 ksi	2.30 sec	Burst Tearing (.185 to .232")
ANO-00-078	16	1.42	Variable	3.950 ksi	4.004 ksi	32.40 min			1.90				Leak Only
ANO-00-079	16	1.42	Variable	Not Used									
ANO-00-080	16	1.42	Variable										
ANO-00-081	16	1.42	Variable							0.006	5.580 ksi	2.63 sec	
ANO-00-082	16	1.42	Variable	4.736 ksi	4.736 ksi	27.13 min			N/A				Leak Only

Table 2-1 (Cont.)
ANO Burst Testing—Burst Test Data

ANO-00-083	14	1.42	Variable	3.600 ksi	3.828 ksi	107.2 min	0.700	0.040 ksi					Leak Only
ANO-00-084	14	1.42	Variable	3.650 ksi	3.872 ksi	182.9 min	0.600	0.200 ksi					Leak Only
ANO-00-085	14	1.42	Variable	4.000 ksi	4.062 ksi	210.0 min	0.473	1.720 ksi			3.400 ksi	1.60 sec	Burst Tearing (.095 to .110")
ANO-00-086	14	1.42	Variable	2.100 ksi	3.325 ksi	320.0 min		1.330 ksi					Leak Only
ANO-00-087	14	1.42	Variable	N/A					N/A	0.006	5.220 ksi	2.58 sec	Burst Tearing (.130 to .170")
ANO-00-088	14	1.42	Variable	N/A					N/A	0.006	5.070 ksi	2.45 sec	Burst Tearing (.150 to .190")
ANO-00-089	14	1.42	Variable	4.200 ksi	4.399 ksi	240.0 min		0.315 ksi					Leak Only
ANO-00-090	14	1.42	Variable	4.000 ksi	4.385 ksi	240.0 min		0.030 ksi					Leak Only
ANO-00-091	14	1.42	Variable	Burn Specimen	4.950 ksi[4]	5.62 min							Intended as EDM verification specimen
ANO-00-092	14	1.42	Variable	Burn Specimen									Intended as EDM verification specimen
ANO-00-093	14	1.42	Variable	N/A					N/A	0.006	5.300 ksi	2.50 sec	Burst Tearing (.085 to .115")
ANO-00-094	14	1.42	Variable	N/A					N/A	0.006	5.300 ksi	2.58 sec	Burst Tearing (.100 to .110")
ANO-00-095	14	1.42	Variable	N/A					N/A	0.006	4.980 ksi	2.35 sec	Burst Tearing (.150 to .140")
ANO-00-096	14	1.42	Variable	N/A					N/A	0.006	5.460 ksi	2.60 sec	Burst Tearing (.090 to .145")

Notes:
1. The presence and thickness of the foil had no effect on the limiting pressure of the test.
2. No effect of the foil, and repeating the test after lining with foil was not successful in elevating the pressure and getting the crack to run in the axial direction. The 0.010" foil was two layers of 0.005" SS foil, 0.006" was brass.
3. Specimen 3.X was fabricated to a profile that did not mimic the R72C72 profile.
4. Specimen 090 was originally produced as a burn specimen, but was never sectioned. It was later burst tested in a separate testing facility and the data included in the cumulative distribution comparison (see Table 2-2).

Table 2-2
ANO Surrogate Specimen Burst Testing Type 14 Specimens' Test Results

Specimen Identification	Test Rate	Measured Pressure (psi)	Median Rank	Notes
ANO-00-086	Slow	3325	6.7%	1.
ANO-00-068	Slow	3433	16.3%	1.
ANO-00-069	Slow	3755	26.0%	1.
ANO-00-083	Slow	3828	35.6%	1.
ANO-00-084	Slow	3872	45.2%	1.
ANO-00-085	Slow	4062	54.8%	1.
ANO-00-090	Slow	4385	64.4%	1.
ANO-00-074	Slow	4395	74.0%	1.
ANO-00-089	Slow	4399	83.7%	1.
ANO-00-076	Slow	4526	93.3%	1.
ANO-00-091	Slow	4950	16.3%	1., 3.
ANO-00-070	Fast	4320	6.7%	1., 2.
ANO-00-095	Fast	4980	26.0%	4.
ANO-00-088	Fast	5070	35.6%	1.
ANO-00-087	Fast	5220	45.2%	1.
ANO-00-093	Fast	5300	54.8%	4.
ANO-00-094	Fast	5300	64.4%	4.
ANO-00-096	Fast	5460	74.0%	4.
ANO-00-077	Fast	5600	83.7%	1.
ANO-00-075	Fast	5700	93.3%	1.

Comparison Statistics		
Slow Rate Average	4085	
Slow Rate Standard Deviation	495	
Fast Rate Average	5217	
Fast Rate Standard Deviation	409	
One-Tailed F-Test	59.9%	Variances are not significantly different. [5]
Two-Tailed t-Test	$3.2 \cdot 10^{-5}$	Means are significantly different.

Notes:
1. SEM fractography performed to determine the actual profile of the tested specimen.
2. Specimen 070 was reported as not exhibiting tearing at the tips of the slot, however, since it was a fast test, burst was judged to be likely imminent and the result included.
3. Specimen 091 was originally prepared as a machined profile verification specimen. It was later tested at a separate facility.
4. Specimen is not available for SEM examination.
5. Significance at a 95% level is not achieved, but close.

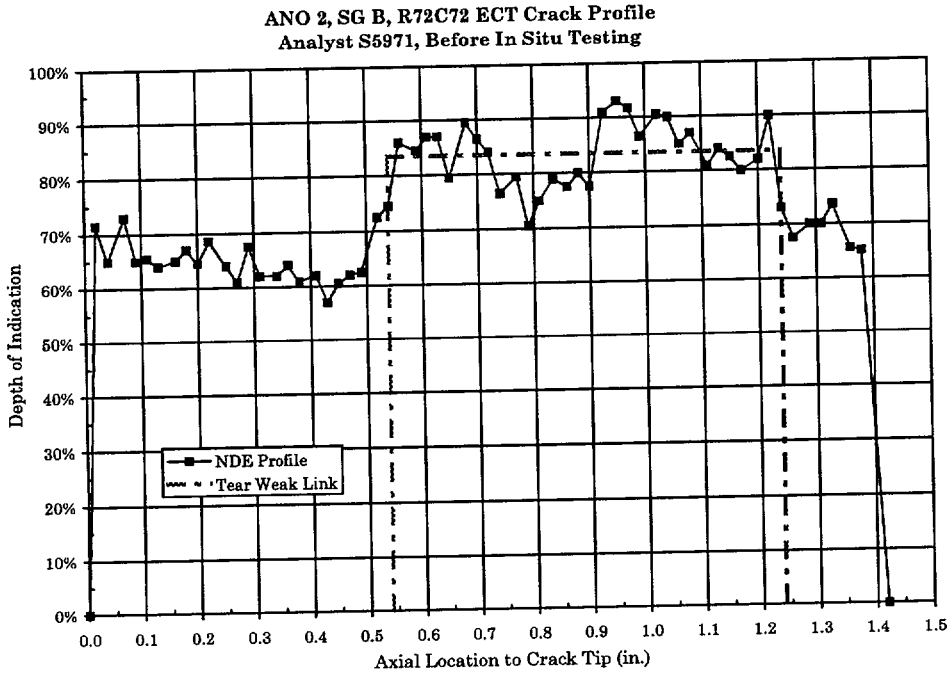

Figure 2-1
NDE Profile of the ANO 2, R72C72 Crack Profile

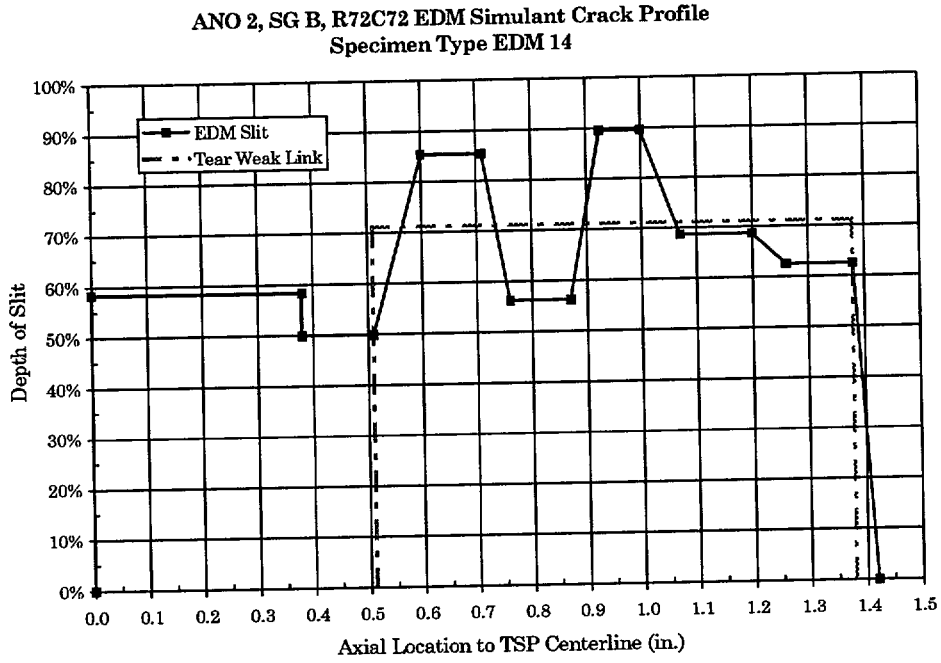

Figure 2-2
EDM Profile of the ANO 2, R72C72 Type 14 Simulant

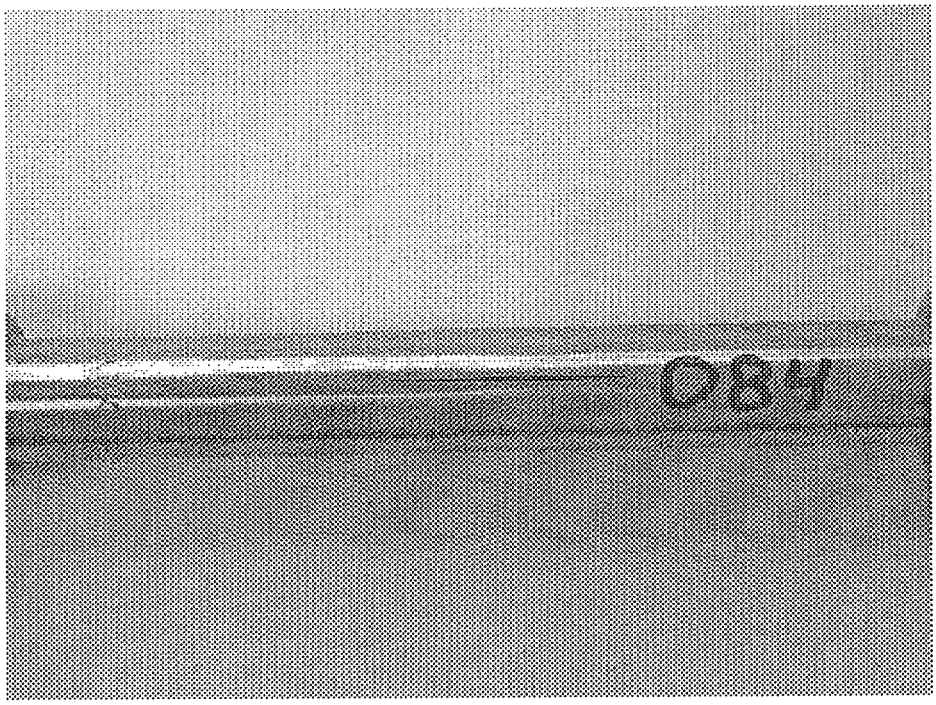

Figure 2-3
Test Specimen ANO-00-084, Small Extent of Throughwall Crack Tearing in a Slow Pressurization Rate Test

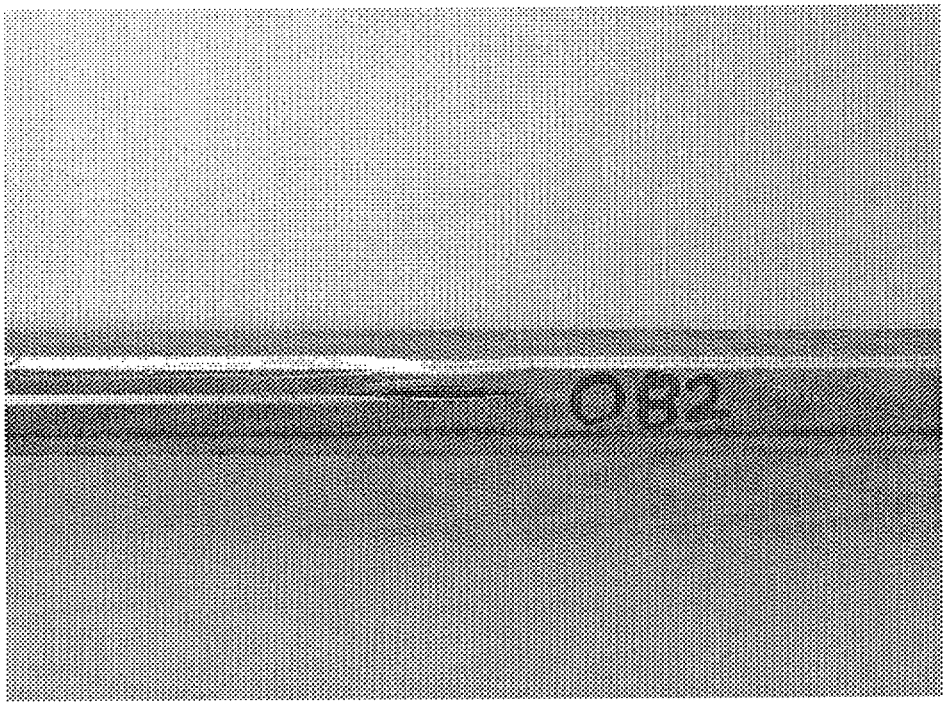

Figure 2-4
Test Specimen ANO-00-082, Relatively Large Opening in a Slow Pressurization Rate Test

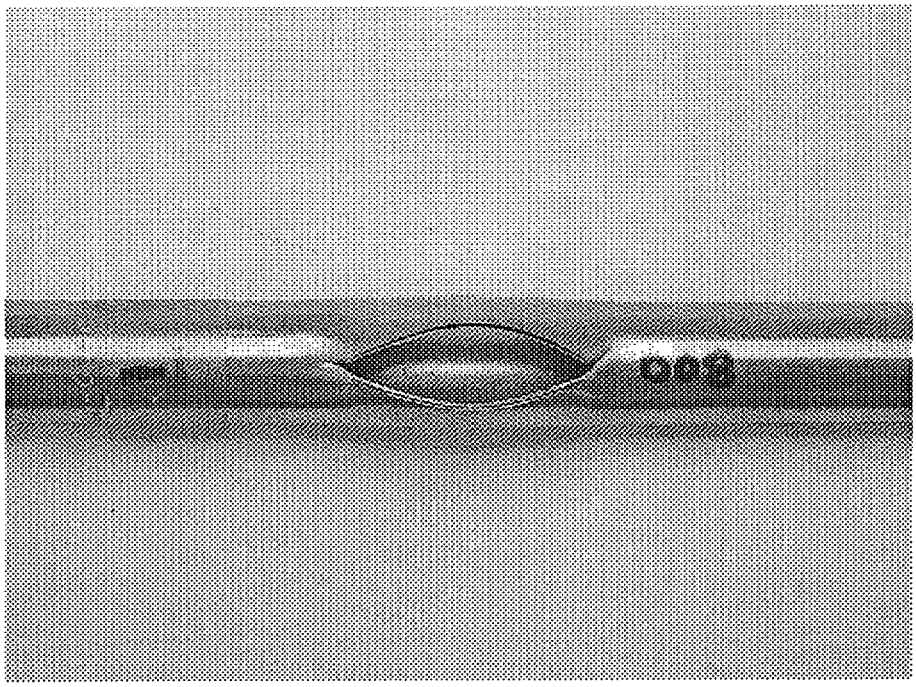

Figure 2-5
Test Specimen ANO-00-008, Burst Opening with Tearing into Full Thickness Material, Fast Rate Test (Type 2 specimen)

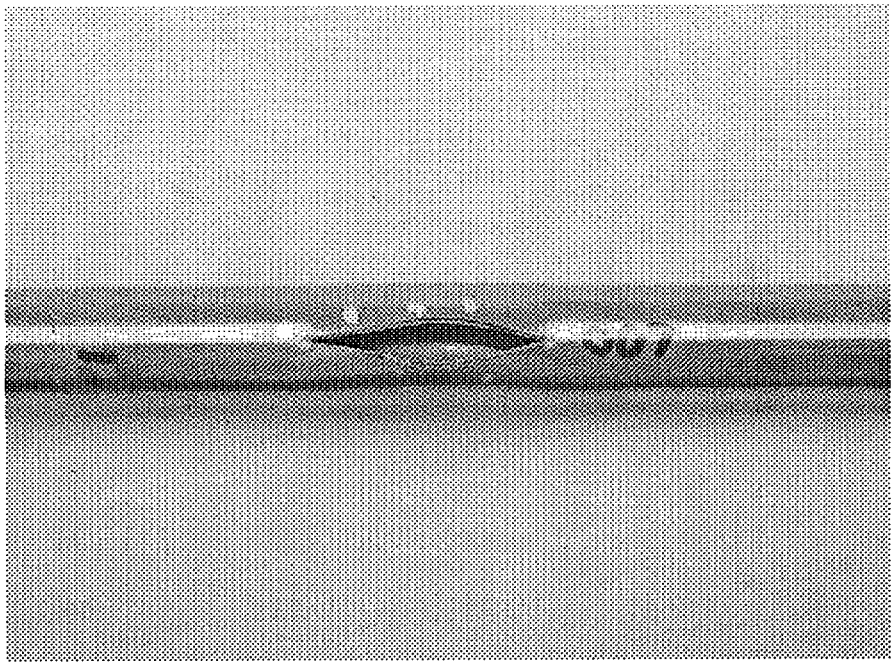

Figure 2-6
Test Specimen ANO-00-007, Large Opening with No Tearing into Full Thickness Material, Fast Rate Test (Type 2 specimen)

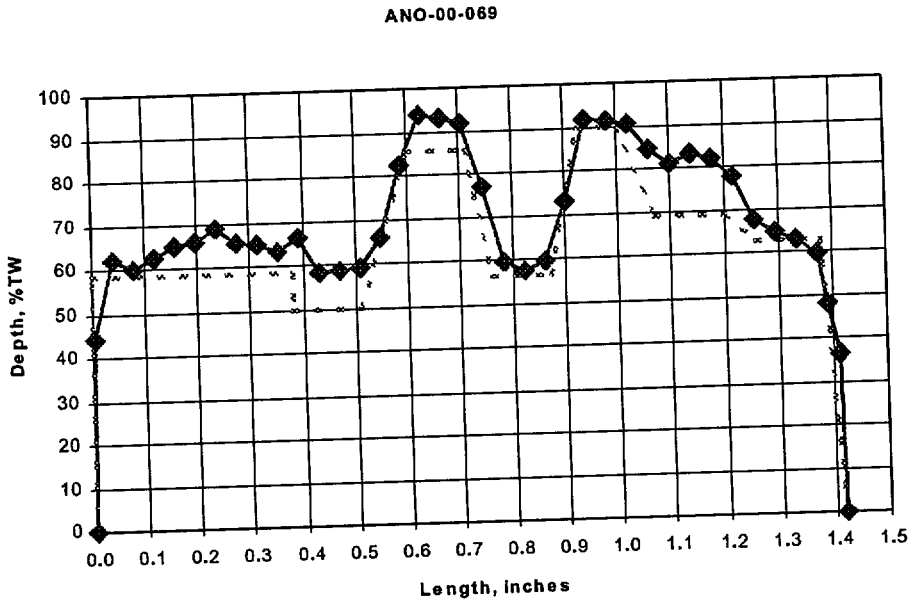

Figure 2-7
Measured EDM Profile Illustrative of Typical Agreement with the Fabrication Drawing

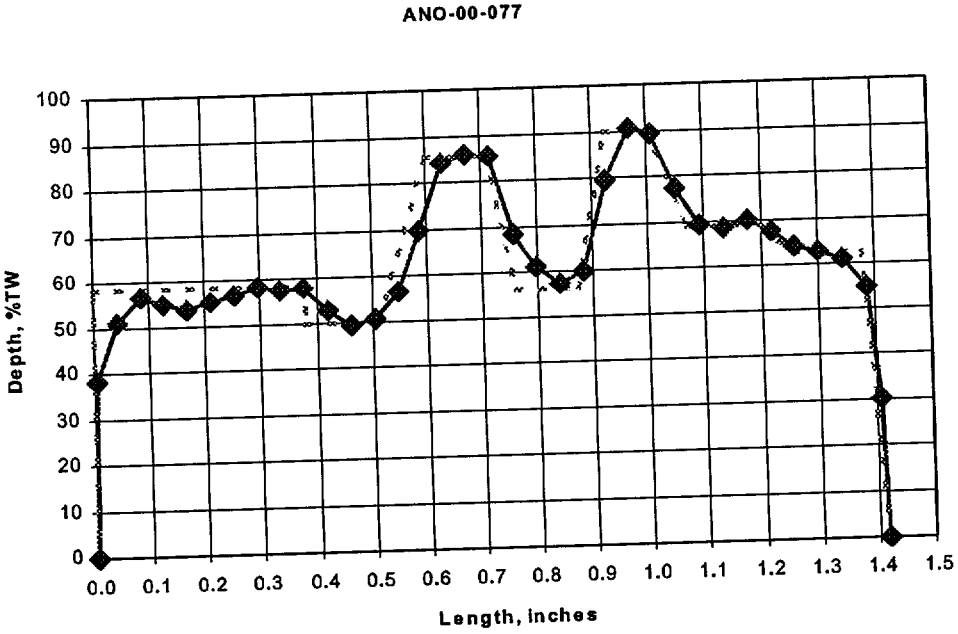

Figure 2-8
Measured EDM Profile Illustrative of Very Good Agreement with the Fabrication Drawing

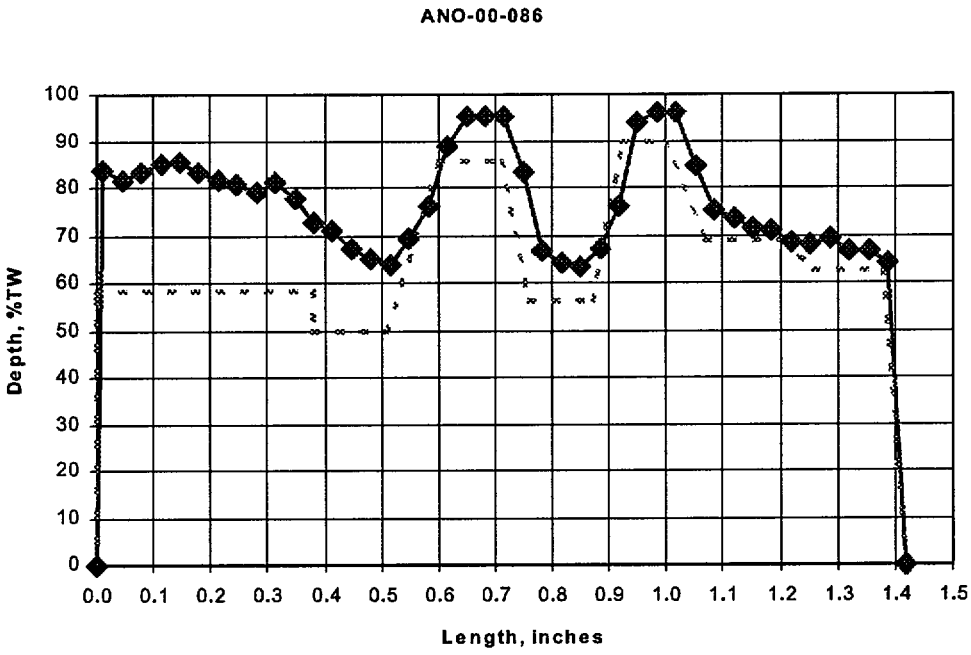

Figure 2-9
Measured EDM Profile Exhibiting the Most Discrepancy from the Fabrication Drawing

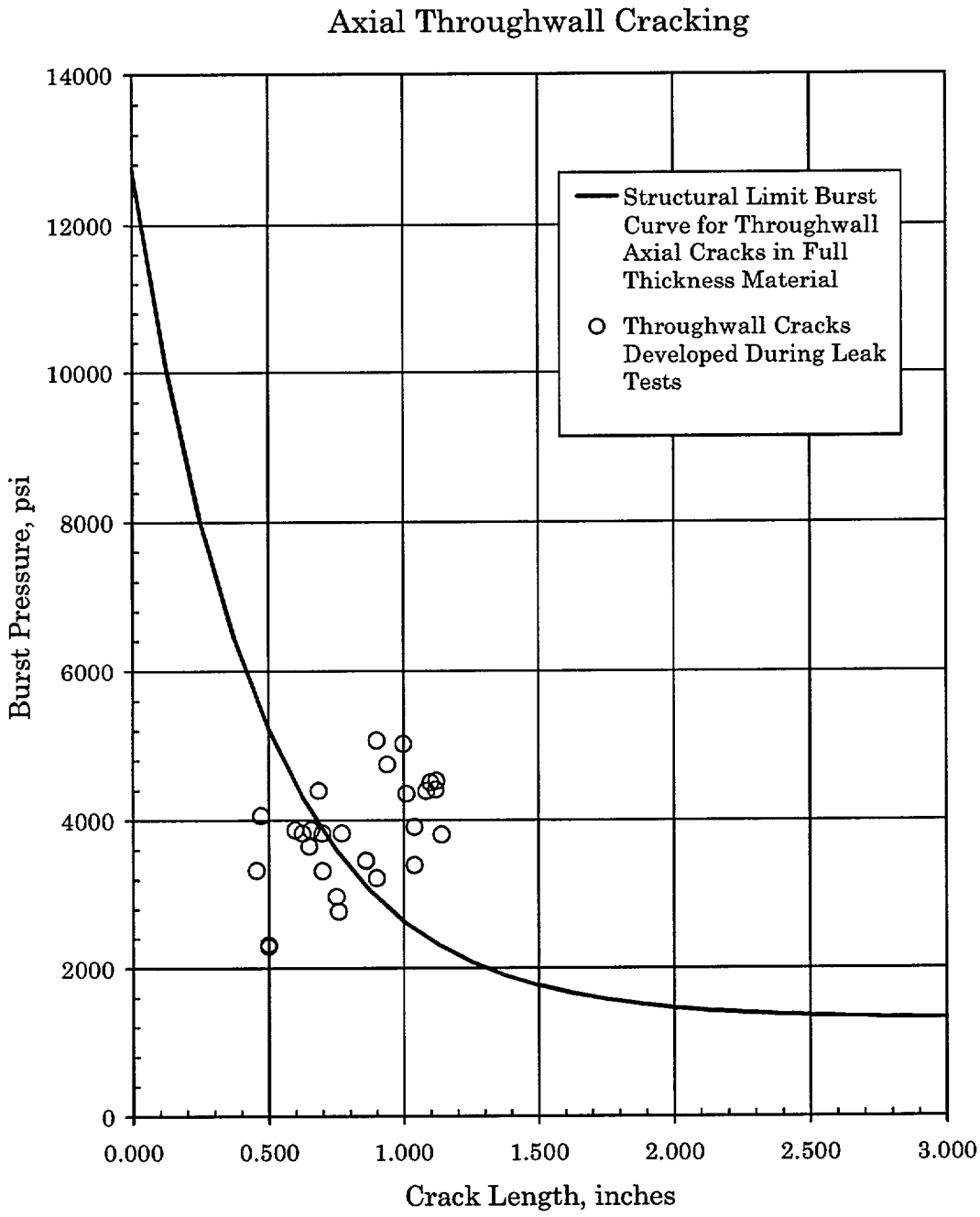

Figure 2-10
Comparison of Maximum Pressure and Length of Throughwall Crack Tearing Produced in Leak Rate Tests with Burst Pressure Curve for a Throughwall Crack in Full Thickness Material

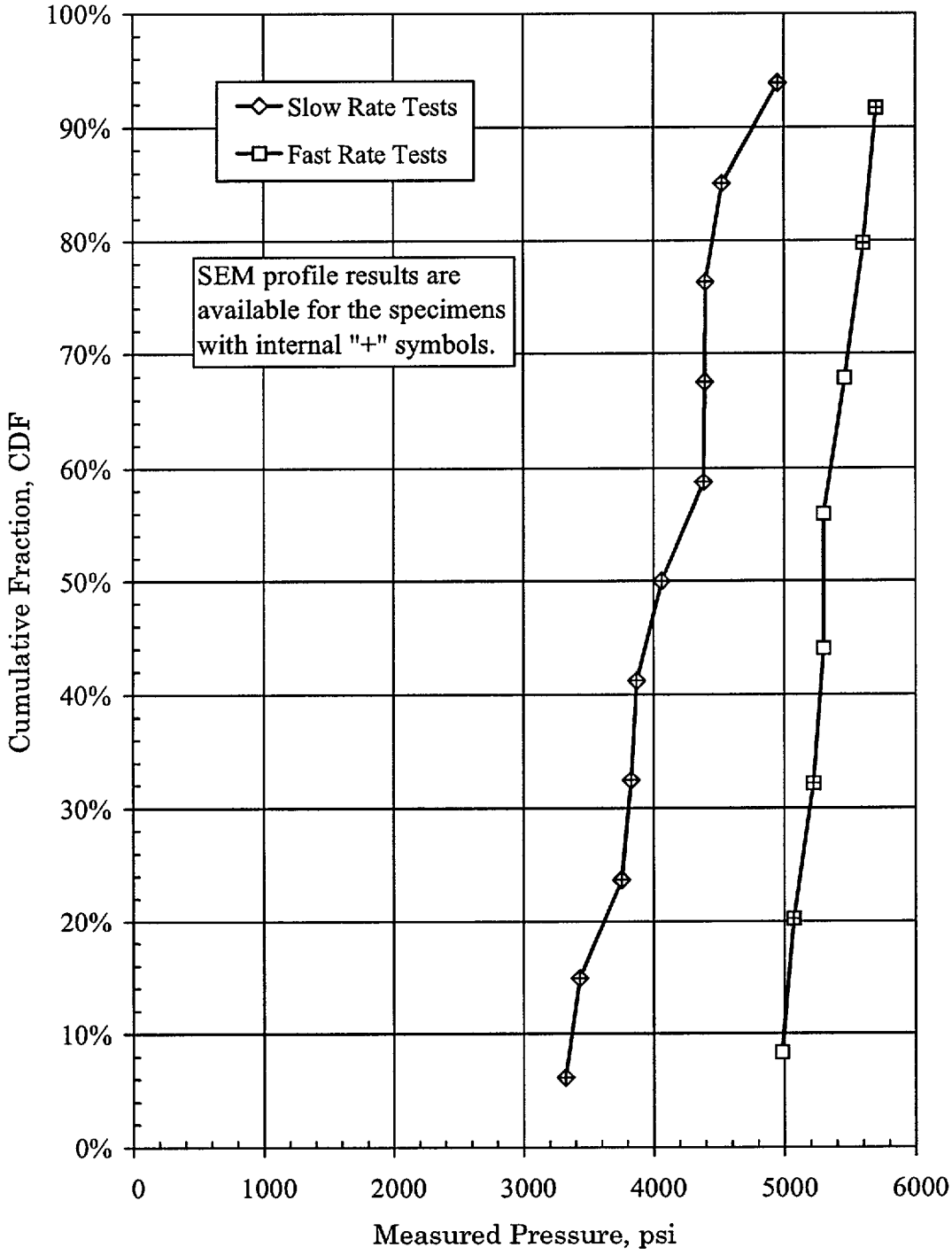

Figure 2-11
Cumulative Distributions of Maximum Pressures in Slow Rate and Fast Rate Pressurization Tests of Type 14 Specimens (Note: Variation with a test category includes a significant contribution due to specimen-to-specimen differences.)

3
BACKGROUND ON BURST TESTING

3.1 Industry Guidelines

The actual performance of burst tests varies from laboratory to laboratory. A joint set of guidelines was developed for EPRI in 1994 by representatives from Westinghouse, Laborelec and Packer Engineering [1]. Comments on the draft guidelines were received from Electricité de France (EdF) in 1995 [5]. A draft revision of the guidelines was prepared in early 1996 to address special considerations associated with circumferential cracking, but has not been formally issued. One of the provisions of the guidelines is the recommendation that the pressurization rate be in the range of 200 to 2000 psi/sec. EdF noted in their comments that they restrict the pressurization rate to 116 psi/sec.

Burst testing is performed on pulled tube specimens, specimens in which cracking has been environmentally induced and on specimens for which the degradation has been fabricated by some machining technique.

Slits are used to simulate cracking and are usually fabricated either by electrical discharge machining (EDM) or by using a narrow beam laser. The former technique generally results in flaws which are on the order of 6 to 8 mils wide, while the laser machining technique usually results in flaws that are about 2 mils wide. Using very low power, which results in long machining times, the laser machining process may result in slits that are on the order of 1 mil wide. The use of slits as surrogate cracks is a long-standing practice and is based on the fact that SG tube materials are ductile and failure is usually typified as being by tensile overload rather than fracture mechanics processes. Moreover, crack tips in SG tube material blunt to widths greater than those of the machined slits before crack extension takes place [11], hence there is essentially no difference between environmentally induced and mechanically fabricated flaws during the failure process. Because EDM results in a thin, brittle surface layer at the plane of machining, it is possible that microscopic extension of such flaws occurs at loads significantly less than those that lead to gross failure of the flawed specimen. There has, however, been no systematic study aimed at investigating this possibility. One significant different difference between environmentally and mechanically produced flaws is the planar nature of the mechanical flaws. Environmentally induced cracks tend to consist of arrays of smaller cracks that are nearly, but are not coplanar. Hence, there are also ligaments or material bridges between the smaller cracks that tend to strengthen the cracked tube relative to its mechanically fabricated counterpart. This is another area where systematic research aimed at characterizing those strengthening effects has not been performed. The omission of such effects leads to some inherent conservatism in the use of planar slits to simulate non-planar cracks.

3.2 Survey of Laboratory Practices

An attempt was made to survey several sources to obtain more information on the various laboratory approaches to burst testing of SG tubes. A letter was prepared and sent to various laboratories/vendors briefly explaining the situation and asking each recipient to prepare a short paragraph describing their approach to testing. A form was also enclosed in an attempt to standardize the responses. The following information was initially requested.

How are the cracks generated or simulated?
How are they measured to verify the dimensions?
What is the pressurizing medium?
Any special preparations, e.g., use of mastic or putty?
What is the pressurization rate and how is it controlled?
Where is[are] the pressure transducer[s] located?
Are there any pressure fluctuations?
What reinforcement is used, when is it used, bladder material, any fiberglass inside, and what foil, how thick, lubricant, etc.?
Can they test without reinforcement?
Do they measure the profile again after the test?

However, it is apparent that all of the requested information is not necessary for addressing the issue associated with the pressurization rate.

The following information, provided by the various vendors, provides a summary of their procedures for performing burst testing of SG tubes.

3.2.1 Westinghouse

Burst tests are performed in accordance with an internal document entitled "Operating Procedure for Burst Testing Degraded Steam Generator Tubes using the STC Burst Test Equipment." The Westinghouse document number is STD-OP-1998-8215. The document provides detail instructions for the performance of the burst tests and it is intended that the conduct of the tests be in accord with the EPRI guidelines [1].

The burst tests are performed in accordance with the EPRI guidelines for laboratory measurements of burst strength of degraded steam generator tubing. Burst specimens are initially prepared by installing an unreinforced plastic bladder into the ID of the test specimen to prevent leakage before burst. The bladder is a clear plastic laboratory tubing with a wall thickness of approximately 0.125 inches. The outer diameter of the bladder is selected to be slightly larger than the inner diameter of the test specimen. The bladder is stretched axially, reducing its diameter, thus permitting the test specimen to be slipped over the bladder. As the stretching force is released, the bladder expands radially and seals the test specimen, the ends of the bladder are then trimmed square using a knife. The specimens are then further prepared by installing a Swagelok plug on one end of the tube specimen and a modified Swagelok adapter to the other. This permits the specimen to be connected to the burst test apparatus via a high pressure connector. The test specimen is pre-filled with de-ionized water and the pressure intensification cycle is initiated with the pressure rising at a rate of 2000 psi per second, until tube burst occurs.

The X-Y recorder is calibrated before each equipment setup by the use of a pressure versus time plot on an X-Y recorder for documentation purposes.

In the event a specimen's flaw depth could possibility rupture before burst, due to through-wall or near through-wall flaws, a metal reinforcing foil made of brass and approximately 0.004 to 0.006 inches thick is used. The foil is installed over the plastic bladder after the stretching process and lubricated using vacuum grease to prevent premature extrusion of the bladder through the defect opening before actual tube burst could occur. In this test program, brass foil was used, having a thickness of 0.006 inches and was positioned such that approximately 0.500 inch on either side of the flaw.

Because of the reasonably high toughness of Alloy 600 tubing, a narrow EDM slit was assumed to be an adequate stimulant of natural stress corrosion or fatigue cracks in terms of affecting the tube burst properties. The burst pressure is dependent on the plastic flow properties of the tubing instead of the fracture toughness. Plastic collapse is reached before the onset of crack tearing. Yielding of the tube in the vicinity of the crack or slit limits the pressure bearing capacity of the tube. If this limit or collapse pressure is maintained, the crack opening will continue to increase until at some point crack tearing develops. The point where crack tearing develops does depend on the fracture toughness of the material but in the geometries of interest here, the maximum pressure capacity of the cracked tube is dominated by plastic response.

3.2.2 Westinghouse (formerly ABB Combustion Engineering)

Burst and leak rate testing of steam generator tubes at the Windsor, Connecticut laboratories are conducted in accordance with Procedure No. 00000-MCC-094, "Procedure for Testing Steam Generator Tubes for Leak before Bursting (Using an accumulator for Bursting). The most recent revision (Number 9, dated 12/3/96) incorporated changes in the pressurization rate (by using an accumulator), as discussed below, to make the procedure consistent with EPRI guidelines. The basic procedure has been used since 1989 to test a variety of specimens representing both tubes removed from operating steam generators and flawed tubes prepared in the laboratory. Flaws tested have included ID and OD initiated SCC, intergranular attack, wastage, wear scars, and pits as well as non-flawed specimens. In addition, specimens with EDM notches (rectangular and more complex shapes) to simulate crack-like flaws have been tested.

Dimensions of SCC and IGA flaws are always determined after burst testing is complete and is accomplished by measurements of the fracture surface from scanning electron micrographs typically obtained at magnifications of 40X or 50X. Depths are typically measured at increments of 0.025 inch. For pits, depths are determined by measurements with light optical microscope (LOM). Wastage and wear scars are determined by either of these techniques. For EDM notches, several techniques have been employed. Measurements from silastic™ molds have been used by the shop producing the EDM notches to demonstrate compliance with specified dimensions. For circumferentially oriented notches, measurements by LOM have been used to measure depths. For axially oriented notches, depths have been determined using LOM differential focus techniques and measurements from SEM micrographs. When using the SEM to measure EDM flaws, fewer measurements along the lengths of the flaws are taken because of the uniformity in depth associated with the notches.

The Westinghouse-Windsor approach to pressurizing specimens has traditionally used an air operated positive displacement pump. The earliest tests used a hand operated pump and, most recently, an accumulator has been used for a few specimens tested at very high pressurization rates. In almost all cases, the pressurizing medium has been de-ionized water. For a few specimens with axial flaws, a non-reinforced bladder was used to apply hoop loads. This approach resulted from qualification testing for in situ pressure testing of through-wall flaws with leakage in excess of pump capacity. Hoop strains in the bladder tests were identical to those recorded in capped tube hydro-tests.

The positive displacement pump results in a small pressure spike whenever the pump strokes. The spike is more significant during leak testing, especially at higher leak rates where significant pressure fluctuations can occur.

Reinforcing bladders are generally not used for burst or leak rate testing. If leakage beyond the pump capacity occurs, the test is interrupted and a bladder is inserted and the test resumed. The bladder is a section of tygon™ tubing. A reinforcing foil of brass (0.004 to 0.008 inch thick) or stainless steel (0.002 to 0.004 inch thick) is positioned over the flaw to prevent the bladder from extruding through the flaw. The bladder is lubricated with vacuum grease for ease of insertion into the specimen. The EPRI guidelines require a reduction in observed burst pressure of 5 percent to account for the reinforcing effect of the bladder (based on results from non-lubricated testing). As part of a CEOG study, Westinghouse-Windsor did evaluate the effect of a bladder on burst pressure by testing six (6) part-throughwall specimens with a bladder and six (6) identical specimens without a bladder. All specimens were from the same tube of Alloy 600. There was not a significant effect (less than 5 percent difference).

A low pressurization rate, target of 2000 psi/minute, was used for most of the burst tests conducted by Westinghouse-Windsor. Burst tests are actually conducted as leak rate tests, regardless of flaw type and characteristics. Specimens were slowly pressurized to a pressure simulating ΔP_{NO} and held for 5 minutes to observe for leakage. If leakage occurred, a leak test of up to 5 minutes duration at this pressure was conducted. Pressure was then slowly raised to P_{SLB} pressure and held for 5 minutes to observe for leakage. A leak rate test of up to 5 minutes duration was conducted if leakage was present. The specimen was then pressurized slowly to $3 \cdot \Delta P_{NO}$ and held for 5 minutes after which the specimen was slowly pressurized to burst. An objective of this procedure was to determine when leakage occurred (ligament tearing) and to determine if leakage at ΔP_{NO} occurred in specimens that were leaking at $3 \cdot \Delta P_{NO}$. Bladders were not used except as noted above.

During burst and leak testing, control of the pressure and pressurization rates is manual. Pressure can be observed by the operator on a pressure gage which taps into the test system tubing about 12 inches downstream of the pump. In addition, pressure is recorded by a transducer at the same location. Transducer output is to an X-Y recorder and to a computerized data acquisition system.

Since the Westinghouse-Windsor procedures were not consistent with the guidelines, the procedures were revised to permit testing at 200 to 2000 psi/second although the revised procedure continued to recommend the slower rate. The higher rate, with a bladder inserted at test initiation, was used for a series of CEOG sponsored tests on notched specimens and has been used on a few pulled tube specimens.

3.2.3 Framatome Nuclear Services – USA

Framatome Technologies Group (FTG) follows the requirements outlined in the "Guidelines for Burst Testing of Steam Generator Tubes" prepared for the EPRI ARC Committee [9, 10]. de-ionized (DI) water is used at a pressurization rate of between 1000 and 2000 psi/second (without hold times). Bladders are used in accordance with the guidelines document, and post-burst flaw dimensions are determined via scanning electron microscope (SEM) fractography. Flaws tested include both electrical discharge machined (EDM) notches and intergranular attack (IGA) and intergranular stress corrosion cracking (IGSCC), and other flaws in tubes' sections removed from SGs. In the cases where burst testing is used in support of a specific project (i.e. thin-walled Electrosleeves), a detailed test plan is written which governs the requirements and objectives of the burst testing to be performed. The results of the testing are recorded in an engineering record where they can be referenced in future calculations or manipulations.

3.2.4 Electricité de France & Framatome – France

There are two significant sources of burst pressure data from France. In both cases the data were obtained for use by Electricité de France and Framatome and later shared with EPRI. The results from extensive testing of tubes with and without various degradation morphologies, other than ODSCC at TSP intersections, is contained in Reference 16. The data from tests performed in support of application of alternate repair criteria (ARC) for ODSCC indications at TSPs are best summarized in Reference 29. Various additional references were used for the compilation of the final set of data which are recorded in Reference 29, but do not need to be cited here.

All of the burst pressure data used to support the ODSCC ARC were obtained from tests which were performed per the Reference 30 procedure specification. Additional information was provided via Reference 31. The procedure provides instructions to be followed for tests performed both at ambient and elevated temperature. Specimens are pressurized with a hydraulic fluid, either water or oil, and a mandrel may be placed inside of the specimen to limit the fluid volume being pressurized. A 0.004" (0.1 mm) thick band of stainless steel foil is glued (the glue may be omitted under specific circumstances) to the inside of the specimen before testing to seal any throughwall degradation and thereby prevent loss of pressure during the test. The pressurizing medium in the tube itself is mastic (putty), which is pushed by the water in the machine. The test specimen is pressurized smoothly at a rate that does not increase the hoop stress more than 4.4 ksi/s, or about 500 psi/s for 3/4" and 7/8" diameter SG tubes. The procedure plans for a pressurization rate of 8 bar/s (116 psi/s), but practically, the device is set to achieve 0 to 2500 bars (0 to 36,300 psi) within 600 seconds, which means a rate of 4.2 bar/s (60.4 psi/s). The testing machine is equipped with a hydraulic control system. There are two (2) pressure transducers; one operates in the 0-200 bars range (0-2900 psi), the other can measure up to 4000 bars (58,000 psi). The pressure transducers are located upstream of the specimen, between the pressure multiplier and the specimen. Each of the pressure transducers can be isolated by valves. The final reported burst pressure is 85% of the measured value to account for the presence of the foil. The crack profiles are examined by scanning electron microscopy (SEM) after the completion of the test.

The results from tests to characterize the strength of degraded SG tubes with forms of degradation other than ODSCC are documented in Reference 16. That report documents the results of tests performed to:

- Characterize the strength of Alloy 600 tube material,
- Determine the burst pressure of tubes without degradation,
- Analyze "the behavior of tubes with one defect (crack) located in the straight portion of the tube remote from discontinuities," and
- Analyze "the behavior of tubes with one or several defects (cracks) located in the roll transition zone."

There is a very extensive amount of data in Reference 16, and various geometries of machined degradation were investigated, i.e., V-notches, EDM slits, machined flats, uniform thinning, and lunar wastage (crescent shaped in the plane perpendicular to the axis of the tube). Typical burst testing rates were on the order of 35 to 60 psi/s, depending on the tests being conducted. The specimens may have been lined with a plastic bladder and the bladder may have been reinforced with a band of metal foil. The interface between the tube and the foil is lubricated to the extent that no adjustment is required from the measured burst pressure to the reported burst pressure.

3.2.5 Laborelec

Much of the information regarding burst testing performed at or for Laborelec may be gleaned from the Reference 11 discussion of the influence of test conditions. In addition, much information regarding test conditions is available in the EPRI report on the Belgian approach to PWSCC [17], the EPRI throughwall burst pressure report [12] and Section 5.1.3 of this document. Testing conditions and procedures at Laborelec are similar to those of the other laboratories. A variety of reinforcing methods have been used with reported burst pressures being reduced from the measured burst pressures to account for the strengthening effect of the reinforcement, e.g., a 5% reduction is applied to account for the presence of a plastic bladder and reinforcing foil. The pressurization rates tend to be slower than those used by Westinghouse in Pittsburgh, but are likely on the order of the rates used by Westinghouse in Windsor.

3.2.6 Argonne and Battelle National Laboratories

Historical data is contained in NUREG reports /CR-0718, /CR-2336 and /CR-5117 [18, 19 and 21]. Data from ongoing programs is reported in the multiple volumes of NUREG/CR-6511 [24]. Pressurization rates on the order of 30 psi/sec were reported in Reference 18 and 19 for tests performed at elevated temperature.

3.2.7 Mitsubishi Heavy Industries

Cracks are generated by EDM slits or by NAOH-IGA [32]. Prior to burst testing the length of the cracks is measured using ECT and UT. Following the tests the profile of the cracks is measured by SEM and macroscopic photography. The pressurizing medium is water. If the cracks are initially thought to be throughwall, the tube is lined with an 80 mil (2 mm) thick bladder

fabricated of nitrile rubber. No tests are performed on throughwall cracks without the benefit of a sealing system. The pressurization rate is not monitored during the test, however, the rate is such that the burst pressure is achieved within about 5 minutes after starting the test. This implies a range of about 10 to 40 psi/s. The burst pressure is measured by means of a pressure transducer located between the pump and the specimen. If the pressurization is stopped during the test, a decrease of the pressure in the system of about 150 psi (1 MPa) is usually observed.

MHI has performed tests with and without reinforcing the bladder with metal foil. They have investigated the effect of unlubricated, 20 mil (0.5 mm) thick by 90° wide stainless steel foil on the measured burst pressure and concluded that it does not have a significant effect. but that thicker or wider foil does elevate the measured burst pressure. This is a contrast to results obtained by Laborelec and Westinghouse. Recall that Framatome (France) has reported no effect of the foil if a lubricant is used [16]. At the time of this writing, additional information was not available, e.g., specific test results, etc.

3.2.8 Bettis and Knolls Atomic Power Laboratories

A personal contact was made by the Westinghouse author of this document with the Bettis Atomic Power Laboratory, however, no qualified data was available for distribution outside of that facility. No specific contact was made with any representatives from the Knolls Atomic Power Laboratory.

4
MATERIAL PROPERTY CONSIDERATIONS

Burst test results presented in Section 2 indicate a rate of pressurization effect for a Type 14 specimen EDM profile. Since burst pressures of degraded Alloy 600 steam generator tubing are generally determined by plastic collapse considerations, a rate effect in burst tests is expected to be a function of a rate effect on plastic flow behavior. A rate effect on plastic flow is simply the result of time dependent plastic deformation. Time dependent plastic deformation occurs across a broad range of temperatures, although high temperature creep deformation is the typical example for time dependent deformation. Room temperature and steam generator operating temperatures are not high enough to activate the mechanisms associated with high temperature creep deformation for Alloy 600. Time dependent deformation of Alloy 600 below the creep regime of behavior does occur. This type of behavior if often referred to as logarithmic creep. Thermally activated motion of dislocations past short range obstacles is a typical operating mechanism. The following paragraphs present and discuss results of tensile tests as a function of strain rate and stress relaxation tests of Alloy 600 at room temperature, 600°F, 680°F, and 750°F.

4.1 Room temperature plastic flow behavior

As part of this program tensile tests of Alloy 600 steam generator tubing were performed at room temperature. The test material was the same as used for burst tests of the Type 14 specimens. Room temperature tests were conducted on sections of tubing approximately 18 inches long using "V" shaped vice grips. An extensometer with a 2.0 inch gage length was affixed at the mid length of the tube. In one series of tests, five minute holds at constant displacement were performed. These hold periods were spaced at increments of 4% strain along the stress strain curve. Figure 4-1 illustrates the load versus displacement history. Time dependent deformation caused stress relaxation to occur during each hold period. The decrease in the load as a function of time was recorded. Figure 4-2 shows an example of the load relaxation curves.

In a second series of tests, a strain rate decrease by a factor of 25 was administered after every 4% strain increment in a standard rate tensile test. Straining at the low rate continued for five minutes whereupon the strain rate was increased back to the normal rate. Figure 4-3 shows that the flow curve was reduced whenever the strain rate decrease was performed. The standard rate of straining was $4.2 \cdot 10^{-4}$/s. The reduced strain rate was $1.7 \cdot 10^{-6}$/s.

Figure 4-4 shows the extent of stress relaxation after five minute holds at strain levels from 4% to about 32%. Replicate test results are shown. Stress relaxation is expressed as a percentage of the flow stress at each strain level. It is seen from Figure 4-2 that time dependent deformation is essentially completed after the first minute of hold time. Figure 4-4 shows that the extent of stress relaxation is about 4% of the flow strength at any given strain level. Figure 4-5 shows that a factor of 25 change in strain rate changes the flow curve (stress strain curve) by about 2.5%.

That is the flow strength at any strain level changes by about 2.5%. Note that if separate specimens had been tested for each strain rate, the specimen to specimen scatter in tensile test results would have obscured detection of any strain rate effect.

Rate effects on flow strength are typically a function of strain rate raised to some exponent. Present results indicate < 2% increase/decrease in flow strength for each order of magnitude increase/decrease in the strain rate (a decrease of 1.4 orders of magnitude in the strain rate reduced the flow stress by 2.5%). In conclusion, testing rate effects on the stress and strain properties of Alloy 600 at room temperature are very small.

4.2 Operating Temperature Plastic Flow Behavior

Tensile tests of five heats of Alloy 600 steam generator tubing at two different strain rates at room temperature, 600°F, 680°F, and 750°F were performed as part of an EPRI program in 1986 and reported in 1990 [8]. Elevated temperature tests were conducted using double leg "dog bone" type specimens, machined from sections of tubing. The strain rates were $5.6 \cdot 10^{-5}$/s and $5.6 \cdot 10^{-7}$/s. Tests were performed on individual specimens. Test to test scatter obscured any strain rate effect on the plastic flow, as illustrated in Figures 4-6 and 4-7 (the figures were obtained directly from the reference and no better copy is available). In retrospect, cyclic strain rate changes on individual specimens were needed to detect the small strain rate effects that are present. Small amounts of time dependent deformation were detected in stress relaxation tests at 600°F, 680°F, and 750°F. A stress relaxation of about 4% was observed in these tests. As in the present room temperature tests, most time dependent deformation occurred early in the test and the overall magnitude was small. Time dependent deformation at operating temperatures of stem generator tubing is still in the range of logarithmic creep. The magnitude and time scale of time dependent deformation of Alloy 600 tubing at operating temperatures is about the same as room temperature.

4.3 Flow Curve Rate Effects on Plastic Collapse Burst Pressures

The times to reach maximum pressure in the fast and slow pressurization test of Type 14 specimens differ by factors between 100 and 1000. In terms of a general plastic collapse mechanism of bursting, rate effects on tensile properties would predict about a 3 to 5% difference between fast rate and slow rate Type 14 burst tests. The mean observed difference is about 25%. Hence a rate effect on global deformation of the burst specimens cannot explain the fast rate and slow rate Type 14 burst test results. The explanation must lie in a factor sensitive to small amounts of time dependent deformation. The fracture of small ligaments beneath very deep partial throughwall cracks or EDM slots is one such consideration. This is discussed in detail in Section 5.1.2.

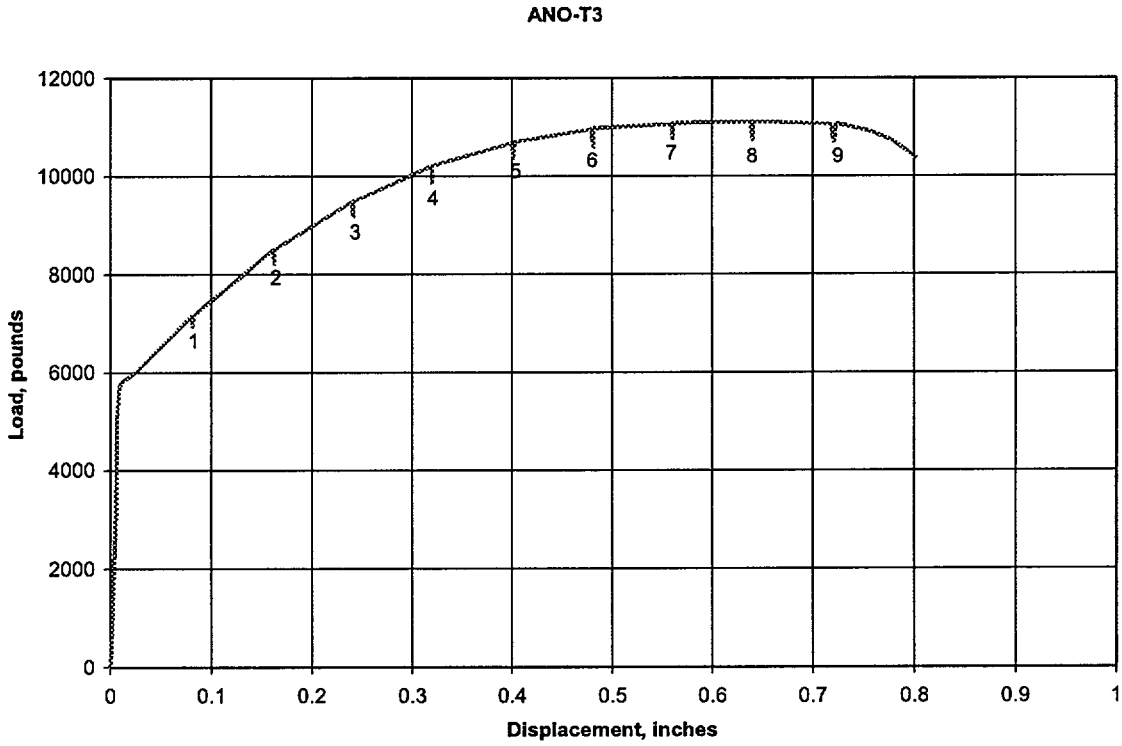

Figure 4-1
Load-Displacement History with Five-Minute Hold Times

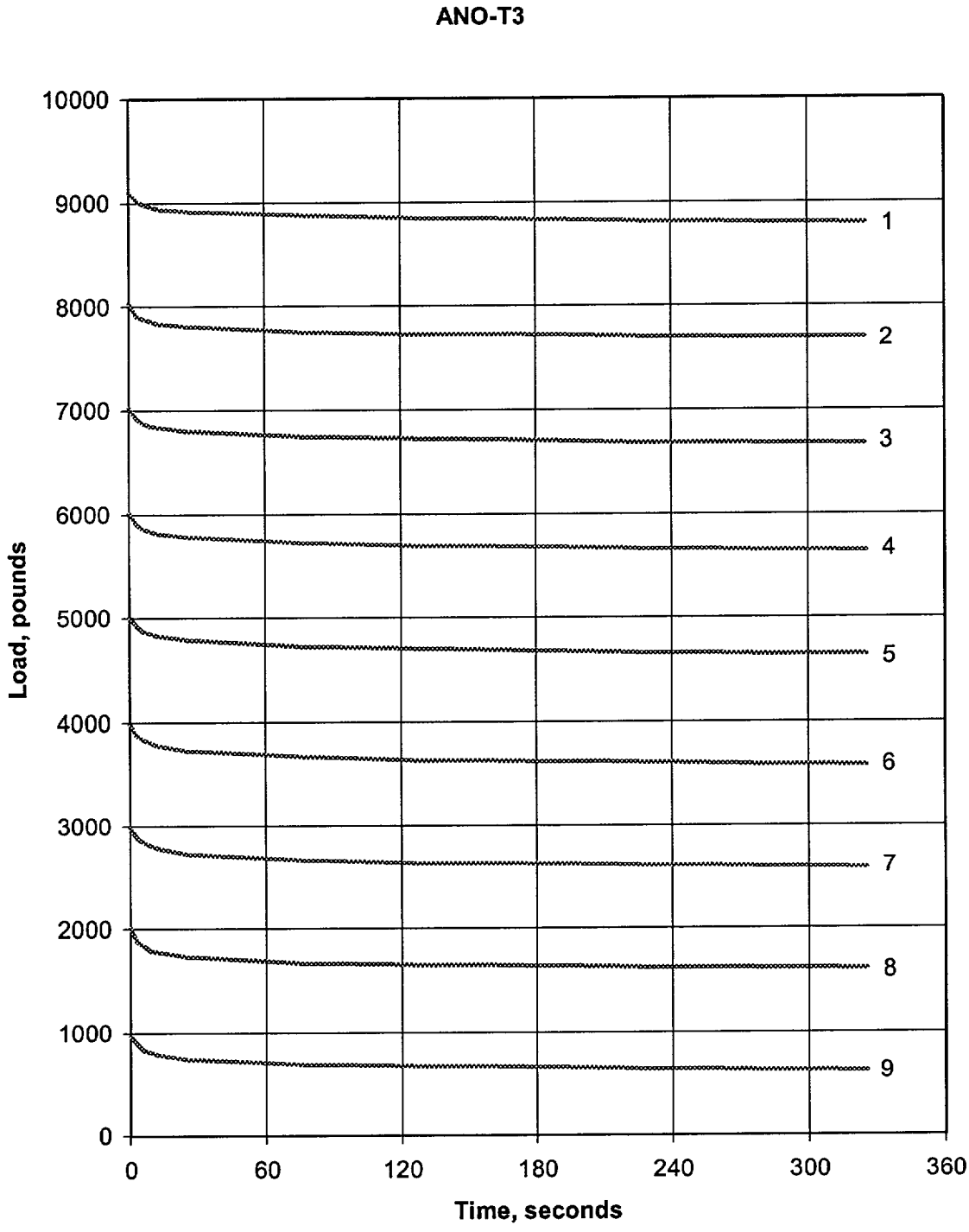

Figure 4-2
Load Relaxation Curves for Alloy 600 Tube Material

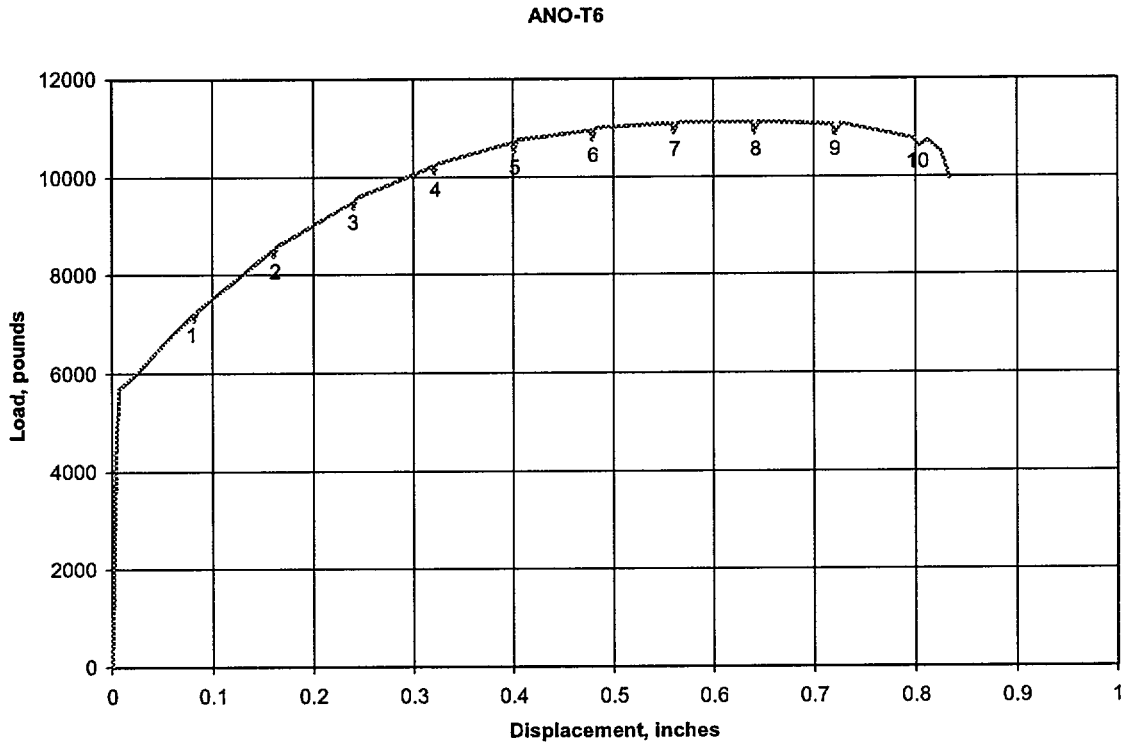

Figure 4-3
Load-Displacement History with Strain Rate Reductions at Specified Intervals

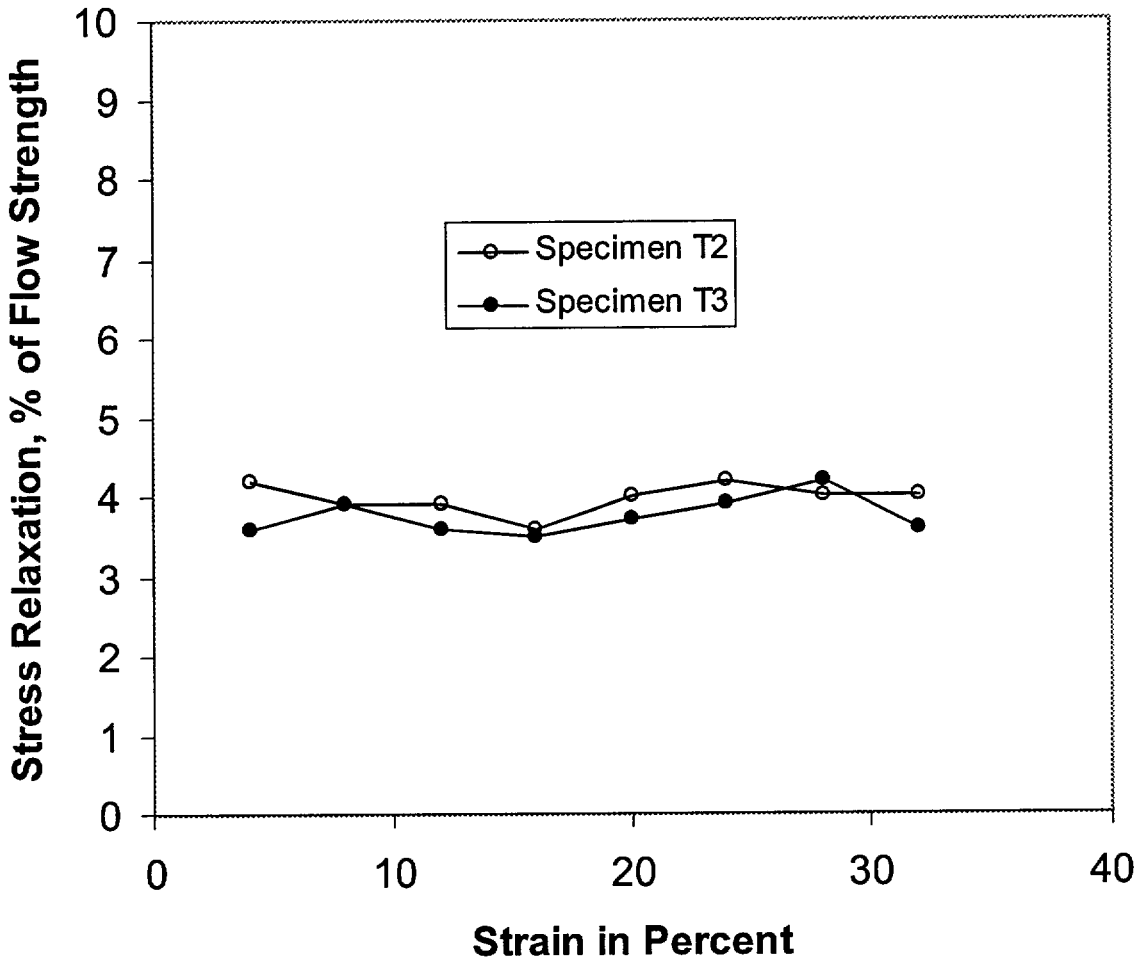

Figure 4-4
Extent of Stress Relaxation After 5-Minute Hold Periods at Strain Levels of 4 to 32%

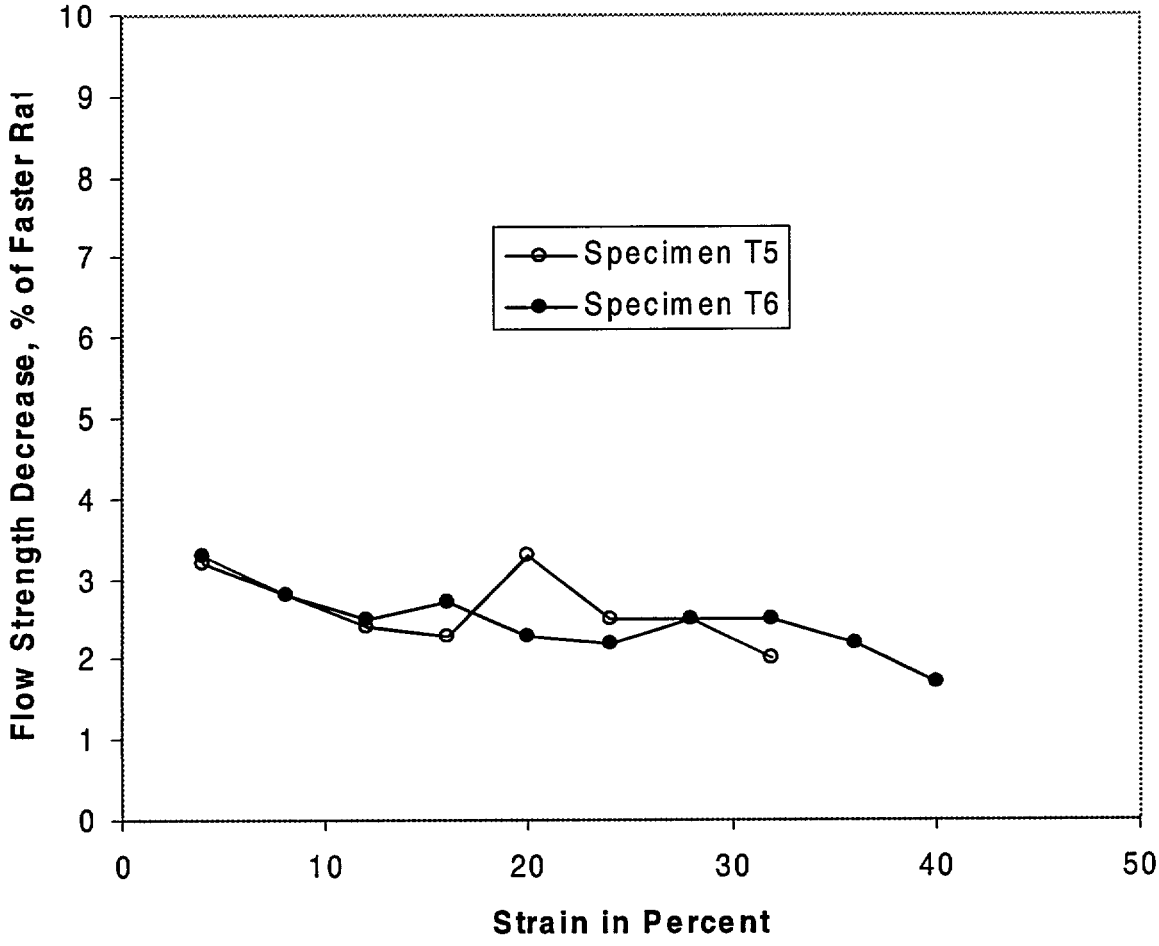

Figure 4-5
Effect of a Factor of Twenty-Five in the Strain Rate on the Flow Stress of Alloy 600 SG Tube Material

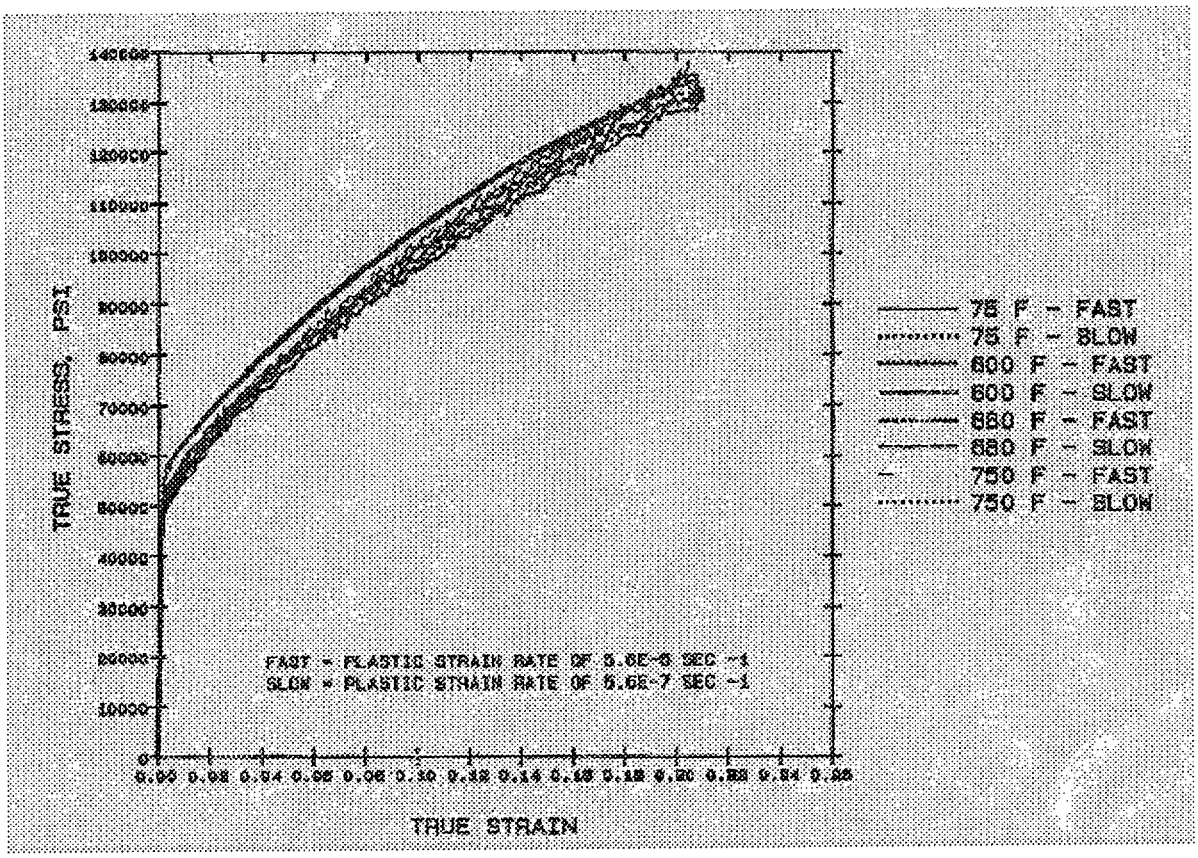

Figure 4-6
True Stress versus True Strain for Specimens from Heat 1019 Mill Annealed Alloy 600 Tubing

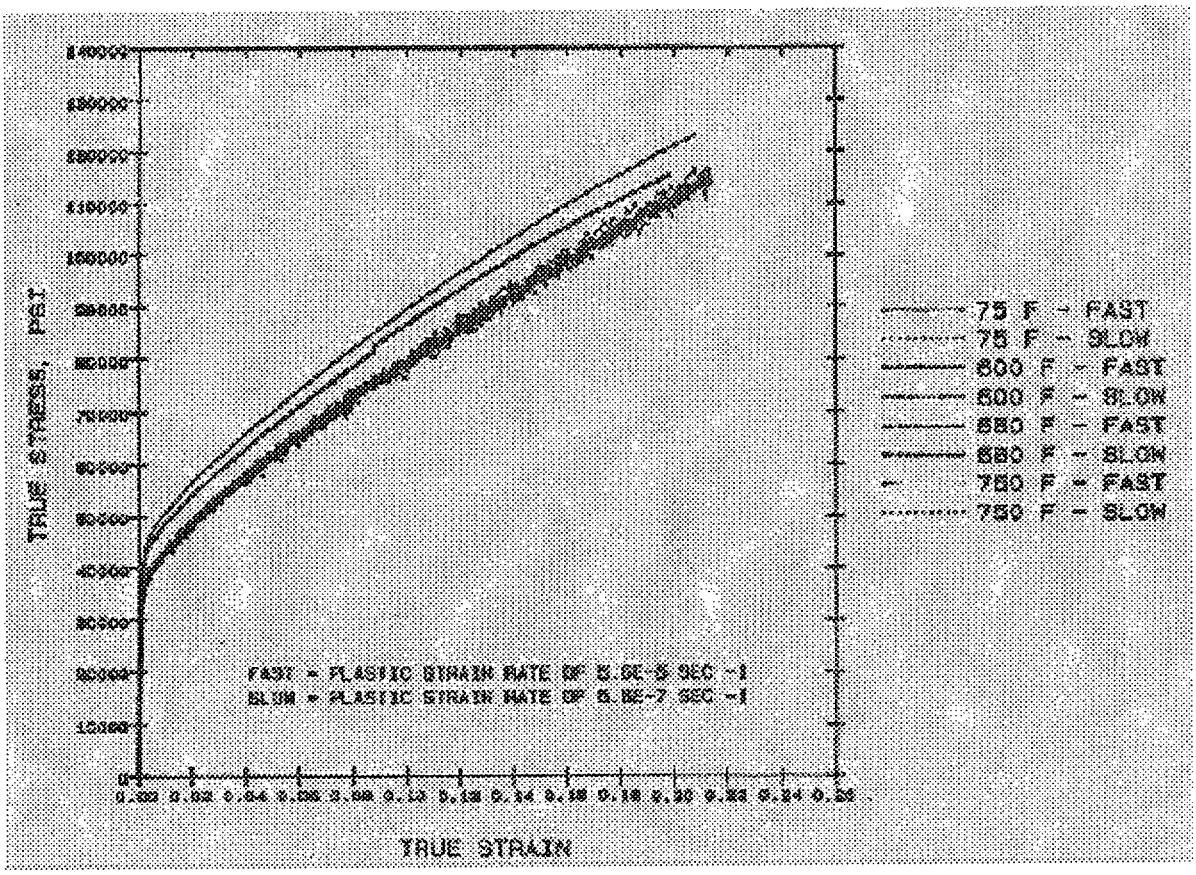

Figure 4-7
True Stress versus True Strain for Specimens from Heat 1991 Series 2 Mill Annealed Alloy 600 Tubing

5
TUBE INTEGRITY EVALUATIONS

This review of tube integrity evaluation methods and the impact and significance of the slow pressurization test results in Section 2 is based on the morphology of the degradation, and sometimes the location of occurrence in the SG. Requirements and implementation procedures for the evaluation of degraded SG tubes is provided in the EPRI Steam Generator Integrity Assessment Guidelines [14]. A comprehensive compilation of evaluation methods and formulae for demonstrating compliance with those requirements is provided in the EPRI Steam Generator Tubing Flaw Handbook [15]. The methods presented are frequently based on empirical correlations derived from the analysis of laboratory test data, i.e., burst tests.

A large number of burst tests have been performed under a variety of conditions and for a variety of degradation morphologies during the last three decades. Testing performed since 1995 likely conforms to the guidelines presented in Reference 1. In the past, pressurization rate effects on measured burst pressures has not been viewed as a significant issue. The data in Section 2 requires a re-evaluation of this viewpoint. Attention is focused on axial cracking. However circumferential cracking is considered as well as volumetric degradation. Tube integrity evaluations typically are based on physical descriptions of degradation. An eddy current bobbin voltage characterization of degradation is applied to axial cracking in some circumstances. Both approaches are included in this review.

The burst behavior of 100% throughwall cracks is presented first, followed by axial partial throughwall cracking. A review of the bobbin voltage methodology is then covered. The allowable extent of circumferential cracking is usually much greater than that of axial cracking. This impacts the permissible conservatism in the analyses. While rate effects on the burst pressure of tubing with axial or circumferential cracking need to be qualitatively the same, allowable margins influence the significance of situations where burst pressure may be rate dependent. High axial loads in once-through steam generators (OTSGs) can create instances where the allowable extent of axial and circumferential cracking is similar. Finally, volumetric degradation is covered. The burst behavior of tubing with volumetric degradation is clearly dominated by global tensile properties of the tubing and the evaluation of rate effects is more straightforward than for axial or circumferential cracking.

Following the above general considerations, specific conclusions and recommendations are provided for each of the degradation modes included the EPRI SG Tubing Flaw Handbook [15].

5.1 Axial Cracking

5.1.1 Freespan Throughwall Axial Cracking

Throughwall cracking is as the name implies, 100% through the wall of the SG tube. The evaluation model is described in Reference 12. The model is empirical, employing an equation form that is simpler than preceding models, some of which were based on theoretical evaluations or numerical solutions to the governing differential equations. The model is consistent with theoretical models, but fits the data better because of the freedom afforded in empirically fitting the coefficients.

The definitive work on measuring the burst pressure of SG tubes with throughwall cracks was performed by Laborelec (Paul Hernalsteen) [11]. In addition to performing multiple tests on laboratory specimens to investigate the effect of various test parameters, a series of specimens were tested to failure using the large capacity pumps at the Schelle fossil power plant in Belgium. The tests were performed without benefit of any lining to prevent leakage from the specimens. The pressure was gradually raised until unstable crack extension was attained. The results from those tests over a wide range of crack lengths confirmed the supposition that burst pressures were greater than had been reported by Westinghouse [12] from tests conducted at high rates and using a plastic bladder to prevent leakage prior to crack extension. They also confirmed that burst pressures were slightly lower than had been reported by others [12], including Laborelec, that used an unlubricated metal foil, like stainless steel, to line the plastic bladder to prevent its expulsion through the crack opening.

A typical pressure versus time history for a Laborelec laboratory test is shown on Figure 5-1 and that for one of the tests performed at Schelle is on Figure 5-2. The rate at which the pressurization of the specimens occurred are also illustrated on the figures (the scale is on the second y-axis). The recorded data is illustrated as the solid line on the figures. The pressurization rates were calculated from the test data and are illustrated as dashed lines. It is apparent that relatively slow pressurization rates were actually achieved during the tests. The pressure versus time histories from the other Schelle tests were requested from Laborelec, however, the response indicated that the original data are no longer available, but that all of the tests were conducted similar to the one plotted [13]. The EPRI database curve for throughwall cracking is shown on Figure 5-3 along with the Schelle data. In fact, the Schelle data were included in the database for the regression analysis. The Laborelec laboratory burst test results, Schelle show pressurization rate and the Westinghouse high pressurization rate data, in the range of 2000 psi/s, demonstrate that the EPRI database for throughwall cracks is free from rate effects. There is no apparent difference in the test results between the forty-three fast-rate and sixteen slow-rate test results illustrated on Figure 5-3.

Additional data were reported by EdF [16] for throughwall cracks with lengths of 0.276" (18 & 435 psi/s), 0.591" (18 to 234 psi/s), and 1.18" (17 to >242 psi/s). The results of these tests add to the database showing no measurable effects of pressurization rates on burst pressure from about 20 psi/s to 2000 psi/s.

It should be noted that all throughwall crack or EDM slot data is geometries where the crack or slot tip resides in full wall thickness material. The extent of crack tip or slot tip blunting prior to

crack tearing is about equal to the wall thickness of the tubing, that is, near 0.040 inches. An extensive database, subjected to thorough reviews and resolutions of sealing bladder issues, shows that the burst pressure of throughwall cracks in full thickness material is not pressurization rate dependent from 20 psi/s to 2000 psi/s.

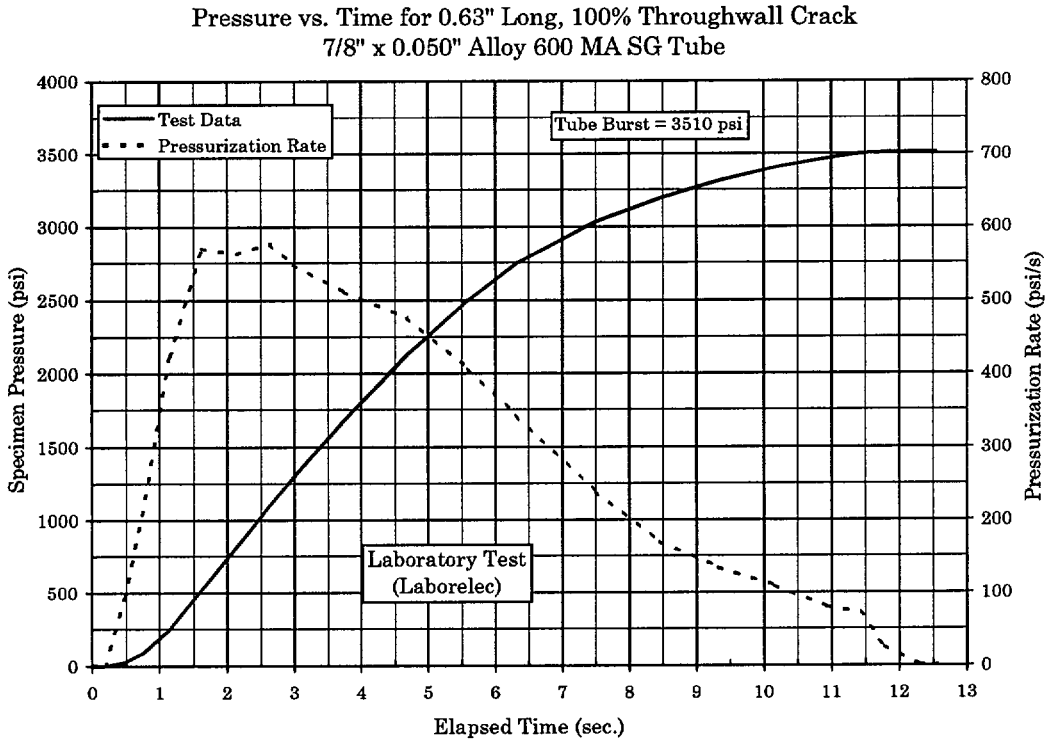

Figure 5-1
Pressure vs. time plot for Laborelec laboratory test

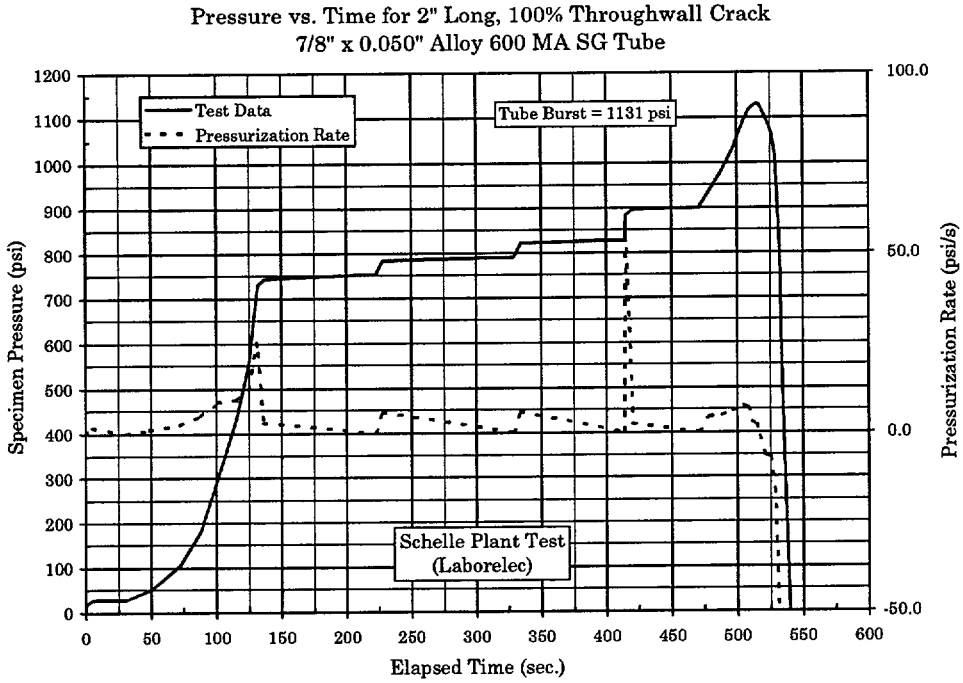

Figure 5-2
Pressure vs. time plot for Laborelec Schelle test

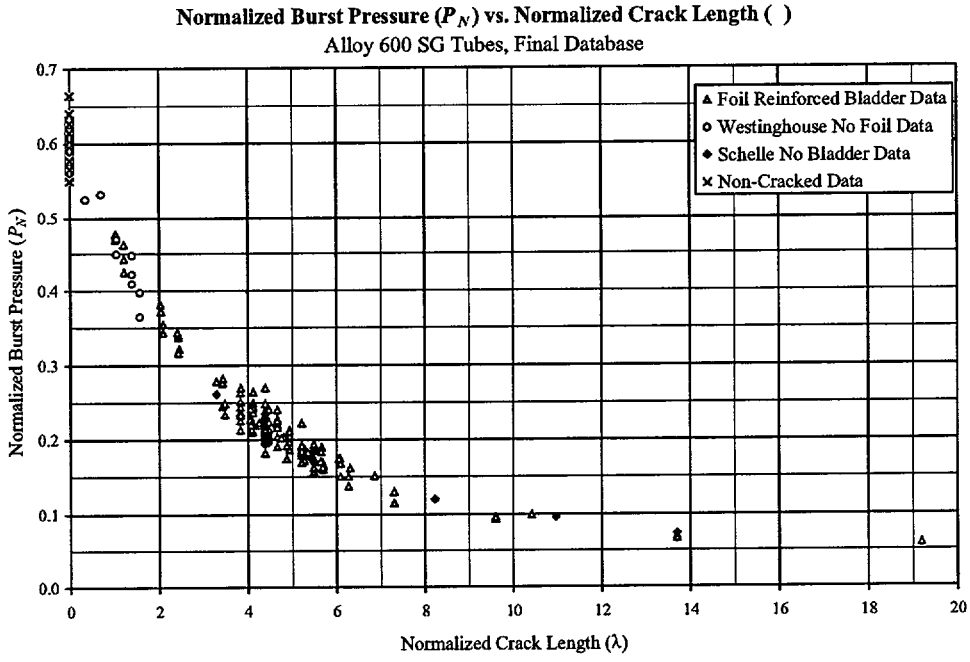

Figure 5-3
Throughwall Crack Burst Pressure Database [12]

5.1.2 Axial Part-Throughwall Cracking

The most definitive set of tests on partial depth crack like degradation was performed at PNL and reported in NUREG CR-0718 [18] and CR-2336 [19]. Narrow rectangular EDM slots were machined into a wide variety of tubing sizes. Testing was performed at 600°F at a pressurization rate of about 30 psi/s. Figure 5-4 shows a plot of calculated maximum test pressure versus measured maximum test pressure. Calculations used the Cochet (Framatome) equation [16] and accurate re-measurements of the sizes of the EDM slots by Argonne National Laboratory personnel, i.e.,

$$P_B = 0.58\left(S_y + S_u\right)\frac{t}{R_i}\left[1 - \frac{L}{L+2t}h\right] \qquad \textbf{Equation 5-1}$$

where S_y and S_u are the yield and ultimate tensile strength of the material, t and R_i are the thickness and inside radius of the tube, L is the effective length of the crack, and h is the relative depth. Equation 5-1 is referred to as the Cochet equation. Calculations are close to a good lower bound compared to measurements. An experimental lower bound in the EPRI Flaw Handbook is a very good lower bound to this data, i.e.,

$$P_B = 0.58\left(S_y + S_u\right)\frac{t}{R_i}\left[0.988 - \frac{L}{L+2t}h\right] \qquad \textbf{Equation 5-2}$$

A value of "1" was used in these calculations since EDM slotted specimens were tested. Calculations are close to a good lower bound compared to measured burst pressures. An experimental lower bound for service induced axial cracks in the EPRI Flaw Handbook is also a good lower bound to the EDM test data. This is because, in the lower limit, some service induced axial cracks are as smooth and planar as EDM slots. The nominal value of the parameter inside the brackets in equation 5-2 is 1.104 with a standard deviation of 0.0705 [15]. Meandering, service induced, partial throughwall, axial cracks have out of plane ligaments which elevate the strength properties relative to smooth, planar EDM slots. The value of 0.988 is obtained as the lower 95th percentile value assuming it is normally distributed. After the uniform ligament slot tears throughwall, the tube is presented with a throughwall crack in full thickness material. At this point the EPRI throughwall burst equation can be applied to determine if a full tube burst will occur compared to just a ligament tearing throughwall in the depth direction. Additional discussion of the tearing and burst phenomena is provided in Section 7 of this report.

Figure 5-5 shows similar test data for tests conducted at a pressurization rate near 2000 psi/s at room temperature. Again the Cochet expression, Equation 5-1, provides a conservatively biased prediction of the maximum pressure that can be achieved during the test. In addition to rectangular EDM slots, Figure 5-5 includes data for triangular and tent shaped slots. Some of these slots had throughwall portions. The weak link or equivalent rectangle method, as described in the EPRI Flaw Handbook (Section 5.1.5), performs well in accounting for dramatic shape effects in addition to the simple rectangle case.

The calculated maximum pressures for the slow and fast pressurization tests of Type 14 specimens are listed in Table 5-1. The tabulated data represents all specimens for which SEM fractography was performed to obtain actual machined profiles. Figure 5-6 compares the measured to the calculated maximum pressures for the slow pressurization tests of those specimens. The Cochet equation together with the equivalent rectangle method provides very good estimates of the measured maximum test pressures obtained at extremely low rates of loading. Figure 5-7 illustrates a definite rate effect on the maximum test pressure of Type 14 specimens evaluated in the same manner. The combined slow and fast rate data are shown on Figure 5-8 and the ratios of the measured maximum to the predicted maximum pressures using the Cochet model are illustrated on Figure5-9. This latter figure illustrates the bias introduced by the rate of pressurization of the specimens. As noted in Section 2, the extent of tearing after both the slow rate and fast rate tests of Type 14 specimens are sufficient to term the final results burst pressures. Again, for the Type 14 specimens with maximum slot depths on the order of 95% TW, a definite rate effect on burst pressure is observed. However, the standard industry method of evaluating results (here as applied to EDM slotted specimens by using the Cochet ligament tearing equation to estimate the burst pressure) is sufficiently conservative to provide a very good description of both ligament tearing and burst pressures. The calculation technique is described later in this section, however, it is appropriate to illustrate the results of the calculations using the profiles discussed in Section 2 relative to typical, good, and poor agreement with the fabrication drawing dimensions. To this end Figures 5-10, 5-11, and 5-12 are included showing the fabrication drawing profile, the SEM fractography measured profile, and the structurally significant or weak link rectangle profile for specimens ANO-00-069, -077, and –086 respectively. The result for specimen –086 provides a striking illustration of why the total ligament tearing pressure was so low. However, once the profile is known, the structural model provides a reasonably accurate prediction of the actual maximum pressure that can be achieved in a slow pressurization test.

Rectangular slot data in Figures 5-4 [18, 19] and 5-5 [20] for depths up to about 90% TW shows that rate effects are not an issue up to this point, i.e., there is no material departure of the results of the tests from the predictions for the slow rate tests of Figure 5-4 or the fast rate tests of Figure5-5. Furthermore, the slow and fast pressurization rate test results are similar for predicted maximum pressures in the range of 1500 to 2500 psi. Test data for larger depths at conventional rates of loading is subject to very high scatter. Remaining ligaments in the depth direction with sizes on the order of 0.005 inches are very to difficult to machine with any degree of accuracy. Ligaments of this size are difficult to measure and small variations in depth along the length of EDM or crack profiles must be carefully considered. A 0.001" variation in depth leads to about a 20% variation in ligament tearing pressure. One approach is simply to use a more conservative analysis technique for very deep planar cracks instead of focusing on detailed test specimen characterizations. An example of a more conservative analysis technique when the depth is greater than $\approx 90\%$ is the ANL equation for ligament tearing of axial cracks [24, 25, 26, 27]. Here, the ligament tearing pressure, P_L, is given as a factor, $1/m_p$, of the burst pressure of a non-degraded tube, P_B, i.e.,

$$P_L = P_B \frac{1}{m_p}, \text{ where } m_p = \frac{1-\alpha^{h/m}}{1-h} \qquad \textbf{Equation 5-3}$$

The expressions for α and m are [26],

$$\alpha = 1 + 0.852\left(\frac{d}{t}\right)^2\left[1 + \frac{1}{m}\right] \qquad \textbf{Equation 5-4}$$

and

$$m = 0.614 + 0.481\lambda + 0.386e^{-1.25\lambda} \qquad \textbf{Equation 5-5}$$

where λ is the dimensionless crack length and non-degraded burst pressure are given by [26],

$$\lambda = \frac{L}{\sqrt{R_m t}}, \text{and } P_B = 0.595(S_Y + S_U)\frac{t}{R_m} \qquad \textbf{Equation 5-6}$$

Here, L is the crack length, R_m is the mean radius of the tube, t is the thickness of the tube, h is the ratio of the depth of the crack to the thickness of the tube, and S_Y and S_U are the yield and ultimate strength of the tube material. It is noted that slight variations of the equation coefficients have been reported because the test program being conducted at Argonne is still ongoing. The expressions presented above were from the most recent reevaluation and analysis of the original Battelle data.

The ANL equation for ligament tearing extrapolates to zero pressure as the crack depth increases to 100% TW while the Cochet equation extrapolates to a very conservative throughwall burst pressure equation as the depth increases to 100% TW. Figures 5-13 through 5-15 illustrate comparisons of the Cochet and ANL equations as a function of depth of rectangular profiles for lengths of 0.5, 0.75 and 1.5 inches. The ANL equation is less conservative than the Cochet equation for depths less than about 85% TW. The ANL equation provides a conservative calculation for ligament tearing. It is more conservative than the slow pressurization test data on Type 14 specimens indicates is necessary. Since the ANL equation extrapolates to zero pressure, if any section of a crack profile is 100% TW, the ANL equation does not provide any estimate of burst pressure; the answer is always zero. In contrast, the Cochet equation provides a conservative burst pressure for crack profiles with throughwall portions. As discussed in Section 7, improved methods of burst pressure calculation are needed for crack profiles with 100% TW portions. The Cochet equation provides conservative burst pressure predictions but, in many cases, these predictions are unduly conservative.

One special case of axial partial throughwall crack analyses is a PWSCC ARC. Testing programs similar to those for ODSCC ARC applications have been conducted at multiple laboratories, e.g., see References 28 and 10, for PWSCC cracked tubes. The tests were of both laboratory specimens and pulled tube sections. The results from the different laboratories were not discernibly different, implying no noticeable effect of pressurization rate. Not as much information is available to discern the differences in the testing procedures for the PWSCC

specimens as for the ODSCC specimens. However, the effect must be limited to the influence of the pressure on the crack flanks. The net effect of the pressure on the crack flanks is to reduce the maximum pressure for an internal axial crack by about 7 to 8% relative to that of a comparable external axial crack. While this is not an insignificant effect, it is apparent that changes to the influence of the internal pressure would be secondary relative to the overall maximum pressure result.

A burst pressure prediction model was developed using available test data [10]. The basic burst pressure, P_B, prediction model equation is that of Cochet [16], Equation 5-1, modified to the following form,

$$P_B = 0.58\left(S_y + S_u\right)\frac{t}{R_i}\left[1 - \frac{L}{L+2t}h\right]\Phi \qquad \textbf{Equation 5-7}$$

where Φ is an adjustment factor, frequently on the order of 0.9, to account for the pressure on the flanks of the crack for PWSCC. A discussion of the derivation of the model, along with the adjustment factor, is provided in the EPRI Flaw Handbook [15]. The model also uses the ASME Code model for the prediction of the burst pressure of throughwall axial cracks in SG tubes. Both the Cochet and ASME Code models, when combined with the weak-link technique of evaluation [15] effectively result in a prediction of the lower bound burst pressure for axially cracked SG tubes. An idealized crack profile is illustrated on Figures 5-16 and 5-17, and the results of predictions of the burst pressure using the model are illustrated on Figure 5-18. The database depicted in the figure is based on using actual material properties from pulled tubes along with the crack profiles obtained from the fractographic examinations of the flanks of the cracks following the burst tests.

The bulk of the burst testing data are from two vendor locations, the Westinghouse facilities in Pennsylvania, and the Westinghouse facilities in Connecticut. The different locations employ different testing equipment and procedures, the latter location being formerly ABB Combustion Engineering. Data from the Windsor site were tested at slower pressurization rates based on the discussion of Section 3.2.2.

Table 5-1
Type 14 Specimen Predictions for Which SEM Profile Data Exists (Sorted by test rate, then maximum pressure)

Specimen Designation	Test Rate	Avg. Depth (%)	Max. Depth (%)	Ratio of Max. to Avg.	Effective Depth (%)	Effective Length (in.)	Measured Tear/Burst (psi)	Cochet Model (psi)	ANL Model (psi)
ANO-00-086	Slow	76	96	1.26	79.6	1.106	3325	3552	3496
ANO-00-068	Slow	71	95	1.34	81.2	0.681	3433	3824	3856
ANO-00-069	Slow	71	94	1.33	80.0	0.705	3755	3927	3994
ANO-00-083	Slow	66	95	1.43	81.8	0.542	3828	4050	4178
ANO-00-084	Slow	75	93	1.24	75.7	1.357	3872	3891	3871
ANO-00-085	Slow	69	95	1.39	79.1	0.673	4062	4086	4210
ANO-00-090	Slow	66	96	1.44	73.9	0.786	4385	4523	4717
ANO-00-074	Slow	66	91	1.37	75.6	0.762	4395	4358	4528
ANO-00-089	Slow	67	93	1.38	75.8	0.770	4399	4329	4488
ANO-00-076	Slow	67	92	1.36	76.9	0.685	4526	4322	4505
ANO-00-091	Slow	61	92	1.52	70.8	0.647	4950	5090	5423
ANO-00-070	Fast	66	92	1.39	76.6	0.659	4320	4397	4620
ANO-00-088	Fast	68	91	1.35	76.3	0.668	5070	4415	4626
ANO-00-087	Fast	70	95	1.35	79.5	0.773	5220	3882	3928
ANO-00-077	Fast	64	91	1.42	73.9	0.672	5600	4690	4944
ANO-00-075	Fast	62	89	1.42	72.8	0.612	5700	4917	5240

Note: Slow pressurization rate data are plotted on Figure 5-6 and the fast pressurization rate data are plotted on Figure 5-7. Specimen 070 was tested at a fast rate, but did not burst.

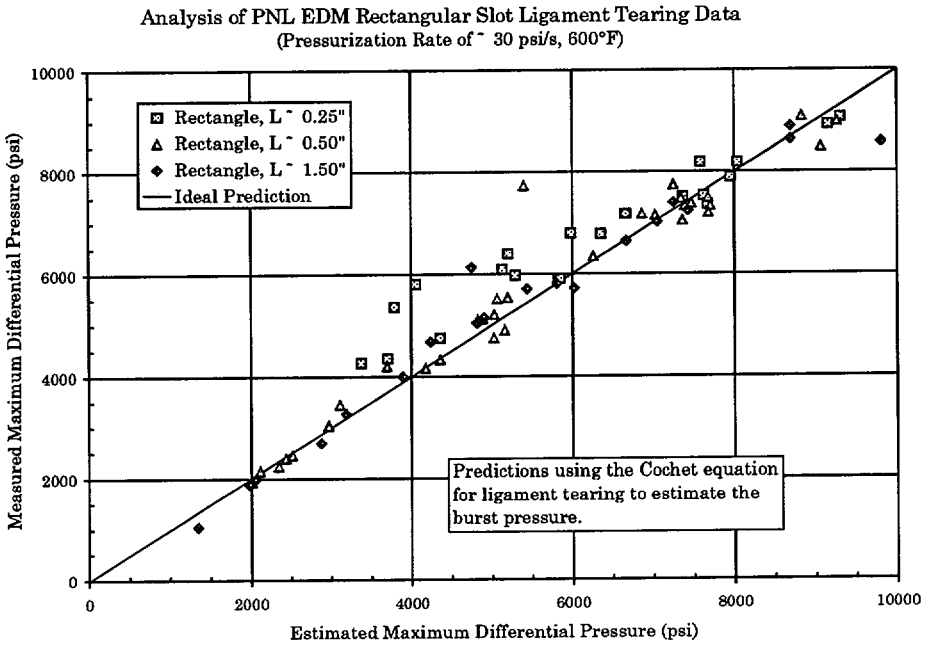

Figure 5-4
Burst Test Data for Rectangular EDM Slots, PNL Test Data, 600°F, 30 psi/s

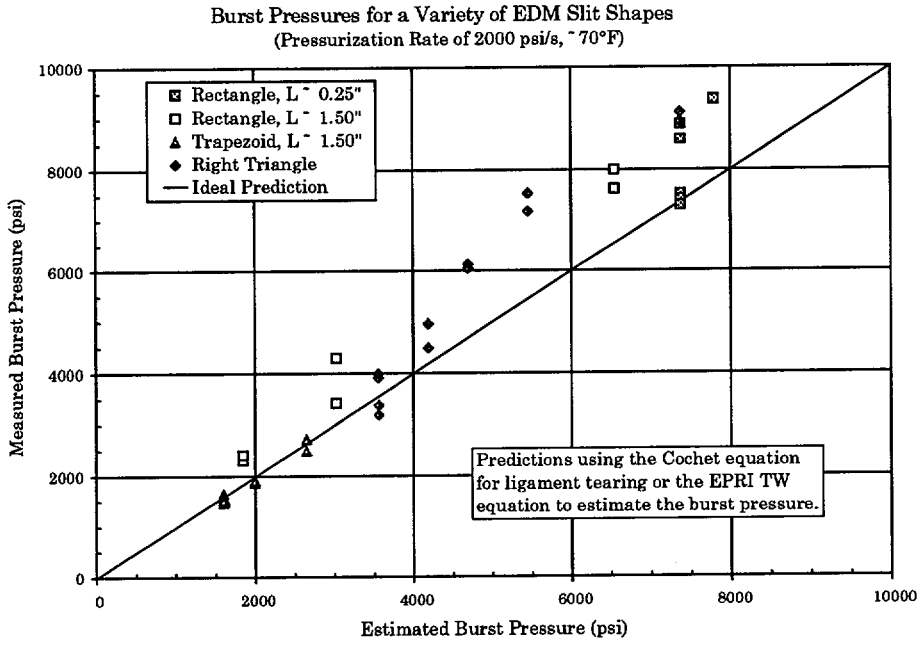

Figure 5-5
Burst Test Data for a variety of EDM Slot Shapes, Room Temperature, 2000 psi/s

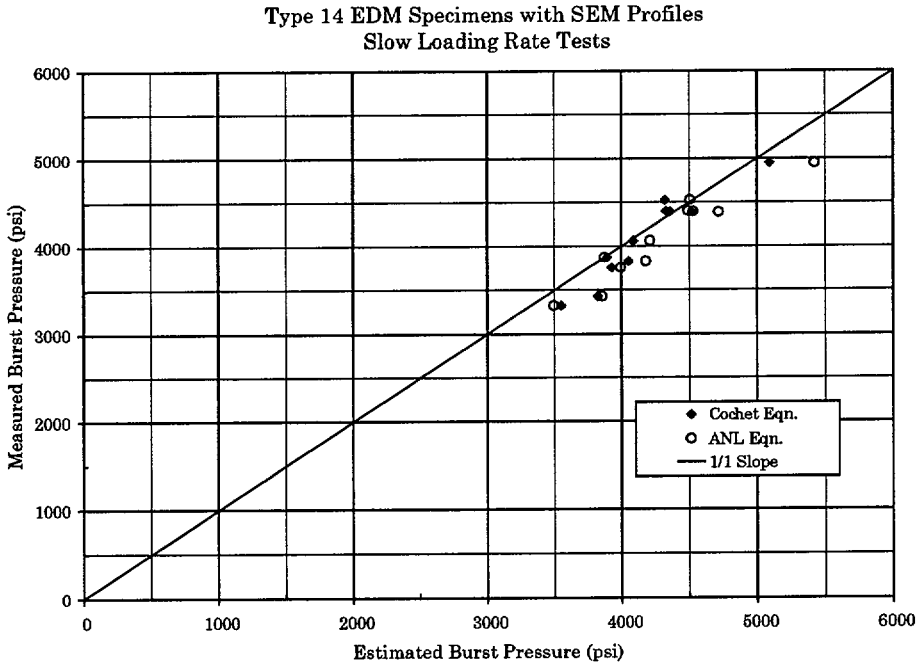

Figure 5-6
Slow Pressurization Rate Results for Type 14 EDM Specimens

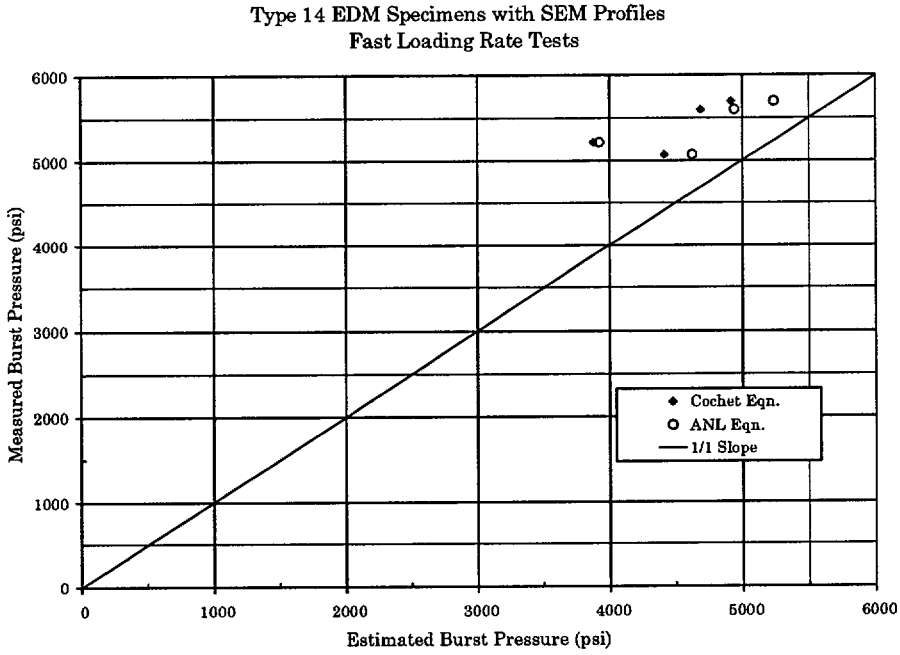

Figure 5-7
Fast Pressurization Rate Results for Type 14 EDM Specimens

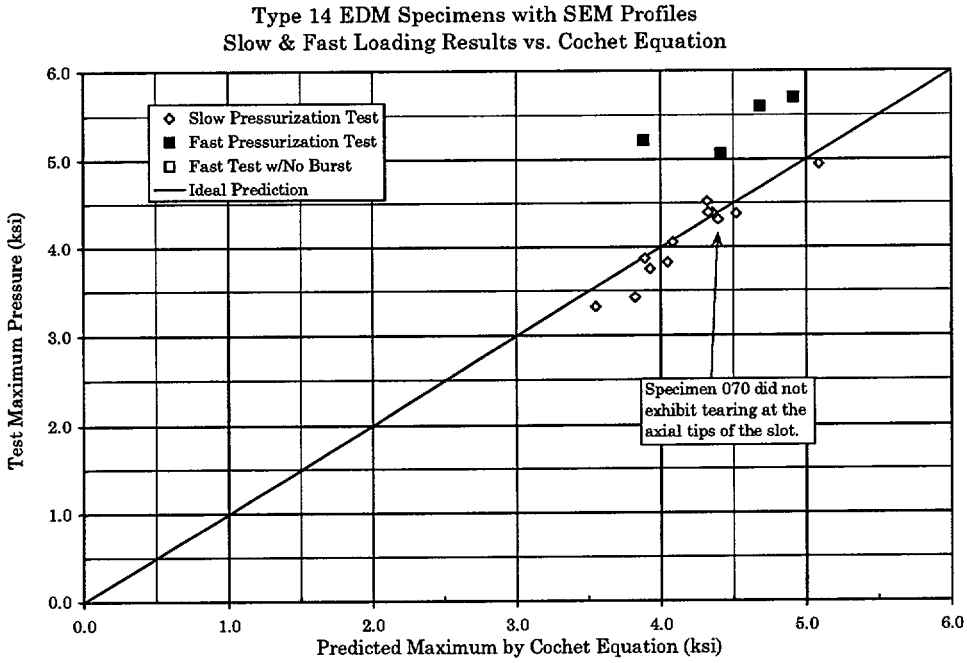

Figure 5-8
Comparison of Slow & Fast Rate Results for Type 14 Specimens

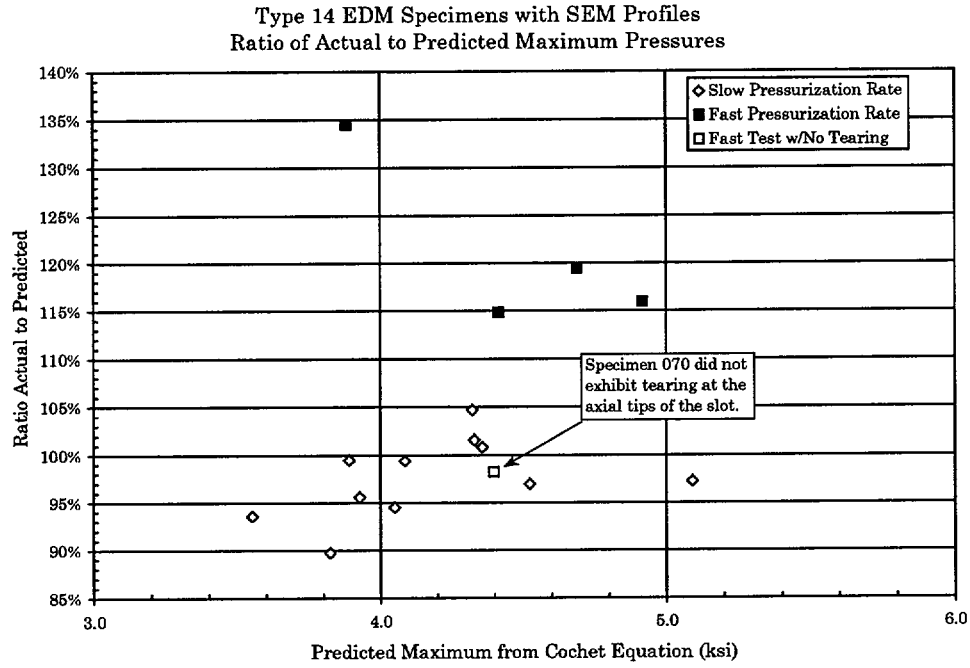

Figure 5-9
Ratio of Measured to Predicted Results for Type 14 Specimens

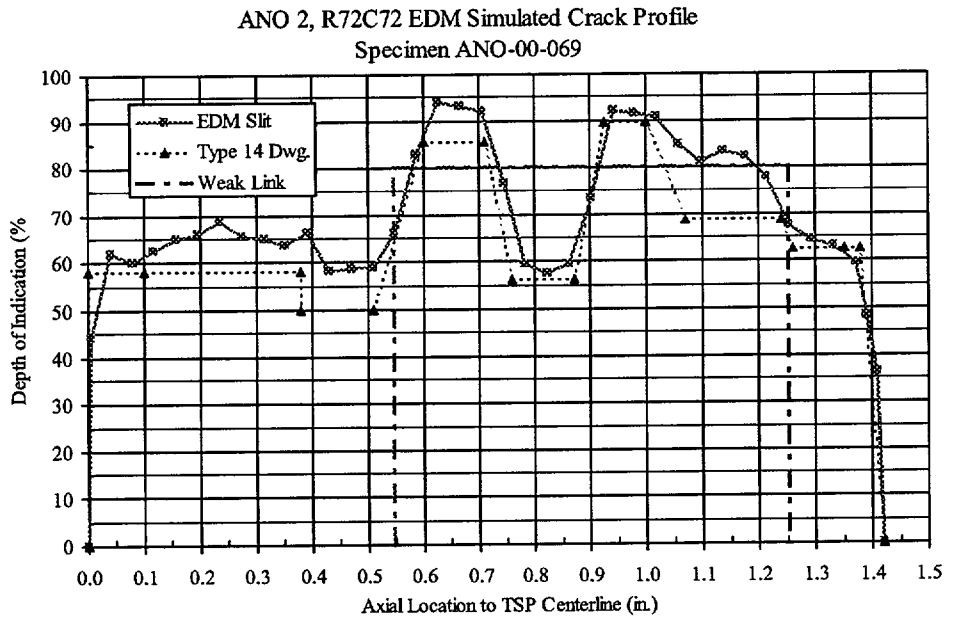

Figure 5-10
Structurally Significant or Weak Link Profile for a Type 14 Profile in Typical Agreement with the Drawing

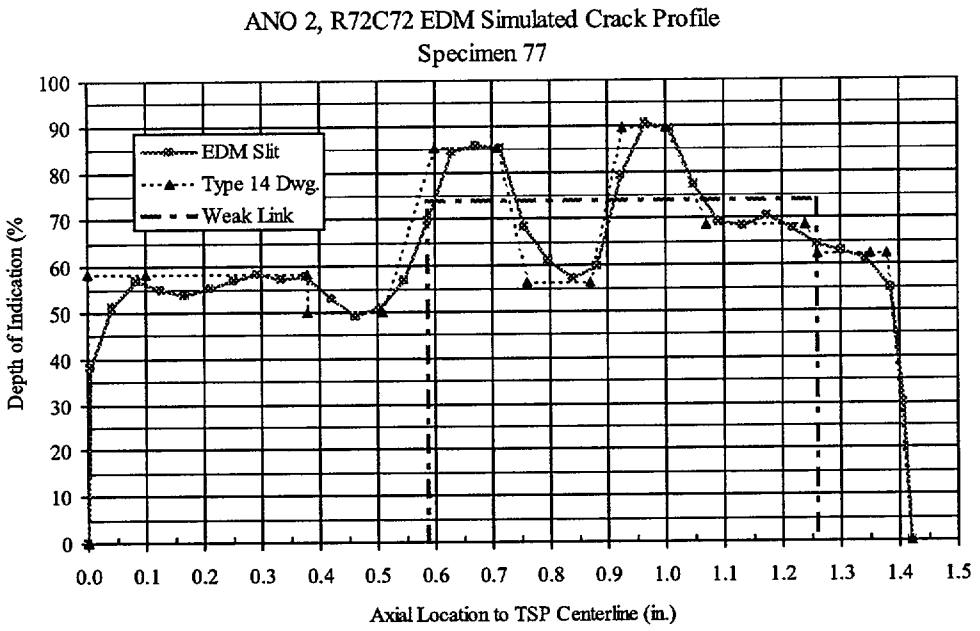

Figure 5-11
Structurally Significant or Weak Link Profile for a Type 14 Profile in Good Agreement with the Drawing

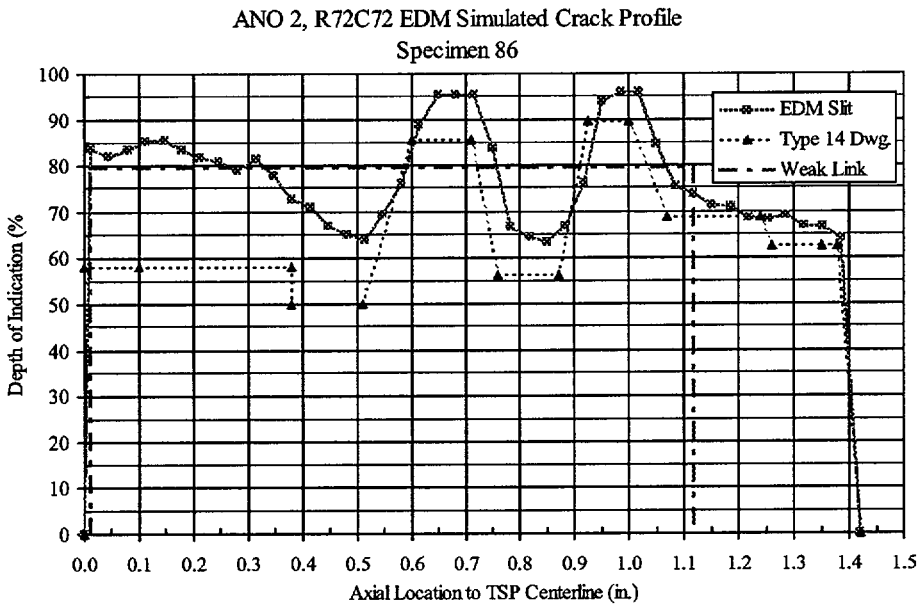

Figure 5-12
Structurally Significant or Weak Link Profile for a Type 14 Profile in Poor Agreement with the Drawing

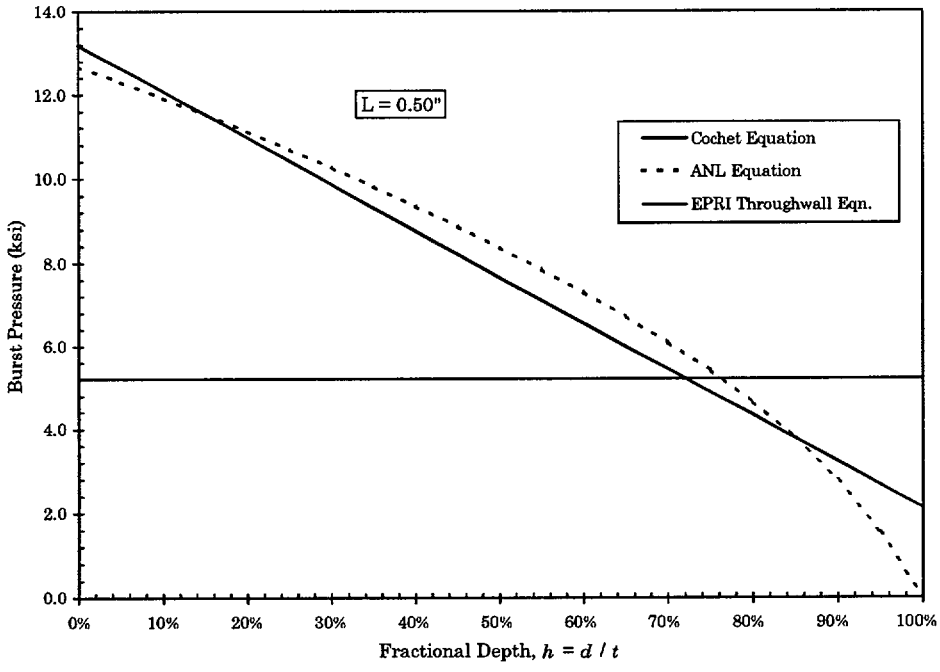

Figure 5-13
Comparison of Cochet and ANL Equations for a Crack Length of 0.5 Inch

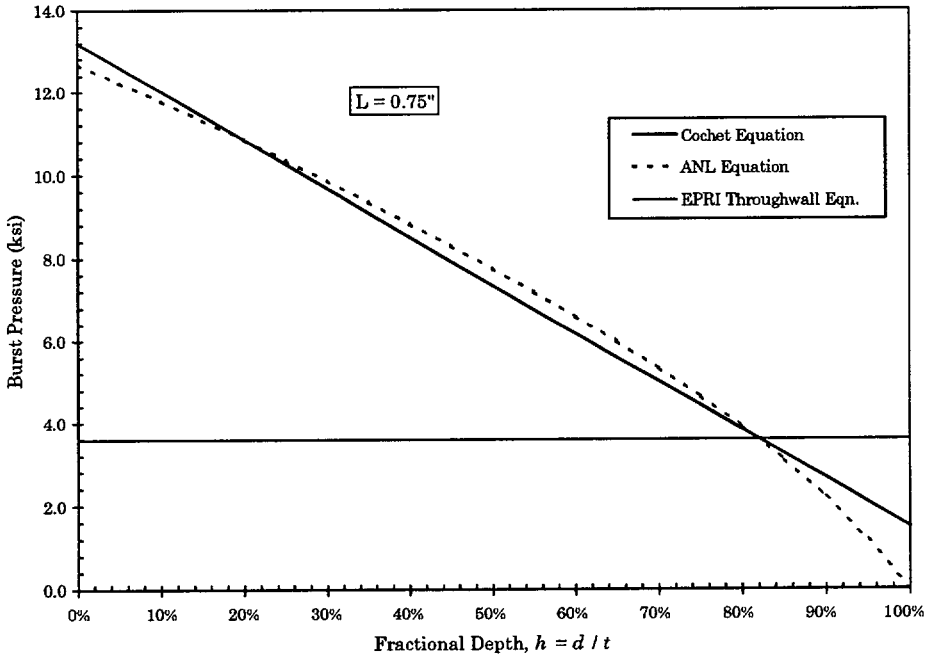

Figure 5-14
Comparison of Cochet and ANL Equations for a Crack Length of 0.75 inch

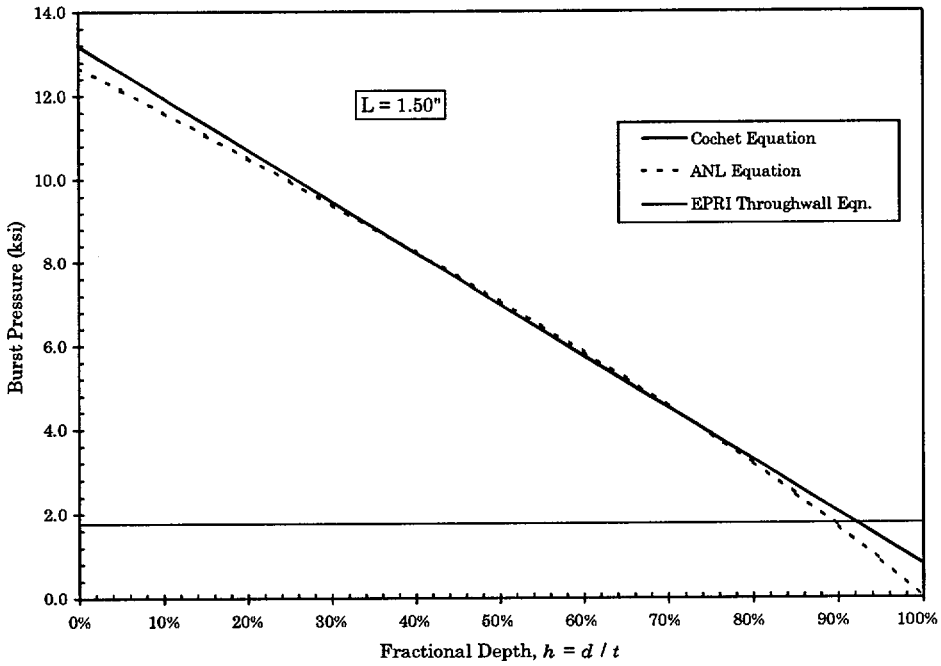

Figure 5-15
Comparison of Cochet and ANL Equations for a Crack Length of 1.5 inch

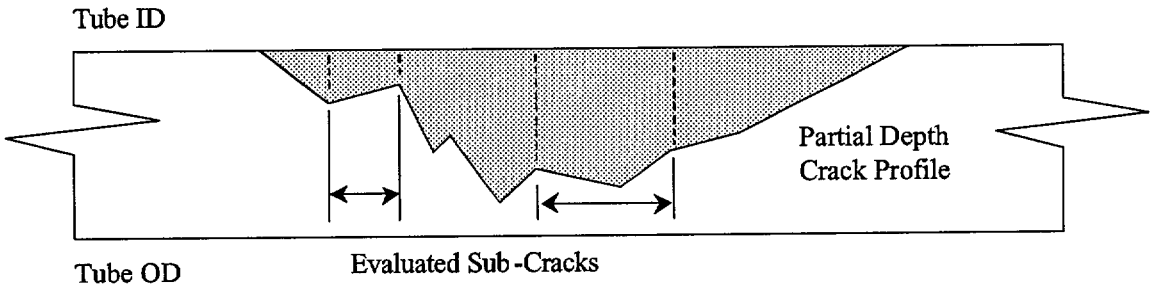

Figure 5-16
Representative Part-Throughwall Axial Crack Profile

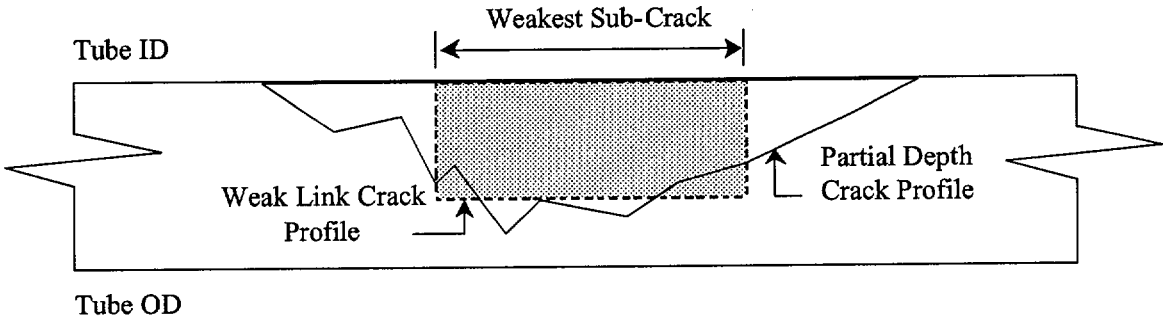

Figure 5-17
Representative Part-Throughwall Axial Crack Profile with the Effective Rectangular Profile Shown

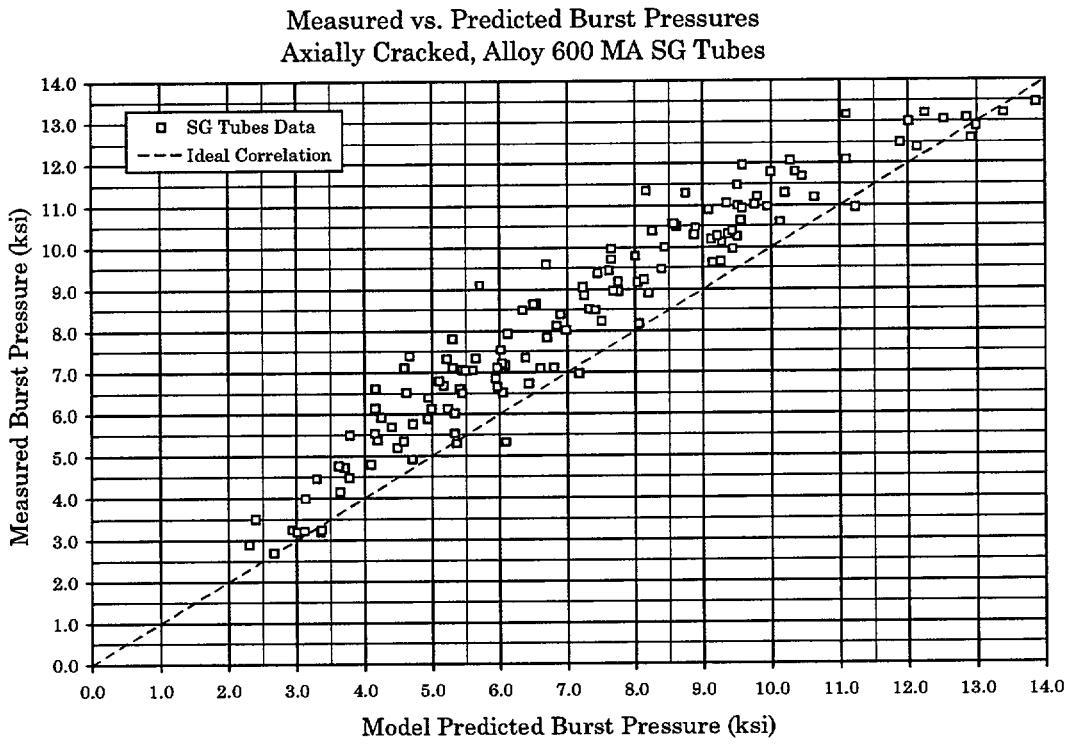

Figure 5-18
Measured vs. Model Burst Pressures for Axial SCC

5.1.3 Bobbin Voltage ARC, Drilled 3/4" Thick Tube Support Plates

Although ODSCC is also part-throughwall cracking, it has been treated separately because of the nature of the degradation and its location, and the fact that the burst pressure has been correlated to the voltage amplitude from a bobbin coil eddy current examination. Burst tests of model boiler and pulled tube specimens were, and may continue to be, performed at several different laboratories in at least three countries, the United States, Belgium and France. Although the testing procedures are different, the test results are similar. Tests performed in the US were typically performed at a rate of about 1500 to 2000 psi/s, while those in France were at a maximum of 500 psi/s and those in Belgium were most likely performed at a rates significantly less than 200 psi/s, see Reference 1 and the discussion of Section 3.2.5. This latter statement is supported by the testing rate reported for throughwall degradation, see Figure 5-1.

The ODSCC voltage limits are 1.0 and 2.0 V for plants with 3/4" and 7/8" diameter tubes respectively. The comparison data for the burst resistance of tubes subject to the ARC is illustrated on Figures 5-19 and 5-20 for 3/4" and 7/8" diameter tubes respectively. Statistical testing of the data is summarized in Tables 5-2 and 5–3. The comparisons are based on standard statistical tests wherein a series of regression models are fit to the data independently and combined. Four models are considered to compare the data as follows:

1. General Model — The data are representative of populations for which both the intercept and slope of the regression lines are different. Four coefficients, two intercepts and two slopes, are obtained from the regression analysis of the data for this model.

2. Parallel Model — The data are representative of populations for which the intercepts are different, but the slopes are the same. Three coefficients, two intercepts and one slope, are obtained from the regression analysis of the data.

3. Concurrent Model — The data are representative of populations for which the intercepts are the same, but the slopes are different. Three coefficients, one intercept and two slopes, are obtained from the regression analysis of the data.

4. Coincident Model — The data are representative of the same population, so the intercepts and the slopes are the same. Two coefficients, one intercept and one slope are obtained from the regression analysis of the data for this model.

The first model is the most flexible in terms of trying to accommodate the variations in the data and results in the smallest value of the residual or error sum of squares (RSS). The fourth model is the most stringent and results in the largest value of the RSS. Models two and three result in RSS values that are less than that of Model 4 and greater than the value from Model 1. A series of general *F*-tests are performed to determine if the improvement in reducing the RSS is statistically significant in changing from a more stringent model to a less stringent model, e.g., the significance of changing from Model 4 to Model 1. In other words, the results of the regression analyses are compared to determine the improvement in the residual sums of squares by adding terms to the model. For example, if all of the data are treated together, Model 4, the regression model of the burst pressure, P_B, as a function of the bobbin amplitude, V, in Volts is given as,

$$P_B = b_0 + b_1 \log(V) \qquad \textbf{Equation 5-8}$$

where b_0 and b_1 are coefficients determined from the regression analysis.

The results from the statistical tests are summarized in Tables 5-2 and 5–3 for 3/4" and 7/8" diameter tubes respectively. The results from testing of pulled tube sections by Westinghouse and Laborelec were compared using the data from 3/4" diameter tubes [28]. The results are quite conclusive in indicating that there is no difference in results obtained from an analysis of the Laborelec data relative to results obtained from an analysis of the Westinghouse data. The table lists the test performed, the models compared, the RSS values calculated, the degrees of freedom of the models, the calculated *F*-test values, and the probability of exceeding those values. Test 2, for example, compares the use of Model 4 against the use of Model 1. The calculated value of *F* is 0.203 and the probability of obtaining a value of *F* greater than 0.203 if the null hypothesis that the intercepts and slopes are equal is true is 82%. The other comparisons all result in values of *F* that would be expected to occur randomly with a probability of greater than 50%. The conclusion that is indicated by the test results is that there is no difference between the set of data from testing performed by Laborelec and testing performed by Westinghouse. The conclusions from the analysis are also visibly apparent from an examination of the information presented on Figure 5-19 where the two regression lines are almost coincident. The Laborelec tests were

performed at a pressurization rate that is significantly less than the Westinghouse rate, see Figure 5-1 for an example of their laboratory practice, therefore implying that the rate of pressurization has no effect on the test results.

The results from the comparison of the Electricité de France (EdF) data and the Westinghouse data are listed in Table 5-3. The results of statistical comparisons of these sets of data were first reported to the NRC in 1996 [29]. The results at that time led to the recommendation that the EdF data be omitted from the ODSCC database. A significant factor leading to that recommendation was the observation that burst pressure predictions based on the EdF data appeared to have a systematic bias to be higher than those based on the Westinghouse data, i.e., the intercepts of the regression lines were indicated to be significantly different. No significant difference in the slopes of the two regression equations was found. Efforts aimed at identifying the cause of the observation did not lead to any meaningful conclusions and the recommendation was not concurred with by the NRC staff. Because of the addition of data subsequent to the 1996 evaluation, the comparisons were repeated for this evaluation. The results are depicted graphically on Figure 5-20 and presented numerically in Table 5-3. The results are similar to the 1996 findings in that no difference in the slope is implied, but a significant difference in the intercept is implied. A comparison of Model 1 (different intercepts and slopes) against Model 4 (same intercept and slope) indicates a significant difference in the RSS obtained from the regression analyses. Further comparisons of Models 4 and 1 against Model 2 (different intercept and same slope) indicates that the results from the first comparison are due almost entirely to an implied difference in the intercept and no difference in the slope. In summary, the models are strongly indicated to be parallel with no difference in the slopes. The EdF pressurization rate is significantly less than the Westinghouse pressurization rate, hence the data indicate no dependence of measured burst pressure on the pressurization rate.

There was no indication of any significant difference when the variances of the prediction errors from each of the models being evaluated for each tube size were compared. For the 3/4" diameter tubes, the standard deviations of the regression residual burst pressures were 0.85 and 0.92 ksi for the US and Belgian data respectively. The variance ratio is then 1.2 which corresponds to performing a two-sided F-test at a confidence level of only 33%. The critical value of F at a 95% confidence level would be 2.2. Thus, there is no implication that a null hypothesis of equal variances should be rejected. For the 7/8" diameter tube data, the variance ratio is 1.3 based on regression residual standard deviations of 0.93 and 0.81 ksi for the US and French data respectively. The variance ratio corresponds to performing a two-sided F-test at a confidence level of 49%. The critical value of F at a 95% confidence level would be 2.2. Again, no implication that a null hypothesis of equal variances should be rejected. For the analysis of the 3/4" diameter tubes, the standard deviation of the residuals of the US data was slightly larger than that of the Belgian data. For the analysis of the 7/8" diameter tubes, the situation was reversed relative to the French data. Hence, there was no consistent difference between the values obtained from the more rapid pressurization rates relative to the slower pressurization rates.

Ancillary information is also available to support the conclusions reached in the preceding paragraphs. Leak rate tests which involved significant hold times were performed at a differential pressure of 3000 psi and at a temperature of 600°F without observing any time-dependent effects [28]. Finally, it is also noted that the average burst pressure for tubes with ODSCC indications is about 7000 psi regardless of the size of the tubing [28]. The average burst pressure for 3/4"

diameter tubes at 1 V is a little over 7000 psi while the average for 7/8" diameter tubes at 2 V is a little less than 7000 psi. This result is to be compared to an imposed pressure during a postulated SLB event of about 2560 psi with a criterion value of about 3600 psi. Therefore, the margin to tube burst during postulated accident conditions is adequate for both tube sizes.

In conclusion, there is no systematic effect of the pressurization rate on the burst pressure to voltage correlations, either the slope or the intercept or the standard deviation of the regression residual values, over the range of interest of application of the ARC, which is bracketed by the data.

Table 5-2
Comparison of Burst Testing of 3/4" Diameter Tubes

Model Testing	Model	RSS	DoF	Test Description & Results
Test 1				
Null Hypothesis:	4	40.1868	62	Same intercept, same slope.
Alt. Hypothesis:	2	40.1307	61	Different intercept, same slope.
Significance:	F / Pr(>F)	0.085	77.1%	**Different intercept NOT indicated.**
Test 2				
Null Hypothesis:	4	40.1868	62	Same intercept, same slope.
Alt. Hypothesis:	1	39.9164	60	Different intercept, different slope.
Significance:	F / Pr(>F)	0.203	81.7%	**Differences NOT indicated.**
Test 3				
Null Hypothesis:	4	40.1868	62	Same intercept, same slope.
Alt. Hypothesis:	3	39.9453	61	Same intercept, different slope.
Significance:	F / Pr(>F)	0.369	54.6%	**Different slope NOT indicated.**
Test 4				
Null Hypothesis:	2	40.1307	61	Different intercept, same slope.
Alt. Hypothesis:	1	39.9164	60	Different intercept, different slope.
Significance:	F / Pr(>F)	0.322	57.3%	**Different slope NOT indicated.**

Table 5-3
Comparison of Burst Testing of 7/8" Diameter Tubes

Model Testing	Model	RSS	DoF	Test Description & Results
Test 1				
Null Hypothesis:	4	65.8347	77	Same intercept, same slope.
Alt. Hypothesis:	2	60.1002	76	Different intercept, same slope.
Significance:	F / Pr(>F)	7.252	0.9%	**Different intercept is very likely.**
Test 2	Model	RSS	DoF	
Null Hypothesis:	4	65.8347	77	Same intercept, same slope.
Alt. Hypothesis:	1	60.0955	75	Different intercept, different slope.
Significance:	F / Pr(>F)	3.581	3.3%	**Reject Null Hypothesis.**
Test 3	Model	RSS	DoF	
Null Hypothesis:	4	65.8347	77	Same intercept, same slope.
Alt. Hypothesis:	3	62.5959	76	Same intercept, different slope.
Significance:	F / Pr(>F)	3.932	5.1%	**Null Hyp. NOT rejected.**
Test 4	Model	RSS	DoF	
Null Hypothesis:	2	60.1002	76	Different intercept, same slope.
Alt. Hypothesis:	1	60.0955	75	Different intercept, different slope.
Significance:	F / Pr(>F)	0.006	93.9%	**Different slope NOT likely!**

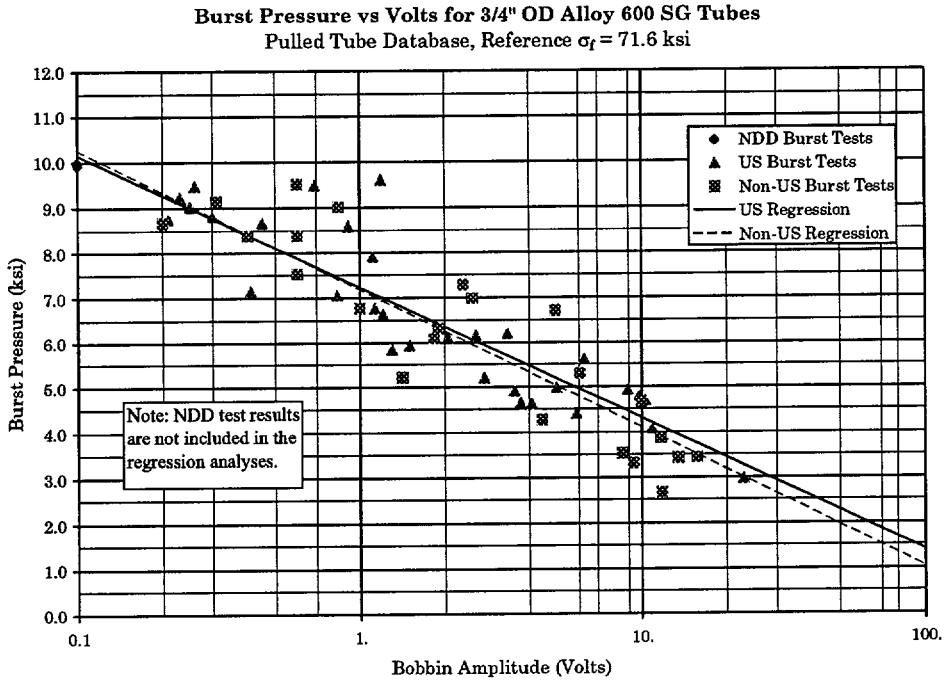

Figure 5-19
ODSCC ARC Data for 3/4" Diameter Tubes

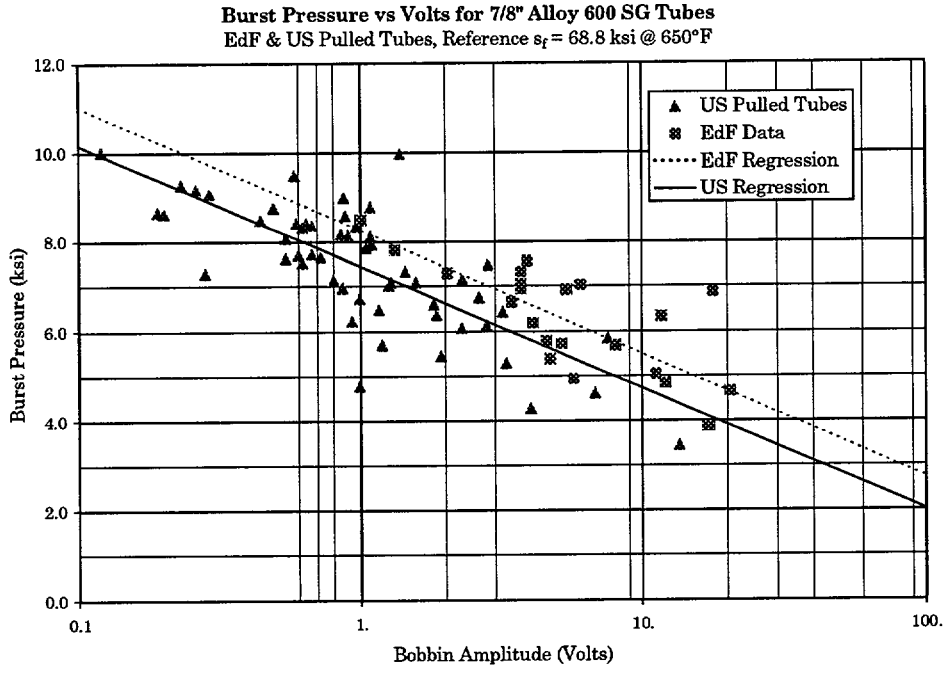

Figure 5-20
ODSCC ARC Data for 7/8" diameter tubes

5.2 Circumferential Cracking

5.2.1 Circumferential Cracking with Limited Lateral Tube Motion

Because of geometry constraints, there is much less bulging of the flanks of circumferential cracks during the bursting process than there is with axial cracks. This means that the stress intensity magnification factor that plays such a significant role in the evaluation of axial cracks is on no practical import relative to circumferential cracks. In addition, the axial load applicable to circumferential cracks is 50% of the hoop load applicable to axial cracks. The post-test geometry of tubes with axial cracks is typified by a "fishmouth" shaped opening at the burst site that is the result of sever deformation of the crack flanks. The flanks of circumferential cracks are curved and are, therefore, significantly stiffer in the radial direction than the flanks of axial cracks. This means that the strain concentration effect that is practically characterized by the stress intensity factor magnification factor for modeling the burst pressure of tubes with axial cracks is not present for modeling the burst pressure of tubes with circumferential cracks. The net result is that the burst pressure of tubes with circumferential cracks should be much less susceptible to rate effects than that of tubes with axial cracks.

The development of the empirical model for predicting for the burst pressure of tubes with circumferential cracks is documented in Reference 36. The burst testing of tube specimens with circumferential cracks was carried out by Westinghouse using the EPRI burst testing guidelines [10]. The pressurization rate of the specimens was likely in the range of 1500 to 2000 psi/s. The empirical model is presented on Figures 5-21 and 5-22. The normalized burst pressure, P_N, is calculated as,

$$P_N = \frac{P_B R_m}{(S_y + S_u)t} \qquad \textbf{Equation 5-9}$$

where P_B is the measured burst pressure, R_m is the mean radius of the tube, t is the thickness of the tube, and S_y and S_u are the yield and ultimate tensile stress of the tube material. The information presented on the two figures leads to an estimate of the maximum crack length for avoiding onset of crack extension during a design basis accident, steamline break, of about 310 to 320°. A purely theoretical solution from one of the national laboratories [37] is 315°. A similar calculation considering a normal operating pressure differential in a tube with a mean radius to thickness ratio of 8.25 and a mean yield plus ultimate stress of 136 ksi leads to an estimate of a maximum crack length of 338°. The reference 37 result is 340°. The theoretical results are irrespective of rate effects and are in concert with the test results, supporting the argument that the effect of the pressurization rate on the measured burst pressure of a tube with circumferential cracking is not significant.

The burst pressure relationship for circumferential cracks is conservative in the sense that all of the degraded area is assumed to reside in a single 100% TW circumferential crack. Although lateral motion is restricted, a bending effect is still present albeit much reduced from the free bending condition. Hence, the burst curves in Figures 5-21 and 5-22 account for a worst case morphology and the associated worst case bending effect. The lower data points which determine

the burst curve are for specimens with 100% TW EDM slots where the slot tips reside in full thickness material. From the axial crack case it is known that no pressurization rate occurs for crack tips in full wall thickness material.

The conclusion from these above considerations is clear, i.e., that there was no pressurization rate effect on the results of tests performed to measure the burst pressure of SG tubes with circumferential cracks.

Tearing of deep circumferential cracks in the throughwall direction is an issue for leakage evaluations of circumferential cracks. Because circumferential cracks are subject to a lower bulging effect than axial cracks and generally lower stresses at SLB conditions only extremely deep circumferential crack sections may experience a pressurization rate effect on ligament tearing in the depth direction. Ligament tearing in the depth direction for circumferential cracks as part of leakage evaluations is an under developed area. There is no generally available test data to consider. Both the Cochet and ANL equations can be adapted from axial cracks to circumferential cracks. As in the axial crack case, the ANL ligament tearing equation will provide the most conservation ligament tearing predictions.

Figure 6-10: TW, Single Slit Circumferential Burst vs. PDA
New Data for 3/4" x 0.043" Nominal, Alloy 600 SG Tubes

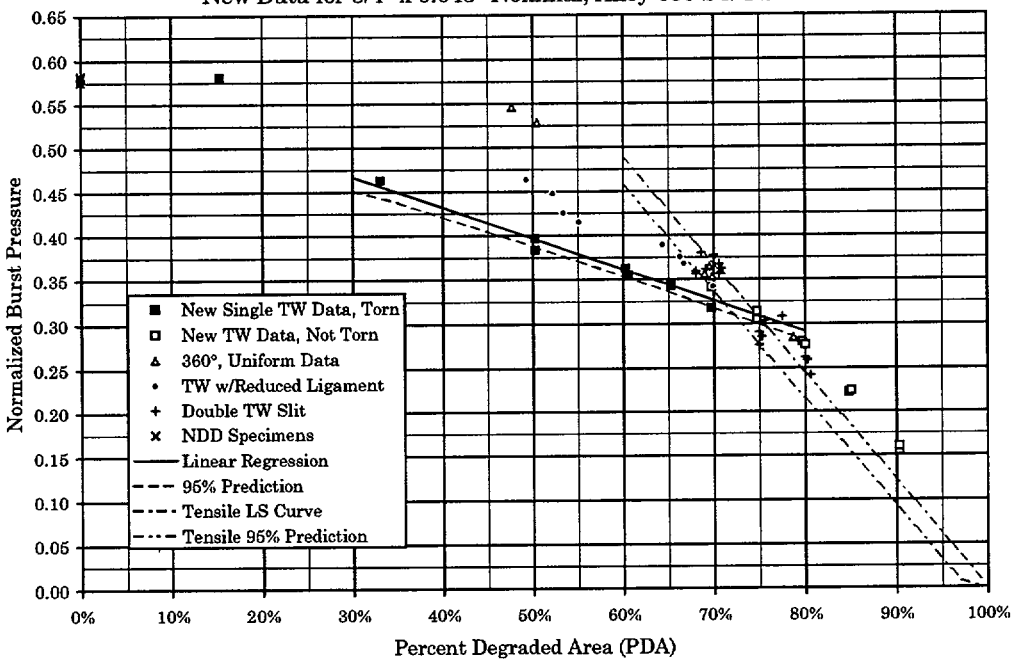

Figure 5-21
Circumferential model for burst

Figure 6-17: TW, Single Slit Circumferential Burst vs. PDA
New Data for 3/4" x 0.043" Nominal, Alloy 600 SG Tubes

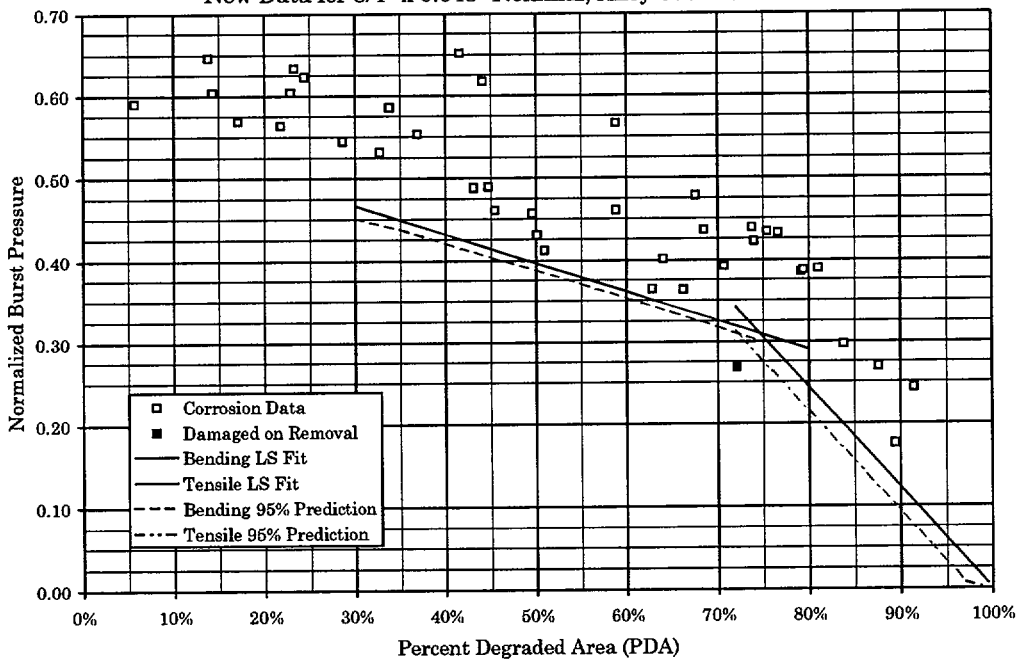

Figure 5-22
Circumferential model relative to pulled tube data

5.3 Volumetric Degradation

The burst pressure of tubes with volumetric degradation depends only on the global tensile properties of the tubing material. Limited amounts of time dependent deformation will not influence the burst pressure even for extreme degradation geometries. From Section 4 it is seen that pressurization rates differing by two orders of magnitude produce changes in tensile flow curves that are essentially within the specimen to specimen scatter. The potential effect of the pressurization rate on burst tests involving volumetric degradation is clearly not an issue.

5.4 Summary Keyed to EPRI Flaw Handbook Category

The following paragraphs summarize conclusions and open issues based on a review of tube integrity evaluation methods and the impact and significance of the slow pressurization test results in Section 2. These conclusion and open issues are arranged by the order of degradation evaluation models in the EPRI Steam Generator Tubing Flaw Handbook.

5.4.1 Freespan Throughwall Axial Cracking

An extensive database [12], subjected to thorough reviews and resolutions of sealing bladder issues, shows that the burst pressure of throughwall cracks in full thickness material is not

pressurization rate dependent from 20 psi/s to 2000 psi/s. If the tube material were strain-rate sensitive, then some effect might be apparent, however, that is not the case and it is concluded that the database for tubes with throughwall axial cracks is unaffected.

The burst pressure of throughwall cracks wherein the crack tips reside is less than full wall thickness material is not an issue because current analysis techniques do not account for the strengthening effect of the full thickness of the tubing at the ends of the crack or would treat the crack as being throughwall over its entire length. This type of crack profile an potential refinements of the evaluation model are discussed further in Section 7.7.

5.4.2 Expansion Transition Axial Cracking

Expansion transition axial cracking results will be identical to the axial throughwall and partial throughwall discussed in Sections 5.4.1 and 5.4.4.

5.4.3 U-bend, Freespan Axial Throughwall Cracking

U-bend, freespan axial cracking results will be identical to the axial throughwall and partial throughwall discussed in Sections 5.4.1 and 5.4.4.

5.4.4 Axial Partial Throughwall Cracking

Crack profiles with maximum depths on the order of 95% TW will exhibit a definite rate effect on burst pressure. However, the standard industry method, of evaluating results is sufficiently conservative to provide a very good description of both ligament tearing and burst pressures. Although, the test data for depths near 95% TW at conventional rates of loading is subject to a large amount of scatter. Instead of focusing on detailed test specimen characterizations, a more conservative analysis technique, such as the ANL equation for predicting the ligament tearing pressure for axial cracks may be useful. However, the ANL equation for ligament tearing extrapolates to zero pressure as the crack depth increases to 100% TW. The Cochet equation extrapolates to a very conservative throughwall burst pressure equation as depth increases to 100% TW. Since the ANL equation extrapolates to zero pressure, if any section of a crack profile is 100% TW, the ANL equation does not provide any estimate of burst pressure; the answer is always zero. In contrast, the Cochet equation provides a conservative burst pressure for crack profiles with throughwall portions. As discussed in Sections 5.4.4 and 5.4.7, improved methods of burst pressure calculation are needed for crack profiles with 100% TW portions. The Cochet equation provides conservative burst pressure predictions but, in many cases, these predictions are unduly conservative.

5.4.5 Effective or Structural Depth and Effective Length for Axial Cracks

There is no test data invalidating the equivalent rectangle approach and use of the Cochet equation in characterizing the burst strength of partial throughwall axial cracks of arbitrary profile.

5.4.6 Bobbin Voltage ARC, Drilled 3/4' Thick Tube Support Plates

A careful examination of the database supporting a bobbin voltage ARC approach shows that any pressurization rate effects on burst pressure do not influence the results of the basic methodology. No modifications are required.

5.4.7 Circumferential Cracking With Restricted Lateral Motion

There is no pressurization rate effect on of tests performed to measure the burst pressure of SG tubes with circumferential cracks. Tearing of deep circumferential cracks in the throughwall direction is an issue for leakage evaluations of circumferential cracks. Because circumferential cracks are subject to a lower bulging effect than axial cracks and generally lower stresses at SLB conditions, only extremely deep circumferential crack sections may experience a pressurization rate effect on ligament tearing in the depth direction. There is no generally available test data to consider. Ligament tearing in the depth direction for circumferential cracks as part of leakage evaluations is an under developed area.

5.4.8 Uniform 360° Thinning

Pressurization rates effects on burst tests involving volumetric degradation are clearly not an issue.

5.4.9 Uniform 360° Thinning Over a Given Axial Length

Refer to uniform 360° thinning.

5.4.10 Axial Thinning with Limited Circumferential Extent

Refer to uniform 360° thinning.

5.4.11 Circumferential Thinning with Limited Axial Extent

Refer to uniform 360° thinning.

5.4.12 Pitting

EPRI Flaw Handbook solutions for pitting deal with leakage rather than burst pressure. Pressurization rate effects may be present for very deep pits. The large leak case is based on global tensile properties and should not be effected by pressurization rate effects. The axial crack limiting case is covered by the conservatism in the Cochet ligament tearing equation. The circumferential crack limiting case for tearing is based on theory and not experiment. The loading conditions for the onset of leakage from pit like degradation, although not necessarily of structural significance, is an area that needs to be more fully developed analytically and supported by test data.

6
IN SITU TEST EXPERIENCES

In situ leak and pressure testing of SG tubes has been commonplace since about 1992. The tests are typically performed to verify leak resistance at differential pressures associated with postulated plant accident conditions, e.g., main steam line break (SLB), and burst resistance at pressures corresponding to the structural criteria associated with demonstrating SG integrity, e.g., [39]. Testing is usually performed in accordance with an industry standard [38], initially developed by EPRI in 1998. There is anecdotal evidence from many tests that ligament tearing after a hold time is a rare event, if it has ever occurred at all.

Some information was gathered by a utility representative relative to the experiences of all of the domestic vendors, Westinghouse-Windsor (formerly ABB Combustion Engineering), Westinghouse, and Framatome Technologies Group. The results of the survey were as follows [40]:

- Westinghouse-Windsor — Based on one plant's in situ pressure test results for Unit 1 in 1999, tubes were tested to the normal operating differential pressure, the main steam line break pressure and three times the normal operating differential pressure. If leakage occurred at the main steam line break (MSLB) pressure, the pressure was held for five minutes before resuming. At each of these hold pressures, the pressure was held for two minutes in the localized test mode or five minutes in the full tube test mode. No information was provided on the pressurization rate.
- Westinghouse — The hold requirement for the leakage test is 5 minutes. The hold time for the proof test is 2 seconds. No guidance is available on the rate of pressurization.
- FTG — The field procedure does not specify hold times. The procedure states that "test pressures, axial loads, hold times, and sequences will be provided in the Task Deployment Letter (TDL). In addition, the tests should be consistent with EPRI Guidelines." So one would have to look at each TDL to actually verify the hold times.

The in situ test plan for tests conducted in 1999 specified "hold times for all locations are 2 minutes (no leakage) or 5 minutes (leakage) at all test pressures."

This vendor believes they have always held pressures for some finite period for any test they have ever done. More definitively, since the 1998 draft EPRI in situ guidelines, this vendor has followed EPRI guidance in section 5.2.3 and 5.2.4, which recommends two minute hold times for systems with real time feedback (which is the new system they have been using for the last 3 or 4 years).

There are certain features of the in situ testing process that should be common to both of the remaining domestic vendors to make it likely that the pressurization rate is slow. The tubes may

be tested either as a whole tube test or using tooling which restricts the length being tested, à la the use of a mandrel, in which case the volume being pressurized is small. The supply lines to the tube are likely to have a small inside diameter which means that a significant pressure drop may occur when the pressurizing water is pumped into the tube. If the test is a whole-tube test, the elastic deformation of the tube will increase the internal volume of the tube and restrict the rate of pressurization. If the tube is significantly degraded, elastic deformation in the vicinity of the degradation may restrict the pressurization rate. If the burst pressure is above the elastic limit of the tube, plastic deformation of the tube will limit the pressurization rate. If the tube is leaking slightly, the rate of pressurization will also be reduced.

Additional information obtained from the in situ test vendors is provided in the following paragraphs. The reader is reminded that the information reported here is subjective.

6.1 Westinghouse

Westinghouse has multiple in situ pressure testing systems because of the acquisition of the ABB Combustion Engineering (CE) nuclear organization in 2000. Thus, there are experiences from two different operating organizations. The following discussion is from the Westinghouse organization that was formerly Combustion Engineering and documents any known observations of a hold time effect during in situ pressure testing (ISPT) of flawed SG tubes. This organization is hereafter referred to as Westinghouse-Windsor to simplify the discussion. Other references to Westinghouse are with respect to the organization headquartered in Pittsburgh, Pennsylvania. The intent of the writing was to address the question of whether or not such an effect has been observed during testing of deep flaw indications in the field.

Westinghouse-Windsor has been conducting ISPT since 1992 and, to date, has conducted about forty (40) ISPT campaigns in at sixteen (16) different Westinghouse and CE designed plants [41]. More than four-hundred (400) tubes have been tested. The defects tested have included essentially all recognized defect types including PWSCC in tubesheet transitions, at supports and in U-bends; ODSCC in tubesheet crevices, in expansion transitions, at free span locations, and at tube supports: pits near the tubesheet; intergranular attack (IGA); volumetric indications; and wear at tube supports. The reported depths of these flaws have ranged from rather shallow to more than 95% throughwall. Since the objective of the testing was to demonstrate tube integrity, most of the flaws selected for testing would be characterized as being deep and/or long.

The Westinghouse-Windsor in situ pressure test system is similar to the laboratory burst test system. This system has the capability of conducting either localized tests (only a small section of the tube is pressurized or a full tube test. An air operated positive displacement pump provides pressurized de-ionized water to the tubes being tested. This system can supply 0.5 gpm of water at MSLB pressures. A high flow system for larger leaks can supply approximately 3.5 gpm at MSLB conditions.

The tools for localized testing were qualified to demonstrate that strains (axial and hoop) produced by the tools were identical to those in a capped tube hydro test. Pressure drop through the tubing and tools during leak tests are estimated based on qualification tests. If leak rates exceed the capabilities of the pump or accumulator in the high flow system, the burst strength of tubes can still be determined by positioning an integral bladder over the defect. Qualification test

of this feature demonstrated that the hoop and axial strains were the same as in a capped tube hydro test.

During ISPT, pressurization is manually controlled and occurs at a slow rate. The current guidelines do not specify a pressurization rate. Pressures are indicated by a pressure gage and by the output of a pressure transducer which goes to a computerized data acquisition system. The taps for the devices are about 12 inches downstream of the pump. A pressure versus time record for each specimen tested is obtained and maintained.

Each ISPT has designated hold points and times. Typically a tube is pressurized to an adjusted ΔP_{NO} (adjusted for temperature and locked tube effects, as applicable) and held for some time. The tube is then slowly pressurized to MSLB pressure and held for the designated time and then pressurized to $3 \cdot \Delta P_{NO}$ and held. Other hold points may be designated by the utility. Hold times in the over 400 tests that Westinghouse-Windsor has conducted to date has varied form as little as 30 seconds to over 20 minutes. The most commonly used hold times are 2 and 5 minutes. If leakage occurs, a leak rate test of up to 5 minutes duration is conducted. The duration is restricted by the amount of water in the reservoir. Leak rates are determined by the number of pump strokes over a given time period or, for the high flow system, a flow meter downstream of the accumulator.

The procedure that Westinghouse-Windsor has always followed has been to slowly pressurize (although a rate has not be specified) to a designated pressure and hold the pressure approximately constant for some specified period of time. Tubes are typically pressurized to the normal operating differential pressure (NODP), ΔP_{NO}, adjusted for temperature and locked tube effects, as applicable, and held at that pressure for a specified time to determine if leakage is occurring. If leakage is observed, a leak test of up to 5 minutes duration is performed; the available water in the ISPT system reservoir dictates the leak test time. This step is followed by slow pressurization to the main steam line break (SLB) differential pressure, P_{SLB}, which is also adjusted to account for temperature and locked tube effects, with a hold period for the same specified time to observe for leakage. A leak test of the same duration as at NODP is conducted. The tube is then pressurized to three times the NODP, again, adjusted to account for temperature and locked tube effects, to demonstrate structural integrity. The practice has been to hold for the same time as at the lower pressures so that each step in the procedure is consistent. Based on the desires and needs of the plant operator, testing may be conducted at other pressures such as 1.4 times the SLB pressure or at pressures beyond three times the NODP. Westinghouse-Windsor has tested a few tubes, most notably at Maine Yankee, at pressures at or slightly above 7,000 psi.

It is concluded that the Westinghouse-Windsor experience is sufficient to permit addressing the NRC staff concern about hold time effects. Interviews were conducted with the personnel who have conducted essentially all of the Westinghouse-Windsor ISPT since the original test. The specific question that was directed to these people was "are you aware of any tests where low or no leakage for several minutes was followed by a sudden increase in leakage that may have indicated a pop-through event (ligament tearing)?" Their response was no direct or hearsay knowledge of any such events related in their responses [41].

Going further, the pressure-time curves for approximately one-hundred (100) ISPT records were reviewed. These are contained in test reports to various utilities. There was not sufficient time to

locate and review all ISPT records that Westinghouse-Windsor has conducted. For the test results that were reviewed, some tubes of which had flaws with indicated depths up to 99% through-wall, there were no indications of an increase in leak rates after several minutes of holding at three times the NODP or any other pressure.

Finally, the same question was asked of the personnel who conducted most of the many burst and leak tests on pulled tube specimens that have been conducted in the Westinghouse-Windsor laboratories. The response was consistent with that from the people intimate with the field service experiences and with the review of the ISPT data. However, time did not permit the review of any pressure-time curves from the laboratory testing the pulled tube specimens. In conclusion, no support was found that would support the aforementioned NRC staff statement that there has been a hold time effect observed during ISPT.

The Westinghouse organization based in western Pennsylvania has been conducting in situ pressure tests (ISPT) since 1996, involving about ten (10) ISPT campaigns and testing of approximately two-hundred (200) tubes [42]. Like the Westinghouse-Windsor field campaigns, the defects tested have included essentially all recognized defect types including PWSCC in tubesheet transitions, at supports and in U-bends; ODSCC in tubesheet crevices, in expansion transitions, at free span locations, and at tube supports: pits near the tubesheet; intergranular attack (IGA); volumetric indications; and wear at tube supports. The reported depths of these flaws have ranged from rather shallow to more than 95% throughwall. Since the objective of the testing was to demonstrate tube integrity, most of the flaws selected for testing would be characterized as being deep and/or long.

The Westinghouse-Pittsburgh in situ pressure test system also has the capability of conducting either localized tests (only a small section of the tube is pressurized) or a full tube test. An air operated positive displacement closed loop controlled pump provides pressurized de-ionized water to the tubes being tested. This system can supply more than 2.0 gpm of water at pressures exceeding 5000 psi. The de-ionized water is a continuous supply which permits long leak test times that are not limited by a reservoir. The system contains three flow meters to cover a wide range of measurement. Pressure and flow measurements are displayed and can be recorded on a computer. The calibrated system measurement range is 0.0001 to about 2.5 gpm.

The tool for localized testing incorporates a sliding mechanism to produce strains (axial and hoop) as in a capped tube hydrostatic test. The pressure drop through the tubing and tools during leak tests are based on qualification testing and displayed real time on the computer to permit the operator to compensate accordingly. If leak rates exceed the capabilities of the pump, the burst strength of tubes can still be determined by positioning an integral bladder over the defect.

During ISPT, pressurization is manually controlled and occurs at a slow rate. Typically, the system is rapidly pressurized to 1200 psi. Above 1200 psi, the pressurization rate would generally not exceed 50 psi/s. Typically, the operator pressurizes at a slower rate to detect the first pressure at which a leak occurs. As the test pressure is approached, the pressurization is extremely slow so as to not overshoot the test pressure.

The minimum hold time for a leak test is 2 minutes provided there is no leakage. If leakage occurs, a leak rate test of 5 minutes minimum duration is conducted. The highest observed leak

rate during the 5 minute hold is used for record. With the real time flow meter, additional flow and pressure data points can be recorded between the desired test pressures.

Finally, there is no information from the Westinghouse personnel at either site to indicate that a hold time effect has been directly observed during ISPT.

6.2 Framatome Technologies [43]

Framatome Technologies Group (FTG) has been performing in situ pressure testing of steam generator tubes since 1993. FTG has tested several hundred tubes, at 25 different plants designed by Westinghouse, CE, and B&W. The defects tested include axial and circumferential SCC, pitting, wear, and various volumetric defects located everywhere from within the tubesheet through the U-bend.

The FTG in situ pressure testing system and probes have undergone significant design changes since 1993. The current system uses a positive displacement pump capable of supplying 4.5 gpm at pressures in excess of 6000 psi. Flow rates from 0.001 gpm through the pump's maximum capacity can be measured. The system maintains a computer record of pressure, time, and flow rate. Various probe designs allow testing of the entire tube or allow a section of the tube to be isolated and tested.

The test procedure has also undergone a number of significant changes. Since EPRI first prepared draft in situ guidelines, FTG has incorporated the recommendations into the test procedure. Key recommendations concerning test points (ΔP_{NO}, P_{SLB}, $3{\cdot}\Delta P_{NO}$) and test hold times (two or five minutes) have been used for the last several years. A number of reports documenting results obtained with previous systems were reviewed and hold times up to ten minutes have been used in the past. Pressures in excess of 6000 psi have been tested based on specific customer request.

The pressurization rate has never been specified or determined during Framatome's tests. However, the pressurization rate has always been low for several reasons:

- The pressure increase is manually controlled and the operators have always been trained not to exceed the designated test pressure. This insures that the pressurization rate is low overall and is usually even slower as the test pressure is reached. [This statement applies to all of the FTG test systems.]
- The operators are also trained to stop the pressure increase if a flow rate is displayed on the mid-range flow meter (>0.02 gpm). This requirement insures a low pressurization rate. [This example only applies to the current system, which has been in use for the last three years.]

A number of test reports were examined and field personnel were interviewed concerning the occurrence of a rapid leak rate increase or tube rupture during a test hold time. There were instances available where leakage was first observed during a test pressure hold time, but no evidence or recollection of a tube rupture during a period where constant pressure was being maintained.

7
ANALYSIS & DISCUSSION

The database of degraded tube burst test results and burst test practices have been described in the preceding sections. It is clear that recent burst test results demonstrate a loading rate and/or hold time effect on burst pressure measurements for a restricted set of test conditions and flaw geometry. It is not evidenced that a loading or hold time effect is evident in the very extensive database of previous burst test results. The following paragraphs describe an analysis of this seeming dichotomy and an explanation of the pressurization rate/hold time effect on the test results from the Type 14 specimens and a crack tearing stability issue of greater significance.

7.1 Time Dependent Deformation

As described earlier, tensile tests with hold times and strain rate changes demonstrated time dependent deformation in Alloy 600 at room temperature. However, a strain rate change by a factor of 25 only changed the flow stress by 2.5 %. This data determines the strain rate sensitivity exponent where the flow strength is taken as proportional to the strain rate to some power [44]. The strain rate sensitivity exponent is 0.008. Alloy 600 has a very low strain rate sensitivity. In a similar vein, hold times at a wide range of strain levels showed only about a 4 % stress relaxation. This stress relaxation and associated time dependent deformation was essentially complete in less than one to two minutes. Strain rate sensitivity and time dependent deformation effects are present in Alloy 600, but these effects are very small. This statement holds true at steam generator operating temperatures, as illustrated by the data presented in Section 4.

The observed rate effect on Type 14 specimen burst pressures cannot be explained as simply a difference in the global tensile properties resulting from the loading rate. If this were true, the ratio of slow to fast burst pressures would be equal to the ratio of slow to fast tensile flow strengths. The ratio of average burst pressure for the slow tests to that for the fast tests was 0.76. The strain rate sensitivity exponent for Alloy 600 would then require the time for the slow rate tests to vary from that for the fast rate tests by 15 orders of magnitude. The actual time difference between the slow and fast rate tests is between 3 and 4 orders of magnitude. This could be expected to lead to an increase in the flow strength of the ligament material on the order of 4 to 6%, with a lesser effect on the burst pressure. In summary, the observed rate effect cannot be explained as being due to the influence of the rate on the tensile properties of the tube material.

7.2 Rate Effect Evaluation of Industry Burst Database

Past and present tensile test data point to essentially negligible rate effects on the burst pressure of degraded Alloy 600 tubing. An evaluation of the industry burst pressure database supports this expectation. The most direct comparison of slow and fast loading rates on burst pressure

available from the previous industry database is provided by burst tests on 100% TW cracks, see Section 5.1.1. Fast or conventional tests, taken as 200 to 2000 psi/second, yield the same burst pressure versus crack length curve as the slow rate, nearly quasi-static tests conducted at Schelle [12], which were on the order of 10 psi/s near the end of the test. Clearly there is no loading rate effects on the burst pressure of tubes with 100% TW cracks. Note that in these tests the crack tips resided in full thickness material.

In a less direct comparison, high temperature tests of tubes with axial EDM slots at 30 psi/second [18] agree with calculated results in about the same manner as a variety of fast, 200 to 2000 psi/second, tests of EDM slotted specimens at room temperature. Again no loading rate effect is evident, Section 5.1.2. The same conclusion was reached in examining burst test data in the bobbin voltage ARC database, Section 5.1.3.

7.3 Conditions needed for the Onset of Loading Rate Effects

Burst test results that are only dependent on global tensile properties should not exhibit and have not exhibited any significant effect of loading rate on burst pressure. A small amount of time dependent deformation and associated stress relaxation occurs in Alloy 600 at low temperatures. This is supported by tensile data at room temperature and 600°F. Low temperature time dependent deformation is not an unusual phenomena and does not occur via the mechanisms usually considered in high temperature creep deformation. A loading rate/hold time effect on the burst pressure of Alloy 600 tubing will occur only in those circumstances where a small amount of time dependent deformation is crucial.

For Alloy 600 tubing, there is a limited set of special circumstances where the absolute extent of deformation and not just the tensile flow curve determines the burst pressure. As described below, long and very deep, axial partial throughwall cracks provides the circumstances where a small amount of time dependent deformation is crucial and some degree of a loading rate/hold time effect on burst pressure should be observed. But, first the process of bursting of Alloy 600 tubes with axial cracks needs to be described

Bursting of Alloy 600 tubes with axial partial throughwall flaws is a two step process. As the pressure increases, the crack first propagates radially through the wall thickness. For a burst to occur, the crack must then propagate along the axis of the tube. Depending on the crack morphology, a substantial increase in pressure may be required to propagate the crack in the axial direction. For some crack geometries, the limiting step is propagation through the wall thickness and once this occurs, propagation down the tube axis could continue at some reduced pressure. Crack propagation through the wall thickness is commonly termed ligament tearing. In summary, ligament tearing triggers a full tube burst for some geometries while ligament tearing just creates some degree of throughwall cracking for other crack geometries and burst will only occur at some higher pressure. In general, ligament tearing triggers burst for long, relatively shallow cracks while deep, short cracks may experience ligament tearing well below the final burst pressure.

Different degrees of plastic deformation are required for radial ligament tearing of part-throughwall cracks versus propagation of the crack (tearing) along the axis of the tube. For a 100% TW crack in a full thickness tube wall, the fracture toughness in terms of crack tip opening

displacement is about 0.040 inches. A crack tip must blunt this amount before the onset of tearing down the axis of the tube. This corresponds to a J integral toughness level near 3000 in-lbs/in^2. This is typically sufficient to ensure that plastic collapse, that is, general yielding, will occur before crack tearing develops. Plastic hinges form, creating crack mouth bulging and allowing the crack tip to blunt. The pressure needed to cause the formation of plastic hinges depends on the global tensile properties (and crack length). Hence a small rate/hold time effect on the tensile flow strength has no discernible effect on the burst pressure. A small amount of time dependent deformation doesn't matter in this case. As plastic hinges operate the pressure will reach a plateau and then tearing develops when sufficient crack tip deformation has occurred to reach a critical toughness level. The amount of crack tip blunting required for tearing in the axial direction will be roughly proportional to the remaining wall thickness at the crack tip if the throughwall crack tip lies in less than full thickness material.

The deformation needed to cause radial ligament tearing of deep, partial throughwall axial cracks is far smaller than the crack tip blunting needed to extend a throughwall axial crack in full thickness material. For example, the ligament beyond the tip of a 95% TW crack will be in the range of 0.002 inches thick. This ligament cannot deform a total of 0.040 inches before it tears to create a throughwall crack. Obviously for small ligaments the amount of deformation they can withstand without tearing is a function of the ligament size. Small ligaments beneath very deep cracks can only blunt a small amount before the onset of ligament tearing. Thus, in this case, small amounts of time dependent deformation can be crucial. It is here where a loading rate effect on tearing may be expected and it is here that a loading rate on burst pressure has been observed.

As noted above, a small amount of time dependent deformation can be crucial for ligament tearing of deep cracks. If the deep crack is long and thus ligament tearing is the limiting step in developing a burst, then time dependent deformation will lower the burst pressure. For short, deep cracks, a time dependent contribution to ligament tearing may affect the pressure at which leakage develops, i.e., development of a throughwall crack, but the burst pressure will not be affected. For short deep cracks, the limiting step is tearing down the tube axis. Hence, only long and deep cracks are at risk of exhibiting a loading rate/hold time effect on burst pressure. The next sections essentially discuss how long is "long" and how deep is "deep".

There is one additional factor to consider in terms of the conditions needed for the onset of loading rate/hold time effects on burst pressure, the absence of crack path tortuosity. Service induced axial cracks in steam generator tubing are typically composed of multiple crack segments which have coalesced, to some degree, out of a network of small cracks to form a single dominant axial crack. The meandering or tortuous path of a service induced crack creates out of plane ligaments which provide strengthening compared to a smooth, continuous, planar crack. The EPRI Flaw Handbook and other similar approaches provide for the probabilistic appearance of ligament strengthening from non-planar ligaments. In the EPRI Flaw Handbook, the variation in strengthening effects of out of plane ligaments is reflected in the term, 1.104, in the axial partial throughwall burst equation shown below. This term has a standard deviation of 0.0705 which was developed from pulled tubes burst test results and destructive examinations of actual crack profiles. The variation in the 1.104 term arises from the range of crack morphologies found in pulled tubes with axial cracks. This variation characterizes the out of plane ligament

strengthening effects expected in Alloy 600 steam generator tubes found in service with axial flaws,

$$P_B = 0.58\left(S_y + S_u\right)\frac{t}{R_i}\left[1.104 - \frac{L}{L+2t}h\right] \qquad \textbf{Equation 7-1}$$

The 95th percentile lower bound of the 1.104 term is a value of 0.988. In essence, the 95th percentile value can be considered as corresponding to the absence of out of plane ligament strengthening effects. A value of 0.988 (or near "1" for convenience) denotes a smooth, continuous, planar crack. This type of service induced crack occurs, but not frequently. An EDM slot models a smooth, continuous, planar crack and this is why a value of "1" should be used to calculated the burst pressure of specimens with EDM slots. In terms of possible rate effects on burst tests results, out of plane ligaments increase the extent of deformation needed for ligament tearing to occur. If significant out of plane ligament strengthening is present, the small contribution of time dependent deformation to the burst process is not crucial. Thus, the additional condition needed for the onset of loading rate/hold time effects on burst pressure is the absence of crack path tortuosity. Not only must axial cracks be deep and long, they must also be smooth, continuous and planar for a loading rate/hold time effect to be observed.

7.4 Flaw Geometries at Risk of Exhibiting a Burst Pressure Rate Effect

Test results from the Type 14 specimens show that a loading rate effect is observed if deep crack sections are in the vicinity of 90 to 95% TW. As shown in Section 5.1.2, high temperature, slow rate tests reported in Reference 18 are consistent with other similar test results at room temperature obtained at significantly higher pressurization rates. In these series of tests of rectangular EDM slots, a wide range of flaw depths were included with maximum depths on the order of 90% TW. On this basis, the question of what is a deep crack leads to an answer of greater than 90% TW.

Recently, tests of Alloy 600 tubing with rectangular EDM slots were conducted at both fast and slow pressurization rates. The EDM slot depth was 50% TW with a length of 0.75 inches. Burst were obtained in about 15 minutes in the slow rate tests compared to about 4 seconds in the fast rate tests. Five nominally identical specimens were tested at each rate. The average burst pressure in the fast rate tests was actually less than the average burst pressure in the slow rate tests by 0.5%. Figure 7-1 shows the cumulative distributions of the slow rate and fast rate burst pressures. Specimen to specimen scatter accounts for the variation in burst pressures. A statistical comparison of the data from the tests yields an F-test value of 87%, equal variances, and a t-test value of 92%, equal means. So, there is no difference between fast rate and slow rate burst tests for an EDM slot depth of 50% TW.

The depth at which burst test data are subject to some degree of a loading rate/hold time effect has been shown by well controlled direct experiments to have occurred at about 95% TW but not at 50% TW. Other fast and slow rate burst test data from separate sources point to the boundary of the onset of loading rate effects on burst test results to be at about 90% TW. It is a straightforward step to continue fast and slow rate burst tests of tubes with rectangular EDM

slots to definitively answer the question of the depth of an axial flaw at which loading rate effects on burst pressure will be observed. Section 8 contains a recommendation for just such a series of burst tests to be conducted. At present, a rational best estimate is 90 %TW.

The requirement of a minimum degraded tube burst strength of $3\Delta P$ provides the context for the question of what is a "long" crack. Typically, depending on the tube size, a 100% TW crack must be greater than ≈0.4 inches long to challenge the minimum $3\Delta P$ strength requirement. Loading rate/hold time effects on the tearing a deep partial throughwall crack with this length will not challenge the required minimum burst strength.

In summary, the flaw geometries at risk of exhibiting a burst pressure rate effect are smooth, continuous, planar cracks with a depth greater than 90% TW and a length greater than 0.4 inches. The next question is the actual significance of possible rate effects on past burst pressure measurements on condition monitoring and operational assessment evaluations.

7.5 Significance of Possible Rate Effects on Burst Pressure Measurements

Given that slow loading rates or hold times can lower the pressure at which tearing develops at the ends of very deep planar slots, the issue at hand is the significance of this observation relative to condition monitoring and operational assessment evaluations. As shown in Section 2, the use of the EPRI Flaw Handbook [15] procedures and equations and actual Type 14 measured profiles gives expected agreement between slow rate measured burst pressures and calculated results. The calculated extents of throughwall tearing are sufficient to cause calculated bursts. Hence, both the pressure calculated for the development of full throughwall tearing and the calculated burst pressure are in agreement with the slow rate test measurements. The slow rate, Type 14 profile, burst test data is in agreement with current industry calculation practices of Reference 15.

Current industry practices correctly predict the burst pressure of long, deep, planar cracks even if a loading rate/hold time effect is present. Re-evaluation of industry burst test databases with and without burst test results for crack depths greater than 90% TW do not significantly change existing burst test correlations. A recommendation is included in Section 8 relative to specifying a hold time requirement for in situ pressure testing.

7.6 Burst Tests on Simulated R72C72 Geometries

The burst tests which motivated this present study were conducted on axial EDM slot profiles which simulated eddy current depth/length profiles of tube R72C72. A number of variations of this profile were tested. Most testing was performed on the Type 14 profile which contained two very deep sections. One of these sections was about 95%TW in many of the specimens. Conventional fast rate and slow rate or long time hold tests of Type 14 specimens demonstrated a rate and/or hold time effect on the measured burst pressure. Test data for other profiles lacked a direct comparison of slow and fast rate results or was inconclusive.

Type 14 specimens in slow rate tests failed by first tearing throughwall (tearing of the radial ligament) at the location of the deepest point of the EDM slot and then tearing along the length of the slot as pressurization continued. In most cases, increases in pressure after the onset of throughwall tearing were small. In one case, the pressure from the onset of throughwall tearing to the full extent of tearing at test termination increased by more than 1000 psi. After excessive leakage terminated pressurization, a sealing bladder with a foil reinforcement was inserted and a fast rate burst test was attempted. In almost all cases, a further fast rate test did not yield a burst pressure higher than that experienced in the initial slow pressurization rate test. Usually this was the expected behavior since slow pressurization created a 100% TW crack long enough to lead to bursting at the maximum pressure in the slow rate test. However, in some tests, the 100% TW crack length after slow rate testing wasn't very long and an increase in maximum pressure could be expected after insertion of a sealing bladder and a subsequent fast rate test. Typically this expected demonstration of increased pressure bearing capacity was not met because the tip of the partially torn crack still resided in a region of much reduced wall thickness. As shown below, this observation, confirmed by evaluation of other test data, is more significant than the observation of a loading rate effect for very deep crack sections.

7.7 Ligament Tearing and Crack Instability

There was one instance where the projected extent of tearing of a Type 14 measured profile did not exceed the 100% TW length for burst at the calculated ligament tearing pressure. Thus, a small increase in the pressure necessary for bursting was predicted in subsequent testing with a sealing bladder. No increase was observed. This fact, together with the observation that some measured extents of throughwall tearing implied increases in the pressure required for bursting that were not realized, led to a re-evaluation of the two-step process (discussed below) for burst pressure prediction for axial cracks.

Typically, the burst pressure of a tube with a partial depth axial crack is calculated using a two-step process. In the first step, the effective structural depth and length are identified corresponding to a minimum calculated pressure leading to tearing radially throughwall (for example, see the weak link profile on Figure 5-17). The second step of the calculation is to examine the stability of the resulting 100% throughwall crack. If the structurally effective length is greater than the critical length of a 100% throughwall crack at the calculated ligament tearing pressure, the crack is unstable and a full burst will develop. If the structurally effective length is less than the critical length of the corresponding 100% throughwall crack, continued tearing is expected to be arrested and the burst pressure is judged to be elevated to the burst pressure of a 100% TW crack with a length of L_e.

This two-step process works well for most axial crack profiles. The phenomenon of crack pop-through, where a crack pops or tears through the wall and then stops while the pressure is elevated until unstable crack tearing occurs, is not uncommon in laboratory or in situ pressure tests. However, if the tip of the partially torn throughwall crack stops along the original crack profile where the remaining ligament in the depth direction is small, then one cannot equate the torn throughwall crack to a 100% TW crack in an otherwise full thickness tube. This is illustrated on Figure 7-2 where the "initial tearing length" terminates in additionally cracked material.

Although the calculation of the pressure for the onset of radial ligament tearing is not an issue, the two step burst evaluation process could be further adjusted to account for the presence or lack of ligaments in the hoop direction. The slow rate Type 14 burst tests agree with present industry procedures. After throughwall tearing commences, the next question is the length of the profile that is torn 100% TW. The present length estimate is the effective structural length. This is portion of the profile where the average flow strength is exceeded. However, this is no more than an educated estimate. It is reasonable, but there is no fundamental argument as to why it should be true. Tearing of small ligaments is ultimately a fracture problem, meaning that the failure mechanism is best described by the equations of fracture mechanics, and not a plastic collapse problem governed by the yield and ultimate strength of the material. The testing results documented in this report indicate it is more likely that additional development work would lead to the identification of strengthening mechanisms associated with the presence of ligaments in the hoop direction rather than deficiencies in the model associated with the initial tearing length terminating in less than full thickness material One rationale for this is that the process of examining all of the possible subcracks and reporting the one with the least tearing pressure is inherently conservative relative to estimating a burst pressure.

One conservative answer to the question of the length of throughwall tearing is to assume tearing continues to the end of the crack profile once it starts. At this point the torn crack tip will be in full wall thickness material and the 100% TW burst equation is certainly applicable to determine if burst occurs. Alternatively, the crack tip could arrest at some location where the material is appreciably thicker, but not necessarily 100% thick, and a similar conclusion would be reached.

One approach to addressing the observation that loading rate effects are a potential issue for deep cracked sections of axial crack profiles could be to attempt to use a ligament tearing equation that is more conservative than the EPRI Flaw Handbook burst solution [15]. Figures 5-13 through 5-15 compare the ANL ligament tearing equation, a modification of an approach developed earlier at the Battelle Columbus national laboratory, and the original Cochet equation [16] which is the basis for the EPRI Flaw Handbook solution. Both equations ignore out of plane ligament strengthening effects that are not loading rate dependent. There is little to chose from, except at very large given depths. Here the ANL ligament tearing equation extrapolates to zero pressure for a 100% deep indication regardless of the length of the indication.

A drawback to this approach is that the use of the ANL ligament tearing equation alone to predict burst can be grossly conservative since it predicts a zero ligament tearing strength for any crack profile which has a throughwall penetration regardless of the length of that penetration. Hence, without a further consideration of the length of throughwall tearing, a tube burst would be predicted if any portion of a crack profile went through the wall. This is demonstrably untrue and a torn length consideration must be added. It is illogical to assume that a 0.4 inch crack profile with one small 100% TW section has zero burst pressure while a 0.4 inch long crack 100% TW meets a $3\Delta P$ burst pressure requirement via the industry standard throughwall burst equation.

As mentioned above, one conservative approach to the question of the length of throughwall tearing is to assume tearing continues to the end of the crack profile once it starts. At this point the torn crack tip will be in full wall thickness material and the 100% TW burst equation is certainly applicable to determine if burst occurs. However, use of the ANL ligament tearing equation together with this conservative torn length assumption would imply than any crack that

penetrates the wall at any point would immediately tear to its full length, irrespective of the applied pressure. Clearly a better treatment of the mechanical tearing of cracks with 100% TW sections is required.

As an interim solution, a loading shedding argument can be used to develop an approximate answer for the question of the stability of crack tearing of axial crack profile with portions that are 100% TW. The field of influence ahead of an axial crack can be approximated by applying the Cochet approach for partial throughwall cracks to 100% TW cracks. The 100% TW cracked section is unable to carry the pressure load that would normally be carried over this length in an unflawed tube. Instead this load is shed to the material in front of the crack. The correct distance over which this load shedding is distributed can be found by adjustment to make the calculated burst pressure equal that of actual test results. The average stress in front of the crack tip for a distance of "k" times the thickness, t, is set equal to the average hoop stress leading to bursting of an unflawed tube. The solution is found by equating the material force of closure to the crack opening force due to the internal pressure. The closure force, $F_{closure}$, is found by considering the material extending a distance of $2k{\cdot}t$ from each end of the crack, the load shedding region, to be at the flow stress of the material, i.e.,

$$F_{closure} = 0.6(S_y + S_u)(2kt)t \qquad \textbf{Equation 7-2}$$

This closure force is set equal to the opening force, $F_{opening}$, which is just the average unflawed hoop stress times the cross sectional area occupied by the crack plus the load shed region,

$$F_{opening} = \frac{P_B R_m}{t}(L + 2kt)t \text{ .(0-1)} \qquad \textbf{Equation 7-3}$$

Thus, the burst pressure is given by:

$$P_B = \frac{0.6(S_y + S_u)(2kt)t}{R_m(L + 2kt)} \qquad \textbf{Equation 7-4}$$

where R_m is the mean tube radius and L is the 100% TW crack length. By setting the burst pressure, P_B, equal to the solution from the EPRI throughwall burst pressure equation, the factor, k, can be solved as a function of normalized crack length, λ. Figure 7-3 shows k as a function of λ for a variety of tube dimensions. The average value for k is about 4. The load over the throughwall portion of a crack is shed for a distance of about $k{\cdot}t$ ahead of each crack tip. If the wall thickness ahead of the crack tip is the full wall thickness, the EPRI throughwall crack burst strength is obtained. If the wall thickness is reduced ahead of the throughwall crack tip, the pressure than can be supported is reduced correspondingly. To estimate the pressure that can be supported, calculate the ratio of the through thickness area over a distance of $k{\cdot}t$ from each crack tip to $2k{\cdot}t^2$. This ratio times the EPRI throughwall burst pressure, P_B, for a crack tip in full thickness material is the pressure that can be supported by a throughwall crack where the crack tips end in less than full thickness material. As a throughwall crack marches down a partial

throughwall crack profile, the maximum pressure bearing capacity without further tearing can be determined. Depending on the crack shape, the pressure bearing capacity can increase, decrease or remain the same as the crack tears and the 100% TW length increases.

7.8 Summary of Rate Dependence Discussion

A small amount of time dependent deformation and associated stress relaxation occurs in Alloy 600 at low temperatures. A loading rate/hold time effect on the burst pressure of degraded Alloy 600 tubing will occur only in those circumstances where a small amount of time dependent deformation is crucial. For Alloy 600 tubing, there are a limited set of special circumstances where the absolute extent of deformation and not just the tensile flow curve determines the burst pressure. Long, very deep, and planar axial partial throughwall cracks provide the circumstances where a small amount of time dependent deformation is crucial and some degree of a loading rate/hold time effect on burst pressure should be observed. The type 14 EDM specimens fall into this category and a loading rate/hold time effect on burst pressure has been observed. The magnitude of this effect could be less than present measurements indicate if the bladder and foil sealing system, used in the fast rate tests but not in the slow tests, caused some degree of artificial strengthening. However, the literature suggest that this is unlikely.

The depth at which burst test data is subject to some degree of a loading rate/hold time effect has been shown by well controlled direct experiments to lie between 50% TW and greater than 90% TW. Other fast and slow rate burst test data from separate sources points to a best estimate of the boundary far the onset burst test of loading rate effects to be at about 90% TW. Fast and slow rate burst tests of tubes with rectangular EDM slots can definitively answer the question of the depth of an axial flaw at which loading rate effects on burst pressure will be observed. Section 8 contains a recommendation for just such a series of burst tests to be conducted.

The practical significance of some degree of a loading rate/hold time on the burst pressure of long, deep, planar axial partial throughwall cracks is small. Current industry practices correctly predict the burst pressure of long, deep, planar cracks even if a loading rate/hold time effect is present. Re-evaluation of industry burst test databases with and without burst test results for crack depths greater than 90% TW do not significantly change existing burst test correlations.

Methods of predicting crack stability when 100% TW throughwall portions of cracks occur such that crack tips reside in less than full thickness material are not developed as thoroughly as needed. One suggested approach to this problem has been presented.

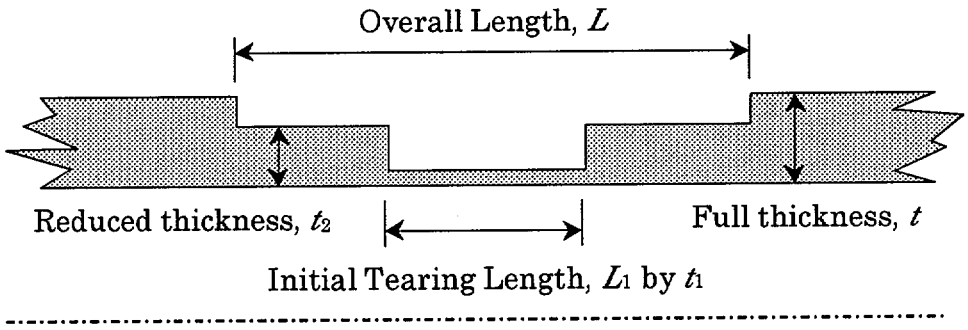

Figure 7-1
Idealization of a PTW crack by multiple rectangular sections

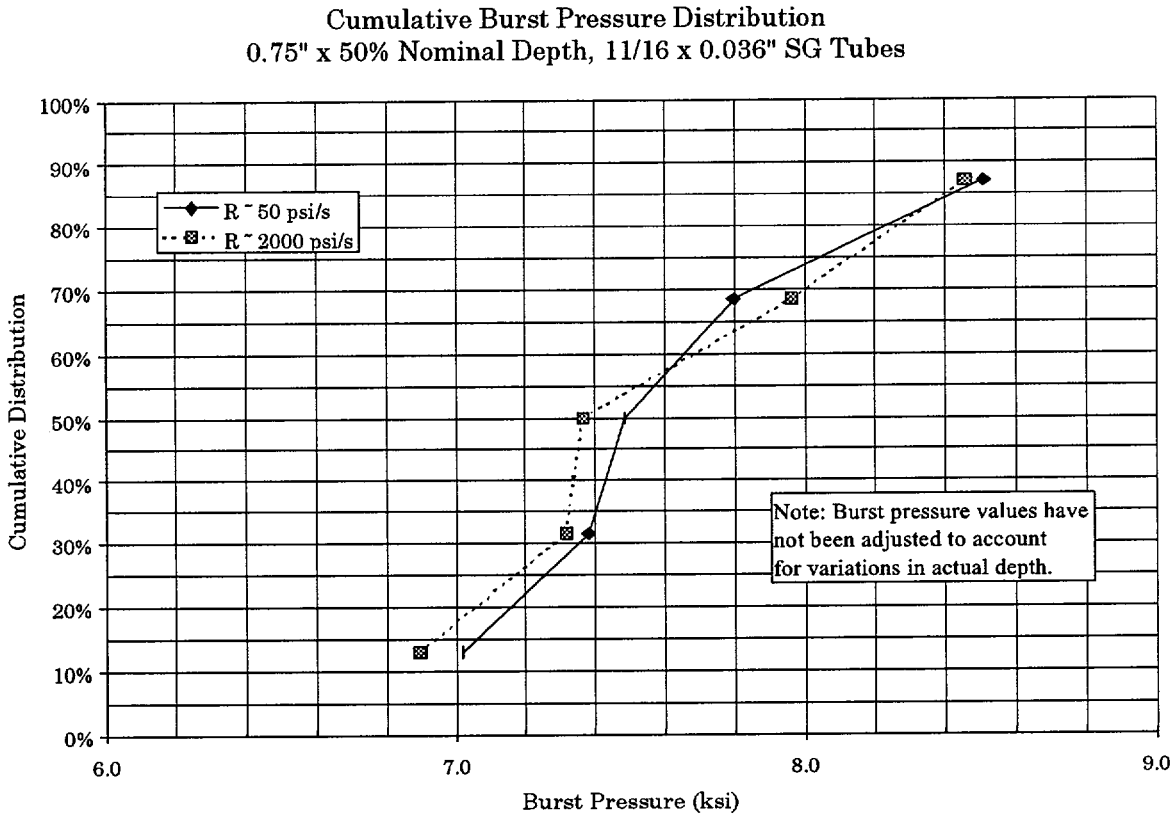

Figure 7-2
Distribution of burst pressures of 0.75" long by 50% deep rectangular EDM slots

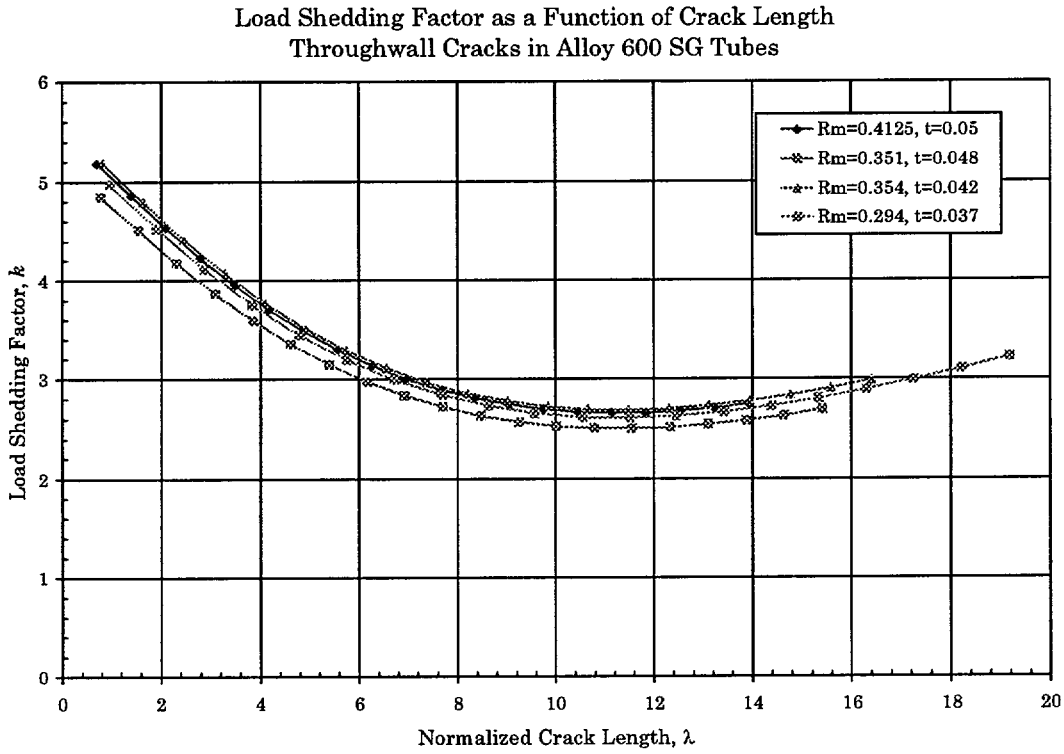

Figure 7-3
Load shedding distance as a function of crack length for various tube sizes

8
RESOLUTION ACTIVITIES

A program was initiated by EPRI to evaluate the implications of the results obtained from the ANO burst testing program. This report documents the work performed and summarizes the results of that evaluation. The results do indicate that a time dependent deformation and burst phenomenon does exist, but that its significance is limited to a specific morphology of degradation or simulated degradation. Specific areas to be addressed by this evaluation were identified as 1) the burst pressure dependence on the pressurization rate, 2) the effects on industry test procedures, and 3) the effects on industry evaluation models. The following paragraphs present the recommendations resulting from the completion of this evaluation. The test procedure recommendations are separated into recommendations for laboratory test procedures and recommendations for in situ test procedures.

8.1 Burst Test Procedure Recommendations

The present burst test procedure, recommended by EPRI, is appropriate for partial throughwall, crack-like (cracks, EDM or laser cut slots) degradation with a maximum depth less than or equal to 90% TW. If the ends of completely throughwall degradation reside at positions where the remainder of degradation is no greater than 20% TW, present test procedures are also appropriate. The relatively narrow set of degradation profiles outside of these considerations may be susceptible to loading rate effects on measured burst pressures. For these degradation geometries, it is recommended that pressurization to failure be performed incrementally in 500 psi steps, say 6 or less, with 2 minute hold times after each pressure increment. The rate at which the pressure is increased in each pressure step should not exceed 200 psi/s (this value results in a strain rate on the order of that specified in the ASME Code for performing tensile tests). Other alternatives may be considered, however, since any number of combinations of ramp rates and hold times are possible which would result in a net *slow rate* test, e.g., see Figure 5-1. After burst testing is completed, for any test geometry, degradation dimensions should be used to verify that the test results are free of possible rate effects.

8.2 In Situ Pressure Testing Recommendations

It is recommended that in situ testing procedures require hold times of at least two minutes at all pressure hold points of interest. Typically these points correspond to P_{SLB}, $1.4 \cdot P_{SLB}$ and $3\Delta P_{NO}$, as adjusted for temperature effects and system uncertainties. In addition, it is recommended that the rate of pressurization between hold points should be practically limited to about 200 psi/s. This is not intended to be severely restrictive and engineering judgment indicates that maximum values of about 500 psi/s early in the time sequence would not lead to invalid results.

8.3 Analytical Model Recommendations

In summary, few changes are recommended relative to the evaluation of tube degradation. Methodologies do exist, however, to conservatively deal with expected degradation in the absence of following through on the recommendations.

- A methodology, backed by test data, needs to be developed to deal with the stability of tearing of throughwall axial cracks down the length of partial throughwall crack profiles. Without such development, the deterministic prediction of the burst pressure should be based on the ligament tearing model, both the Cochet and the ANL model are satisfactory for this purpose.
- A recommendation was delineated in Section 2.5 to perform a series of burst tests at a high pressurization rate to quantify the effect of the sealing bladder and lubricated brass foil on the results from the tests of the Type 14 specimens.
- A corresponding tearing methodology needs to be developed for the future development of generic methods for performing leakage evaluations of circumferential cracks.
- A methodology and test data needs to be developed for dealing with the tearing of material at the bottom of pits in order to develop appropriate models to deal with leakage paths that could be created in service. The current approach would be to treat the pit as a planar crack and apply either the Cochet or ANL ligament tearing equation to the prediction problem.
- In the condition monitoring evaluation of single axial cracks, the statistical nature of ligament strengthening needs to be recognized. For operational assessments, the statistical nature of the strength of flawed tubes appears to be adequate without change.

A summary of recommendations as a function of degradation morphology is provided in Table 8-1. It is noted that none of the previous recommendations or those listed in the table is essential for demonstrating structural integrity beyond current practice. However, several of the current practices are seen as significantly conservative and the intend of carrying out the actions recommended would be to improve the analytical models and the accuracy of their predictions.

Table 8-1
Recommended Changes to the Analytical Models Used for Degradation Evaluations

Morphology of Degradation	Recommendations
Axial Throughwall	Develop methodology for throughwall cracks in less than full thickness material (as an interim conservative approach use the Cochet or ANL ligament tearing equations and assume 100% TW cracking along the full crack length once tearing starts).
Expansion Transition	No changes recommended.
U-bend Freespan Axial	No changes recommended.
Axial Part-Throughwall	For single cracks the ligament tearing model should be used to estimate the burst pressure. The nominal model may be used for the distribution of pressures.
PWSCC ARC	Keep the statistical model for the distribution of burst pressures about the nominal prediction.
ODSCC ARC	No changes are recommended.
Circumferential Cracking	Develop methodology for tearing throughwall for leakage evaluation
Uniform 360° Thinning	No changes are recommended.
Uniform 360° w/Limited Axial Length	No changes are recommended.
Axial Thinning w/Limited Circumferential Extent	No changes are recommended.
Pitting	Develop methodology for tearing throughwall for leakage evaluations (as an interim conservative approach use the Cochet or ANL ligament tearing equations and assume 100% TW cracking along the full crack length once tearing starts).

9
CONCLUSIONS

The introduction of this report ended with a summary of issues that ensued from consideration of the results of the testing program that was carried out on the tube specimens that were fabricated to simulate the ECT estimated degradation profile of the ANO 2 R72C72 tube. The evaluations and considerations of this report have led to the following conclusions relative to those issues:

1. Is the burst pressure of degraded tubing a function of the pressurization rate, including the consideration that a hold-time is a zero pressurization rate, used to test the tubing? The answer is yes, but only for a limited type, or types, of degradation morphology. For most degradation modes there does not appear to be any meaningful influence of the pressurization rate on the measured burst pressure of the degraded tubing. The morphologies that are affected are readily identified by inspection of the recommendations in Table 8-1. Specifically, axial, part-throughwall cracks with segments that are greater than about 90% deep and a crack length longer than the $3\Delta P$ throughwall length (about 0.4 inches) would be expected to demonstrate a rate dependent burst pressure, with higher pressurization rates leading to higher measured burst pressures.

2. Should changes be made to industry test procedures to account for the potential dependence of the burst pressure on the pressurization rate? The answer is yes, again, and recommendations have been summarized in Sections 8.1 and 8.2 of this report for laboratory and in situ testing respectively. Those recommendations include changes relative to the pressurization rate and the inclusion of hold times during the testing.

3. Are there industry evaluation models that were empirically derived or qualified using data which might be pressurization rate dependent, e.g., data used for the ODSCC ARC? As for item 1 above, the answer is yes, but it appears that the only time the measured burst pressure is influenced by the pressurization rate is when an axial crack is tested, and that crack has portions that are greater than 90% deep and terminate in sections that are too deep to lead to arrest of the running crack once the deeper radial ligament has torn. The ODSCC ARC data do not appear to be sensitive to the test pressurization rate below or within the range permitted by the EPRI guideline. Cracks with lengths and depths sufficient to cause a concern regarding a rate effect burst pressure issue are not left in service via the use of ARC.

4. Do the industry evaluation models need to be modified to account for the potential dependence of the burst pressure on the pressure rate, i.e., to account for the potential for ligaments to tear prior to burst, thus reducing the burst pressure? Recommended changes to the industry models are summarized in Table 8-1. For a single axial crack, the use of the analysis model must involve consideration of the potential for the database burst pressures to have been influenced by the rate of pressurization. This simply means that a model developed for the evaluation of shallower indications, where any potential rate effects were

not significant, should not be extrapolated to predict the burst pressure of indications where rate effects could be significant. In general, the potential will only exist for the evaluation of single, axial, cracks with maximum depths greater than about 90% throughwall.

For a one-time estimate of the burst pressure of an individual crack when the maximum depth exceeds about 90%, the Cochet [15], using a constant value of 1.0, or the ANL [27], ligament tearing model should be used to predict the burst pressure of the tube. To calculate the distribution of the expected burst pressures of a crack, the techniques developed based on burst testing of cracked tubes should be employed.

10
REFERENCES

1. 2CAN050008, "Arkansas Nuclear One – Unit 2, Docket No. 50-368, License No. NPF-6, Additional Information Regarding the ANO-2 Deterministic Operational Assessment of Steam Generator Tubing for the Remainder of Cycle 14," Entergy Operations, Russellville, AR (May 17, 2000).

2. 2CAN060009, "Arkansas Nuclear One – Unit 2, Docket No. 50-368, License No. NPF-6, Additional Testing Results Supporting the ANO-2 Deterministic Operational Assessment of Steam Generator Tubing for the Remainder of Cycle 14," Entergy Operations, Russellville, AR (June 6, 2000).

3. NSD-EPRI-0646, "EPRI Guidelines for Leak & Burst Testing of SG Tubes," Westinghouse Electric Company, Madison, PA (July, 11, 1994).

4. CE NPSD-1125-P (Proprietary), Revision 2, "Methodology for Evaluation of Axial Degradation in Steam Generator Tubing – Laboratory Testing Program," Combustion Engineering, Windsor CN (August 1999).

5. Berge, P., "EPRI Guidelines for Leak and Burst Testing of Steam Generator Tubes," Electricité de France, Paris, France (January 8, 1995).

6. Riley, J., "SG News," electronic mail to distribution, NEI, Washington, DC (June 21, 2000).

7. TP-SGDA-00-1, Rev. 0, "Burst Testing of Degraded Steam Generator Evaluation of the Estimated Structural Integrity of the R72C72 Tube Failure (ANO Unit 2)," Westinghouse Electric Company, Pittsburgh, PA (May, 2000).

8. NP-7008, "Strain-Rate Damage Model for Alloy 600 in Primary Water," EPRI, Palo Alto, CA (October 1990).

9. Fleck, J., "Steam Generator Tube Bursting Test Procedures," electronic mail to distribution, Framatome Technologies, Inc., Lynchburg, VA (August 14, 2000).

10. TR-016743-V4R1, "Guidelines for SG Tube Section Removal, Test and Examination," EPRI, Palo Alto, CA (December 1997).

11. Hernalsteen, P., "The influence of Testing Conditions on Burst-Pressure Assessment for Inconel Tubing," IJPVP, **52**, pp. 41-57 (1992).

12. TR-105505, "Burst Pressure Correlation for Steam Generator Tubes with Throughwall Axial Cracks," EPRI, Palo Alto, CA (October 1997).

13. Laire, Charles, "Re: Request for Schelle Data," electronic mail, Laborelec, Belgium (July 06, 2000).

14. TR-107621-R1, "Steam Generator Integrity Assessment Guidelines," EPRI, Palo Alto, CA (March 2000)

15. 1001191, "Steam Generator Degradation Specific Management Flaw Handbook," EPRI, Palo Alto, CA (January 2001).

16. NP-6865-L, "Steam Generator Tube Integrity Volume 1: Burst Test Results and Validation of Rupture Criteria (Framatome Data)," EPRI, Palo Alto, CA (June 1991).

17. NP-6626-SD, "Belgian Approach to Steam Generator Tube Plugging for Primary Water Stress Corrosion Cracking," EPRI, Palo Alto, CA (March 1990).

18. NUREG/CR-0718, "Steam Generator Tube Integrity Program Phase I Report," Prepared by the Pacific Northweat Laboratory for the U.S. Nuclear Regulatory Commission, Rockville, MD (September 1979).

19. NUREG/CR-2336, "Steam Generator Tube Integrity Program/Steam Generator Group Project," Prepared by the Pacific Northwest Laboratory for the U.S. Nuclear Regulatory Commission, Rockville, MD (May 1990).

20. Woods, J. P., "The Effect of Ligament Size on the Burst Pressure of Alloy 600 Tubing Containing Axial Cracks, Department of Metallurgical Engineering, Illinois Institute of Technology, Chicaco, IL (December, 1995).

21. NUREG/CR-5117, "Steam Generator Tube Integrity Program Phase II Final Report," Prepared by the Pacific Northwest Laboratory for the U.S. Nuclear Regulatory Commission, Rockville, MD (August 1988).

22. NP-7474, "Evaluation of Leak and Burst Characteristics of Roll Transitions Containing Primary Water Stress Corrosion Cracks," EPRI, Palo Alto, CA (May 1993).

23. NP-6864-L (Draft Report), "PWR Steam Generator Tube Repair Limits: Technical Support Document for Expansion Zone PWSCC in Roll Transitions – Rev. 2," EPRI, Palo Alto, CA (August 1993).

24. NUREG/CR-6511, Volumes 1 through 6, "Steam Generator Tube Integrity Program," U.S. Nuclear Regulatory Commission, Rockville, MD (April 1997 through October 1999).

25. Diercks, D., "Steam Generator Tube Integrity Program Monthly Progress Report for January 2000," Argonne National Laboratory, Argonne, IL (March 1, 2000).

26. Diercks, D., "Steam Generator Tube Integrity Program Monthly Progress Report for February 2000," Argonne National Laboratory, Argonne, IL (April 3, 2000)

27. NUREG/CR-6664, "Pressure and Leak-Rate Tests and Models for Predicting Failure of Flawed Steam Generator Tubes," U.S. Nuclear Regulatory Commission, Rockville, MD (August 2000).

28. NP-7480-L, Addendum 3, "Steam Generator Tubing Outside Diameter Stress Corrosion Cracking at Tube Support Plates Database for Alternate Repair Limits, Addendum 3, 1999 Database Update," prepared by Westinghouse Electric Company for EPRI, Palo Alto, CA (May 1999).

29. NP-7480-L, Addendum 1, "Steam Generator Tubing Outside Diameter Stress Corrosion Cracking at Tube Support Plates Database for Alternate Repair Limits, 1996 Database Update," prepared by Westinghouse Electric Company for EPRI, Palo Alto, CA (November 1996).

30. D.5004/BRD/RB.90.126, Version 2, "Procedure for Performance and Analysis of Opening Tests by Placing Tubular Test-Pieces Under Internal Pressure," Electricité de France, Production Transport Laboratories Group, Paris, France (December 2, 1992).

31. Cattant, François, "Ref.: Steam Generator Tube Burst Testing Procedure," electronic mail to Robert Keating (Westinghouse), Electricité de France, Paris, France (August 8, 2000).

32. PET-0049-00, "Steam Generator Tube Burst Testing," T. Iida, Mitsubishi Heavy Industries, Yokohama, Japan (September 18, 2000).

33. EPRI NP-7008, "Strain-Rate Damage Model for Alloy 600 in Primary Water," Electric Power Research Institute, Palo Alto, CA (October 1990).

34. AES 96112906-1Q-2, "Aptech Axial Crack Burst Pressure Methodology," prepared by Aptech Engineering Services for the CEOG Steam Generator Task Force, Sunnyvale, CA (December 1997).

35. WCAP-15129, Revision 3, "Depth-Based SG Tube Repair Criteria for Axial PWSCC at Dented TSP Intersections," Westinghouse Electric Company, Madison, PA (February 23, 2000).

36. TR-107197-P1, "Depth-Based Structural Analysis Methods for Steam Generator Circumferential Indications," EPRI, Palo Alto, CA (Interim Report, December 1997).

37. Majumdar, S., *Failure and Leakage through circumferential cracks in steam generator tubing during accident conditions*, International Journal of Pressure Vessels and Piping, Vol. 76, pp. 839-847 (1999).

38. TR-107620-R1, "Steam Generator In Situ Pressure Test Guidelines: Revision 1," EPRI, Palo Alto, CA (1999).

39. RG 1.121 (draft), "Bases for Plugging Degraded PWR Steam Generator Tubes," United States Nuclear Regulatory Commission, Rockville, MD (issued for comment, August 1976).

40. Pearson, R., "RE: In Situ Procedures," electronic mail, Northern States Power, MN (August 21, 2000).

41. Hall, J., "Hold Time Effects During In Situ Pressure Testing," electronic mail, Westinghouse Electric Company, Windsor, CN (August 3, 2000).

42. Hawkins, P. J., "Input for the EPRI PTW Burst Report," Westinghouse Electric Company, Madison, PA (December 1, 2000).

43. Fleck, J., "Re: In Situ Experience," electronic mail, Framatome Technologies Incorporated, Lynchburg, VA (September 19, 2000).

44. Lubahn, J. D., and Felgar, R. P., Plasticity and Creep of Metals, John Wiley & Sons, New York, New York (1961).

A
MACHINED DRAWINGS EDM PROFILES, TYPE 1 THROUGH TYPE 16

Type 1 EDM Profile

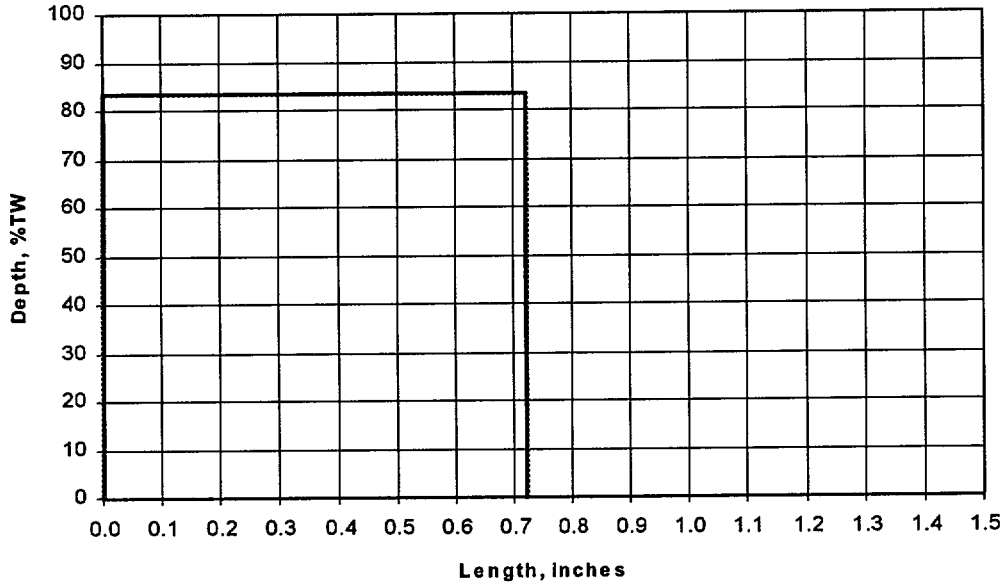

Type 2 EDM Profile

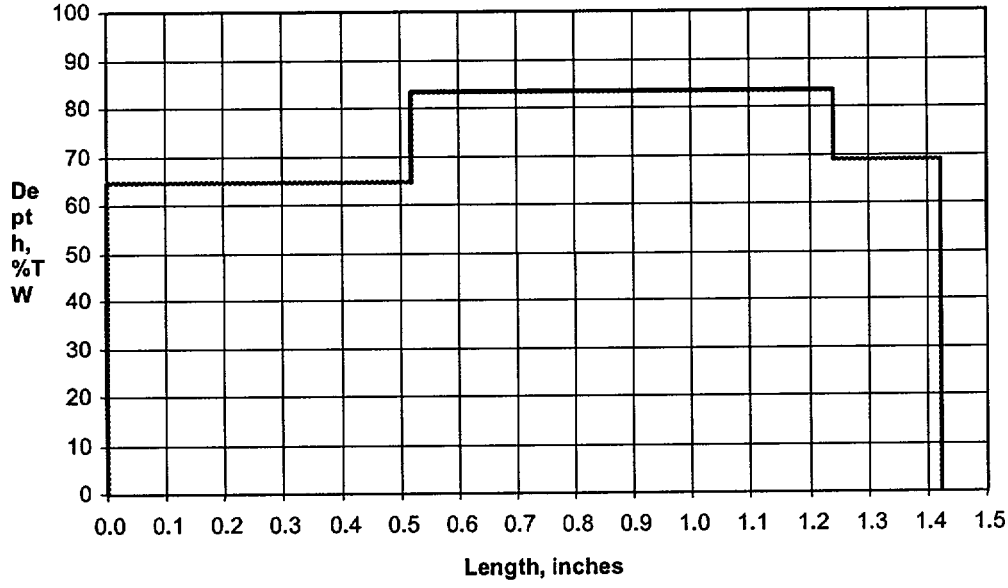

Type 3 EDM Profile

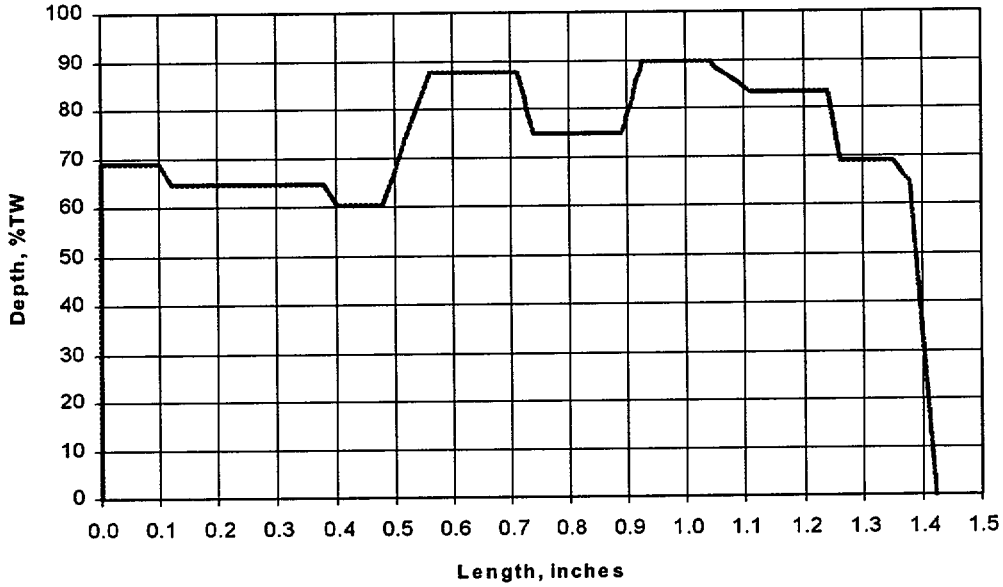

Type 4 EDM Profile

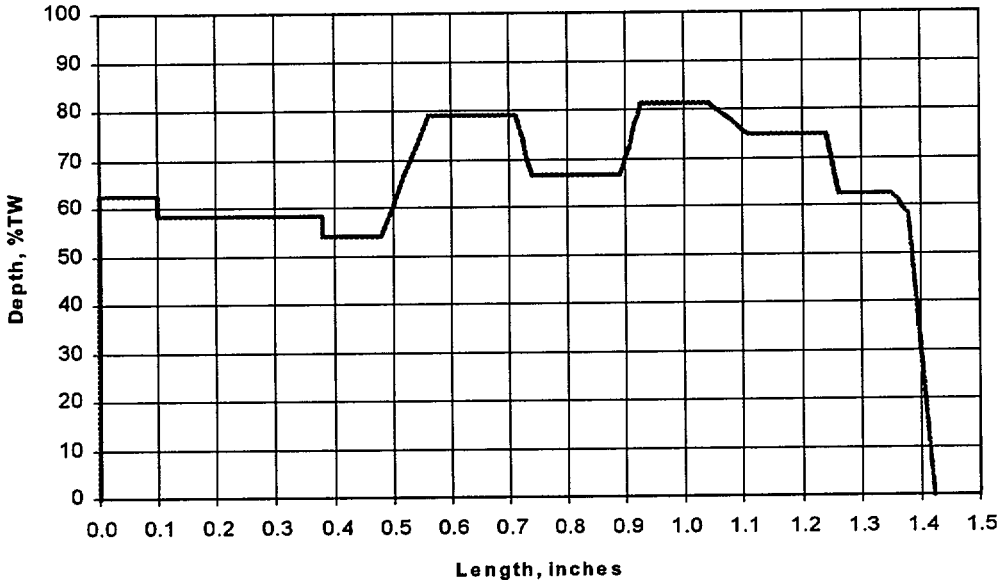

Type 5 EDM Profile

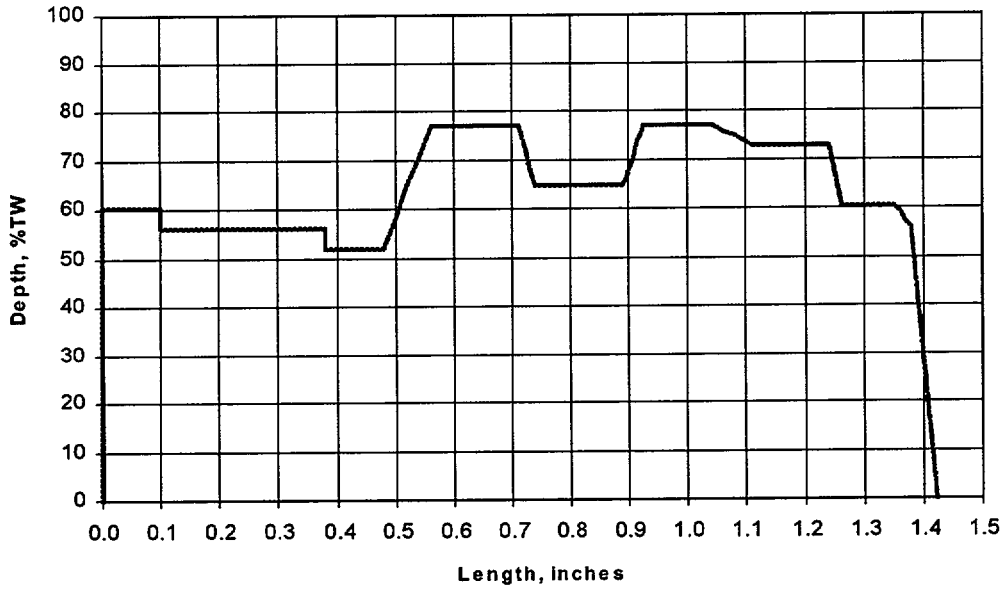

Type 6 EDM Profile

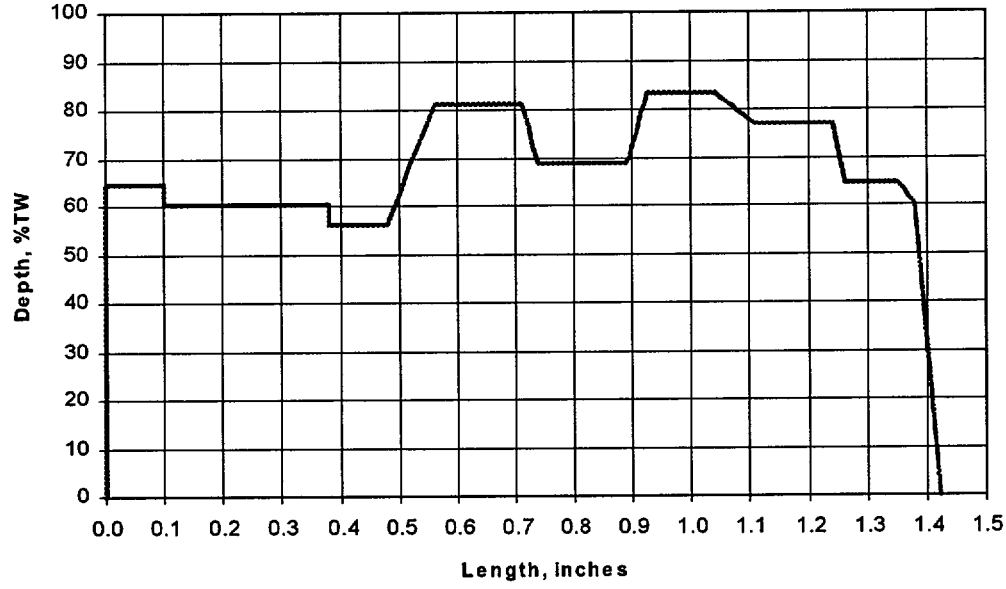

Type 7 EDM Profile

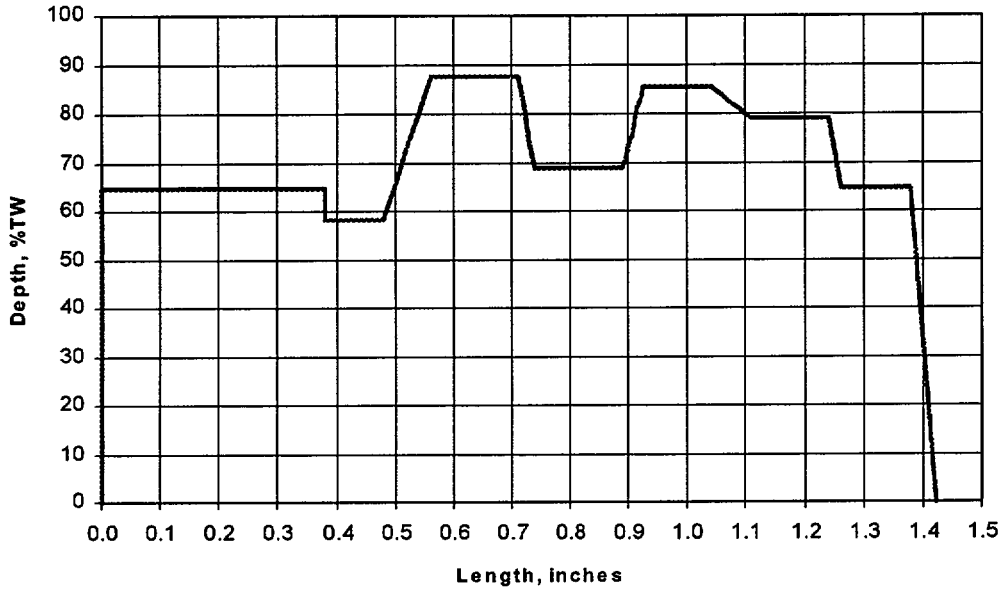

Type 8 EDM Profile

Type 9 EDM Profile

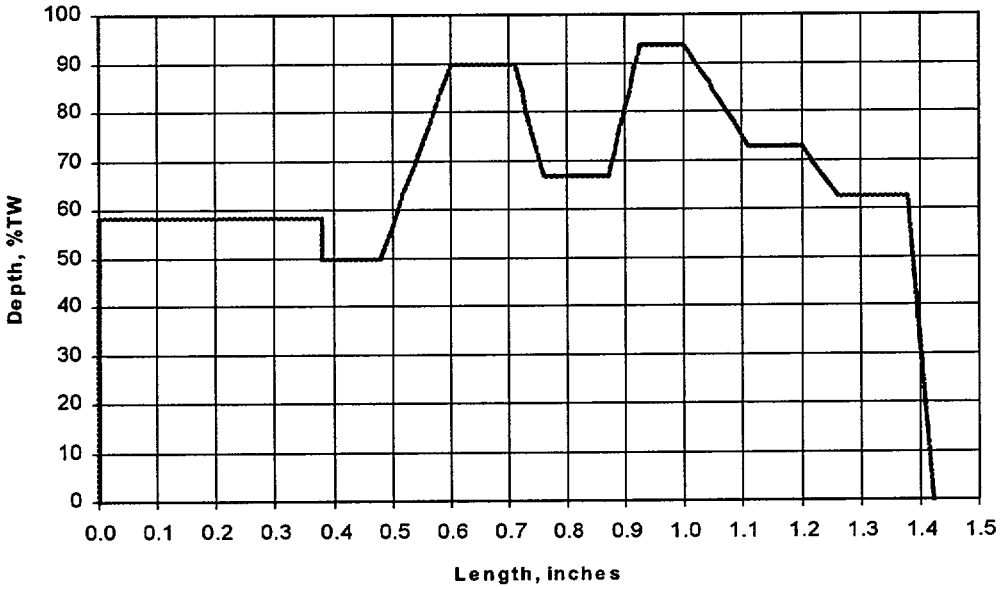

Type 10 EDM Profile

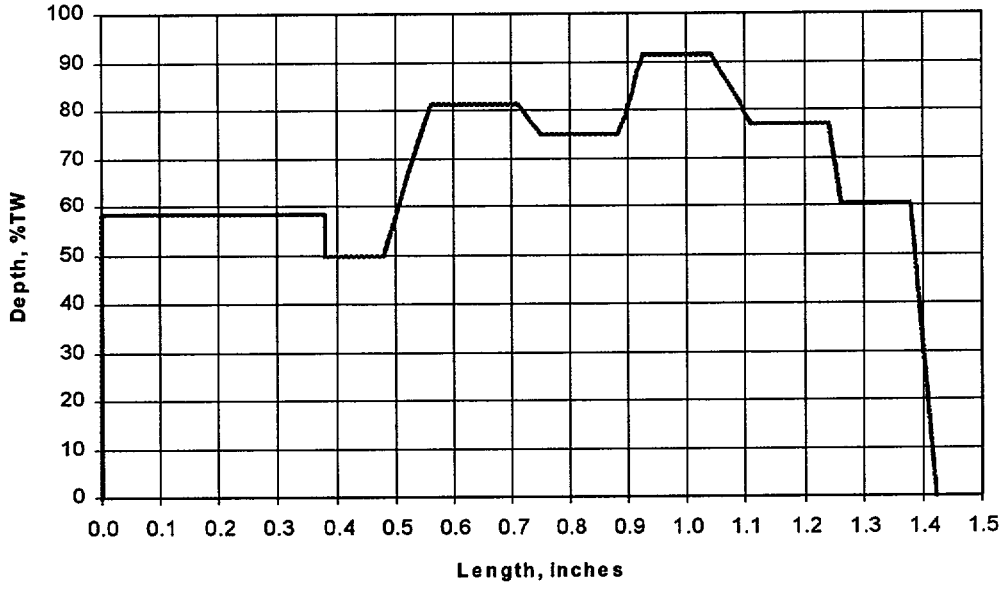

Type 11 EDM Profile

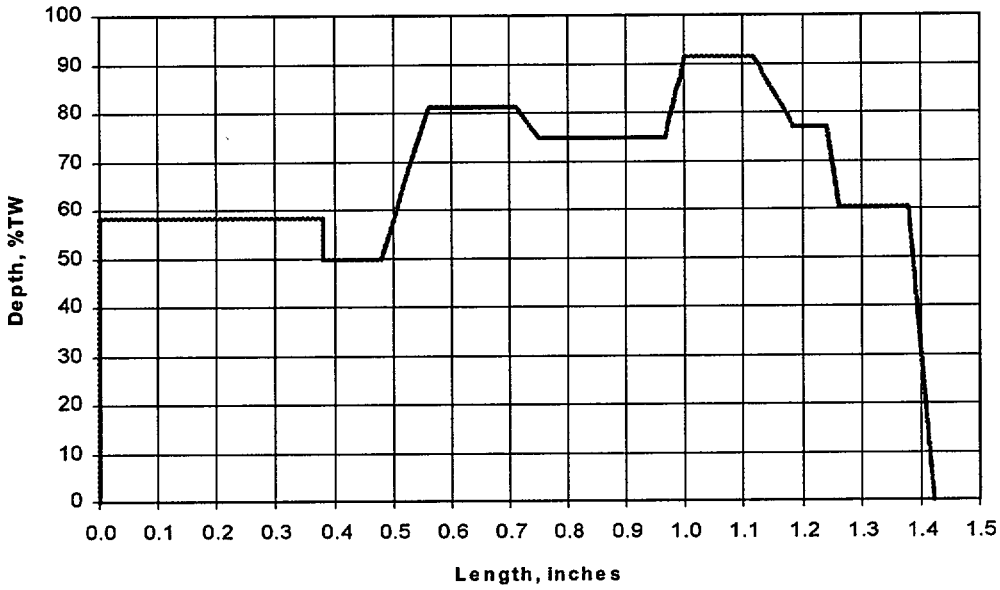

Type 12 EDM Profile

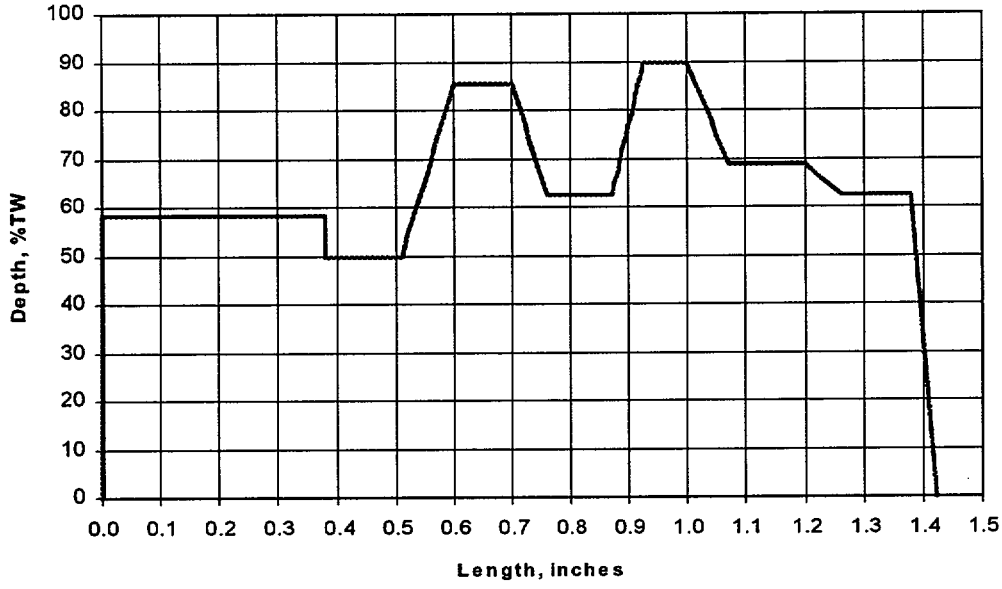

Type 13 EDM Profile

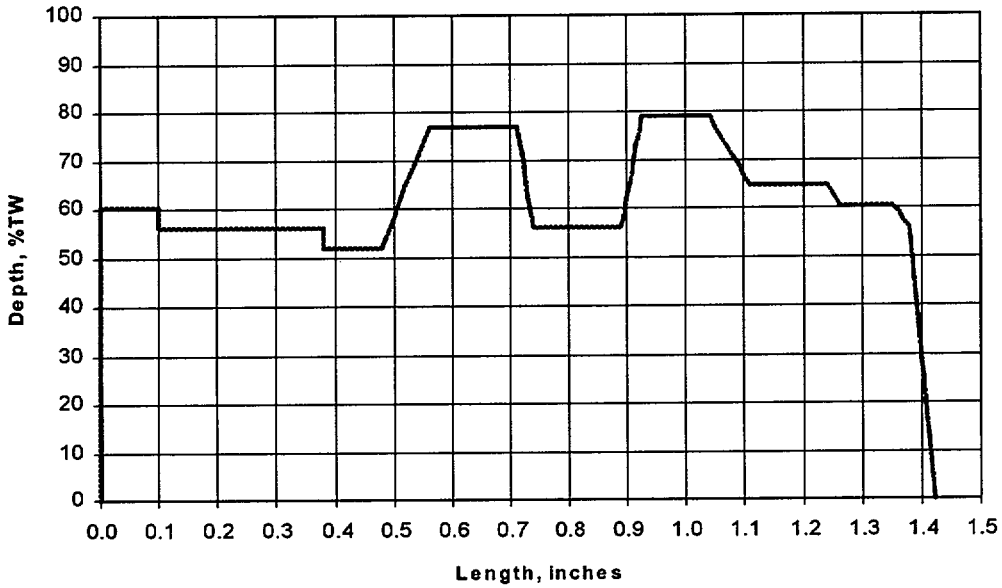

Type 14 EDM Profile

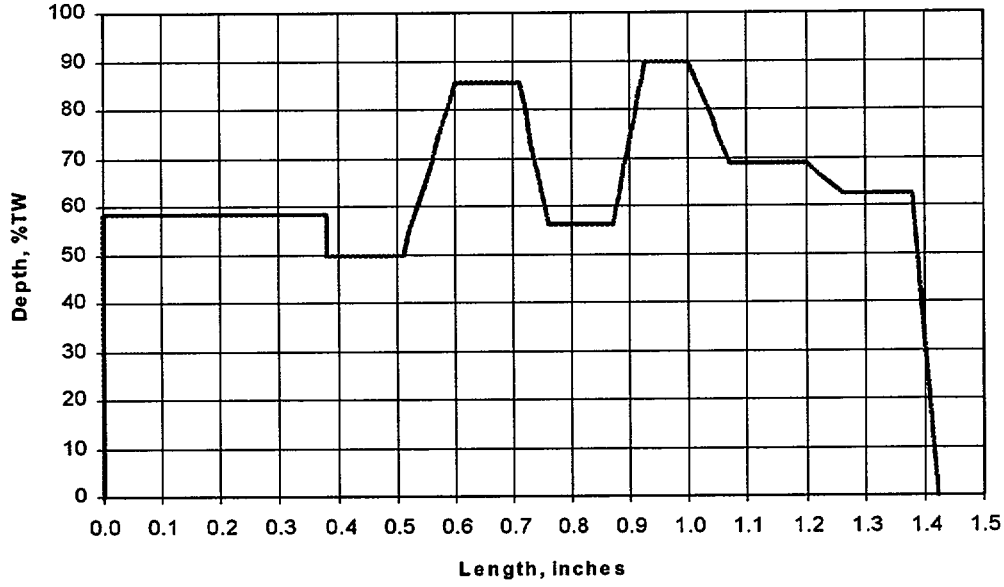

Type 15 EDM Profile

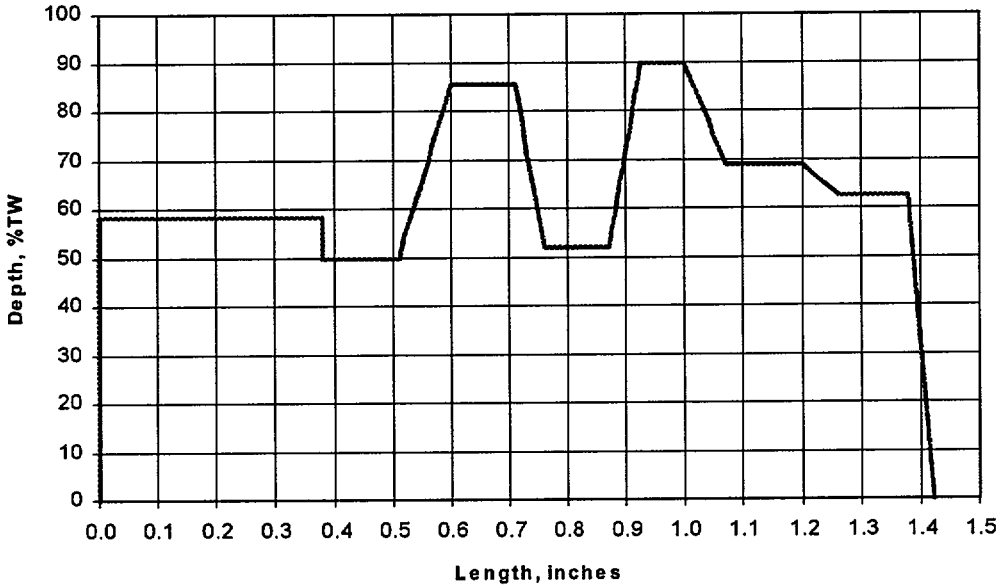

Type 16 EDM Profile

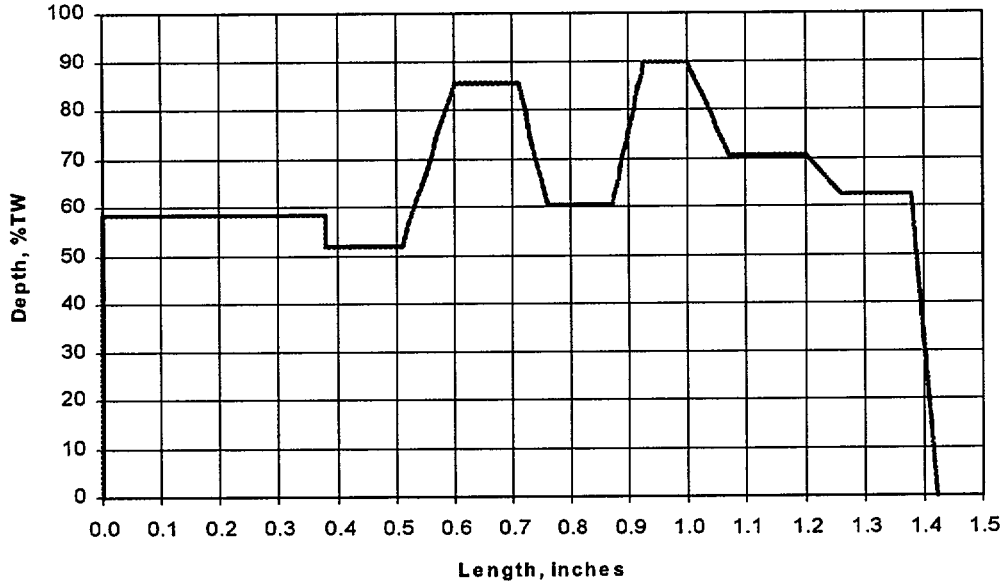

B
WESTINGHOUSE PRESSURE AND FLOW VS TIME PLOTS

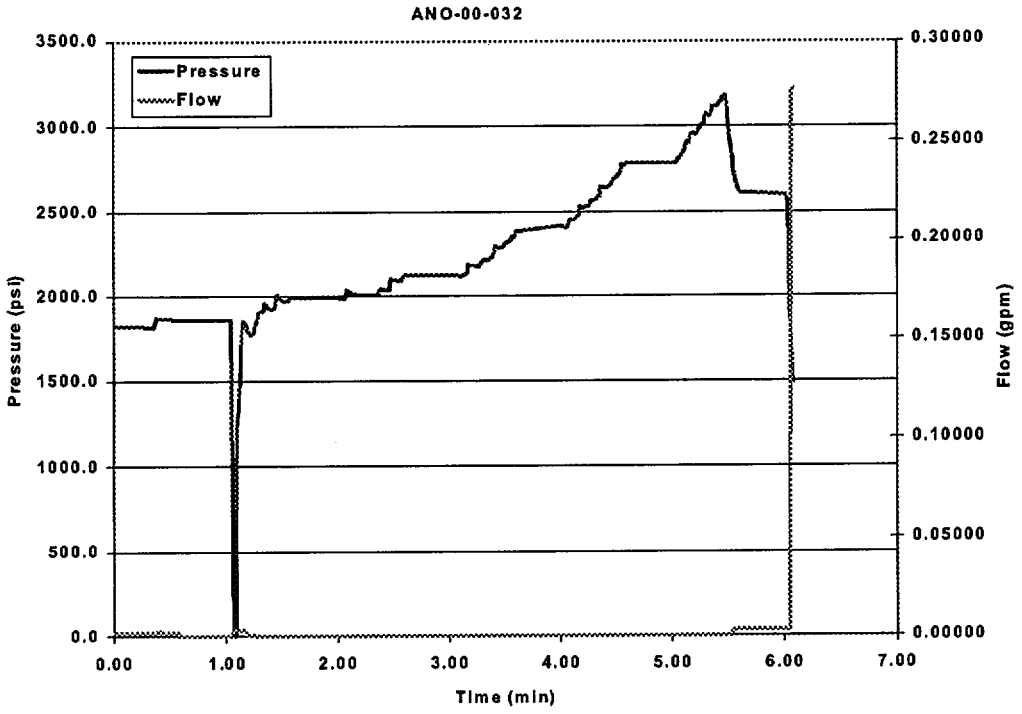
ANO-00-032
Pressure
Flow
3500.0
3000.0
2500.0
2000.0
1500.0
1000.0
500.0
0.0
Pressure (psi)
0.30000
0.25000
0.20000
0.15000
0.10000
0.05000
0.00000
Flow (gpm)
0.00
1.00
2.00
3.00
4.00
5.00
6.00
7.00
Time (min)

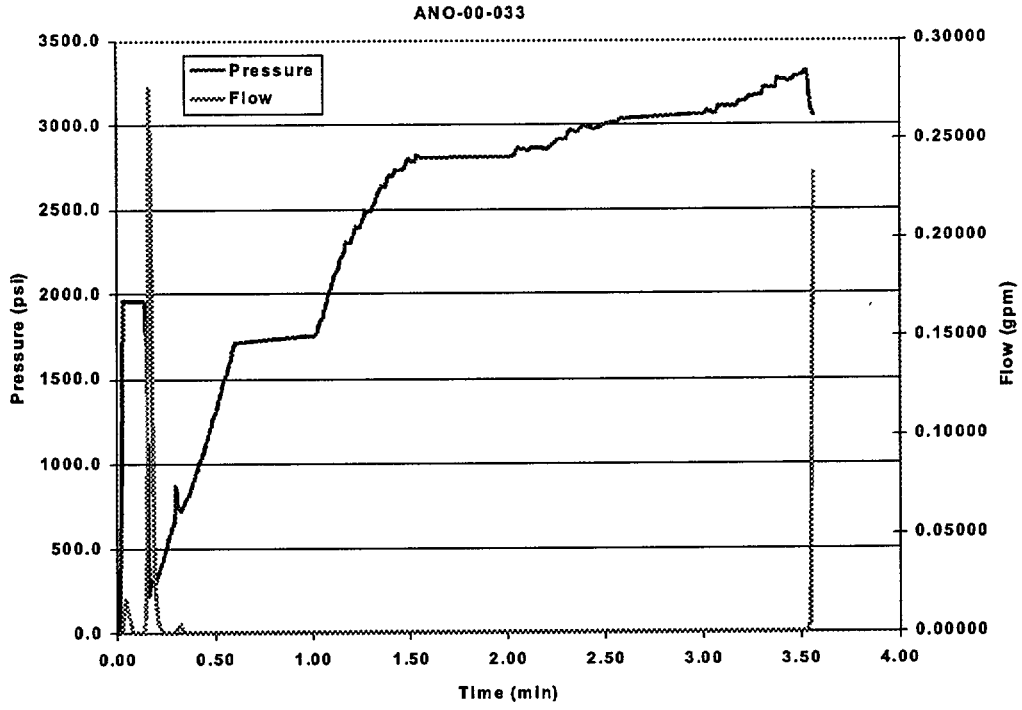
ANO-00-033
Pressure
Flow
3500.0
3000.0
2500.0
2000.0
1500.0
1000.0
500.0
0.0
Pressure (psi)
0.30000
0.25000
0.20000
0.15000
0.10000
0.05000
0.00000
Flow (gpm)
0.00
0.50
1.00
1.50
2.00
2.50
3.00
3.50
4.00
Time (min)

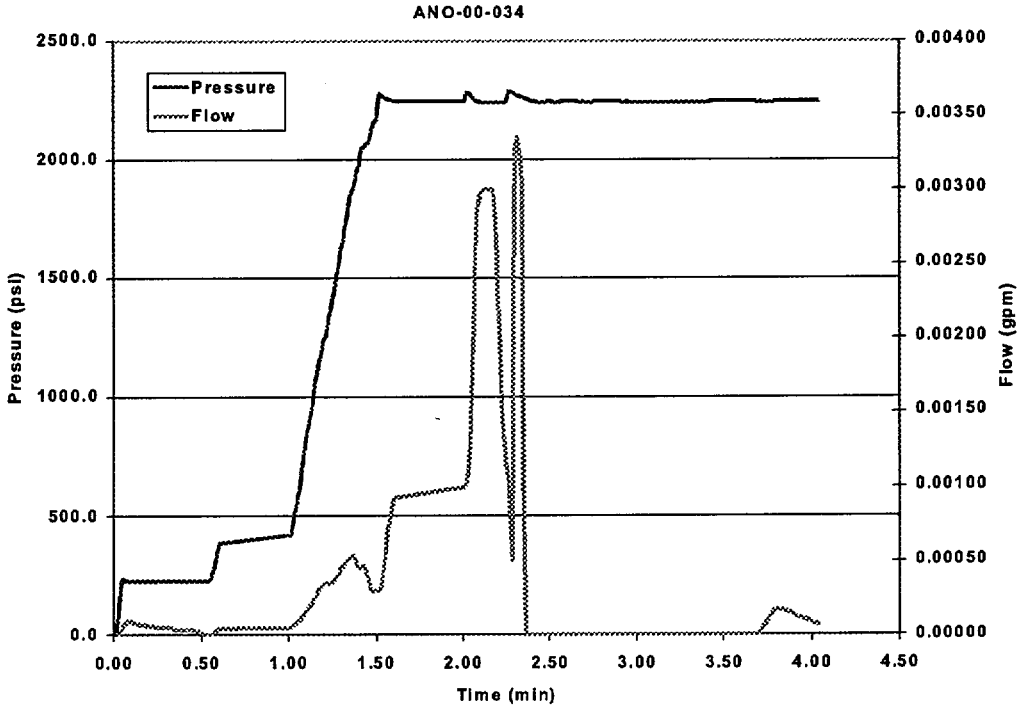
ANO-00-034
Pressure
Flow
Pressure (psi)
Flow (gpm)
Time (min)
2500.0
2000.0
1500.0
1000.0
500.0
0.0
0.00400
0.00350
0.00300
0.00250
0.00200
0.00150
0.00100
0.00050
0.00000
0.00
0.50
1.00
1.50
2.00
2.50
3.00
3.50
4.00
4.50

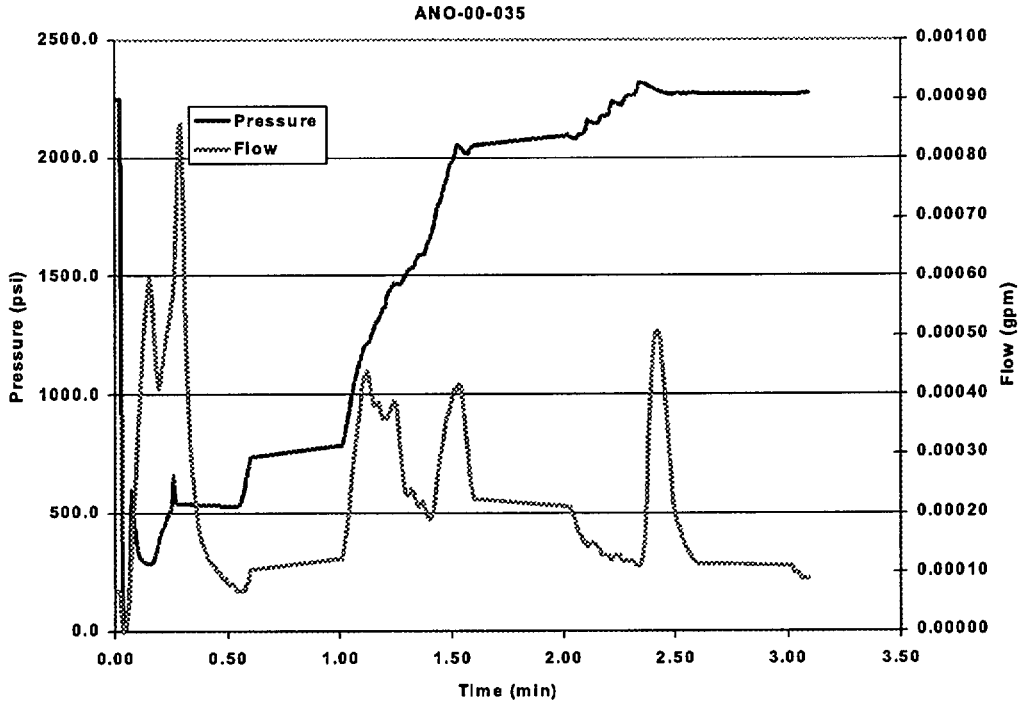
ANO-00-035
Pressure
Flow
Pressure (psi)
Flow (gpm)
Time (min)
2500.0
2000.0
1500.0
1000.0
500.0
0.0
0.00100
0.00090
0.00080
0.00070
0.00060
0.00050
0.00040
0.00030
0.00020
0.00010
0.00000
0.00
0.50
1.00
1.50
2.00
2.50
3.00
3.50

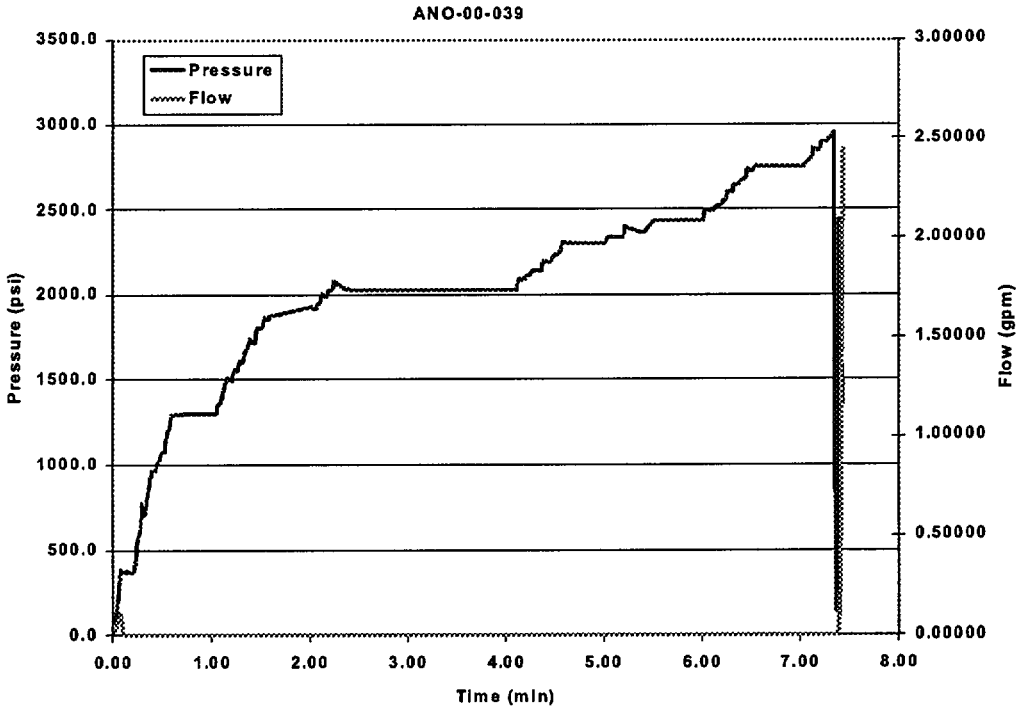
ANO-00-039
Pressure
Flow
3500.0
3000.0
2500.0
2000.0
1500.0
1000.0
500.0
0.0
Pressure (psi)
3.00000
2.50000
2.00000
1.50000
1.00000
0.50000
0.00000
Flow (gpm)
0.00
1.00
2.00
3.00
4.00
5.00
6.00
7.00
8.00
Time (min)

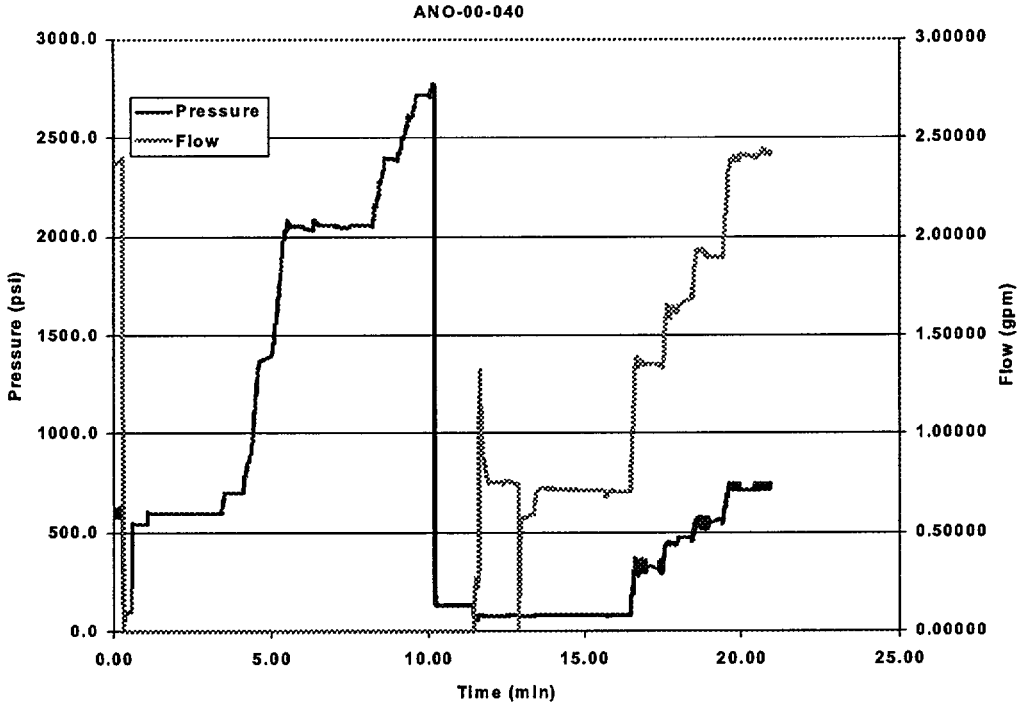
ANO-00-040
Pressure
Flow
3000.0
2500.0
2000.0
1500.0
1000.0
500.0
0.0
Pressure (psi)
3.00000
2.50000
2.00000
1.50000
1.00000
0.50000
0.00000
Flow (gpm)
0.00
5.00
10.00
15.00
20.00
25.00
Time (min)

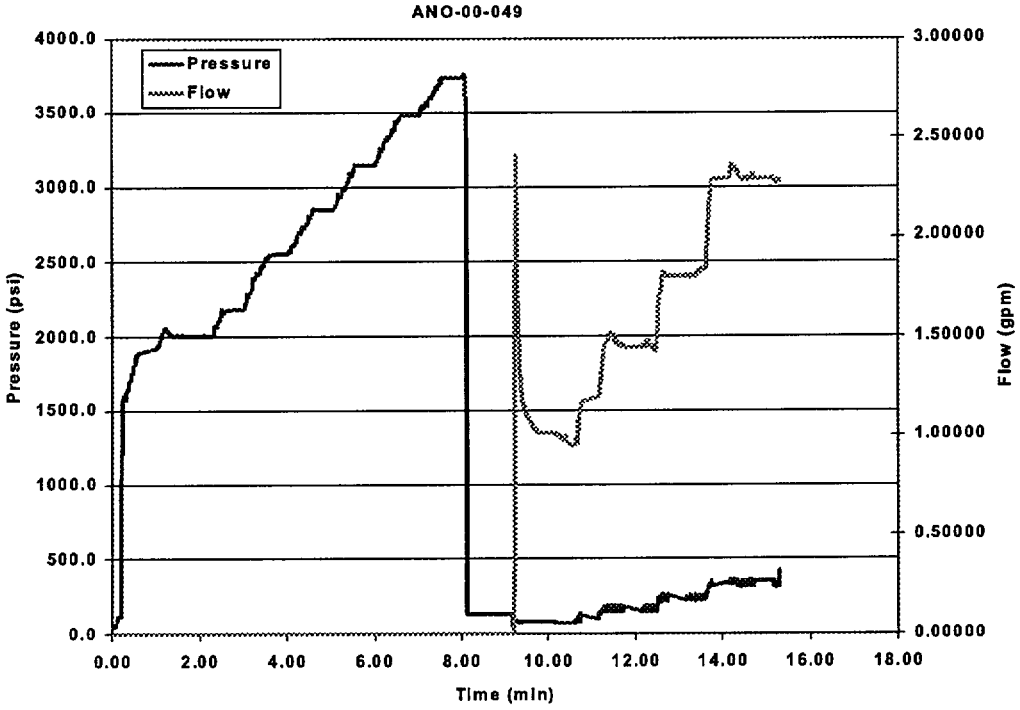
ANO-00-049
Pressure
Flow
Pressure (psi)
Flow (gpm)
Time (min)
4000.0
3500.0
3000.0
2500.0
2000.0
1500.0
1000.0
500.0
0.0
3.00000
2.50000
2.00000
1.50000
1.00000
0.50000
0.00000
0.00
2.00
4.00
6.00
8.00
10.00
12.00
14.00
16.00
18.00

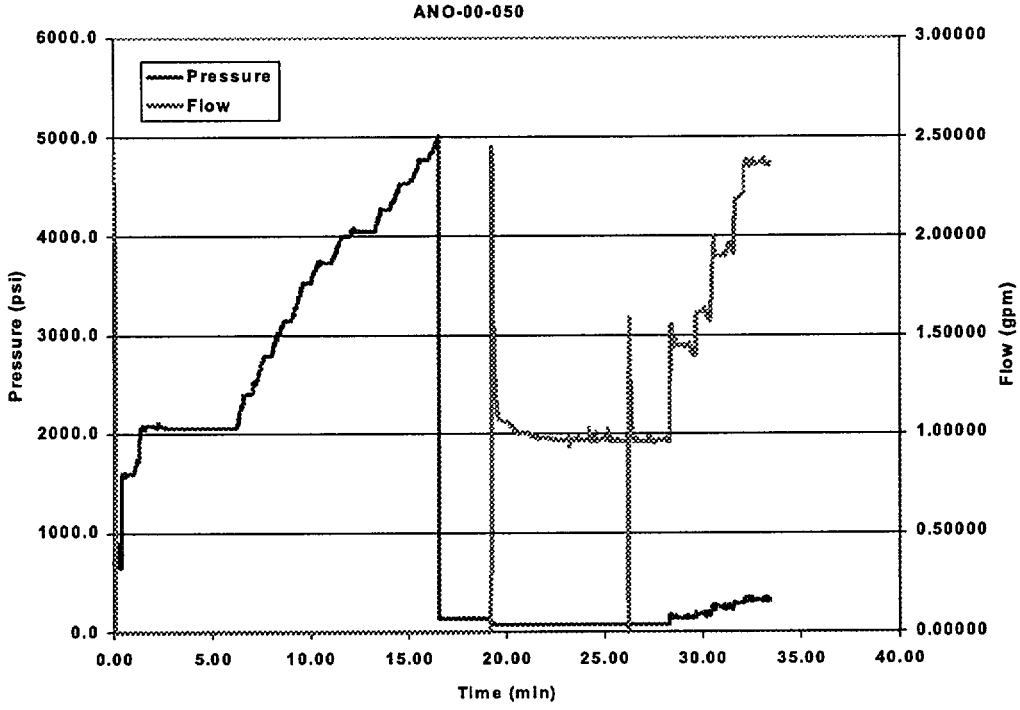
ANO-00-050
Pressure
Flow
Pressure (psi)
Flow (gpm)
Time (min)
6000.0
5000.0
4000.0
3000.0
2000.0
1000.0
0.0
3.00000
2.50000
2.00000
1.50000
1.00000
0.50000
0.00000
0.00
5.00
10.00
15.00
20.00
25.00
30.00
35.00
40.00

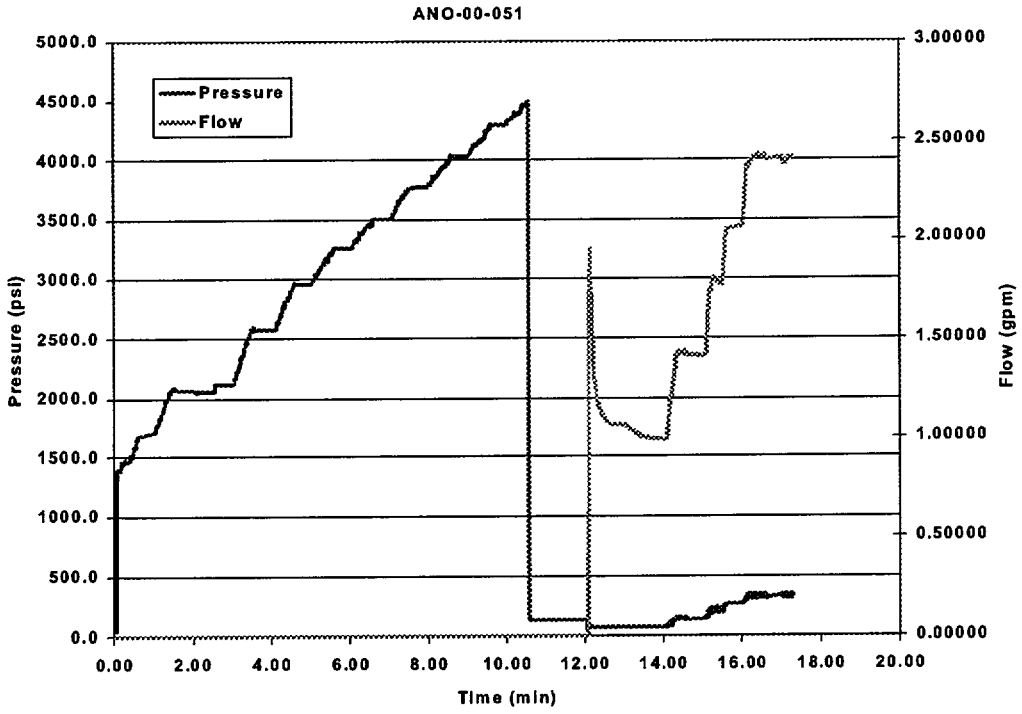
ANO-00-051
Pressure
Flow
Pressure (psi)
Flow (gpm)
Time (min)
5000.0
4500.0
4000.0
3500.0
3000.0
2500.0
2000.0
1500.0
1000.0
500.0
0.0
3.00000
2.50000
2.00000
1.50000
1.00000
0.50000
0.00000
0.00
2.00
4.00
6.00
8.00
10.00
12.00
14.00
16.00
18.00
20.00

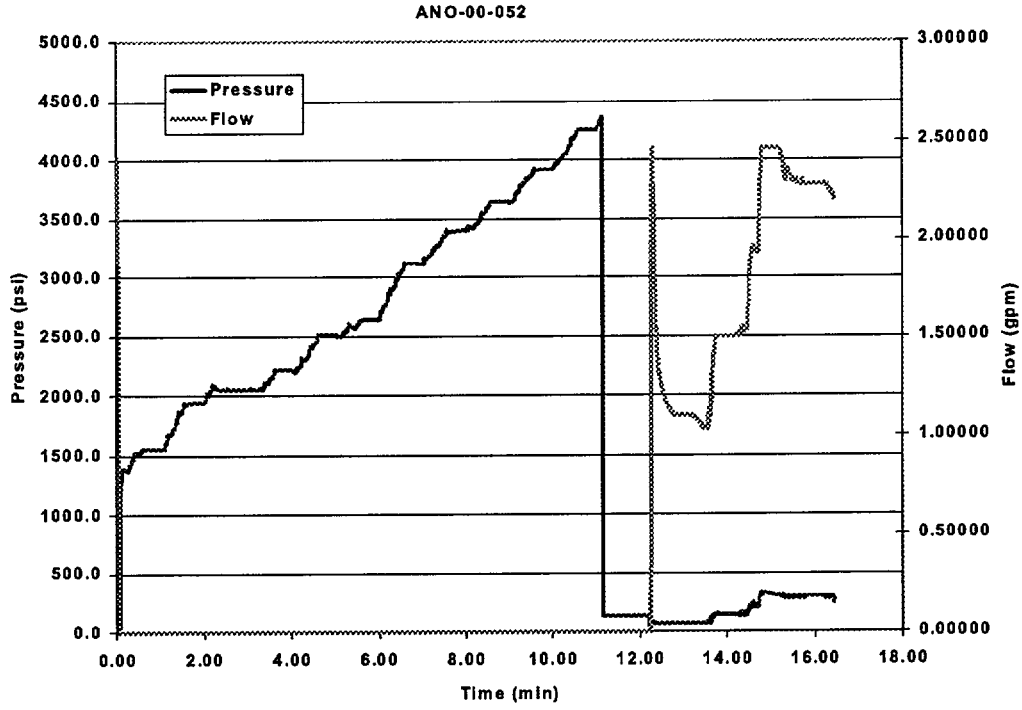
ANO-00-052
Pressure
Flow
Pressure (psi)
Flow (gpm)
Time (min)
5000.0
4500.0
4000.0
3500.0
3000.0
2500.0
2000.0
1500.0
1000.0
500.0
0.0
3.00000
2.50000
2.00000
1.50000
1.00000
0.50000
0.00000
0.00
2.00
4.00
6.00
8.00
10.00
12.00
14.00
16.00
18.00

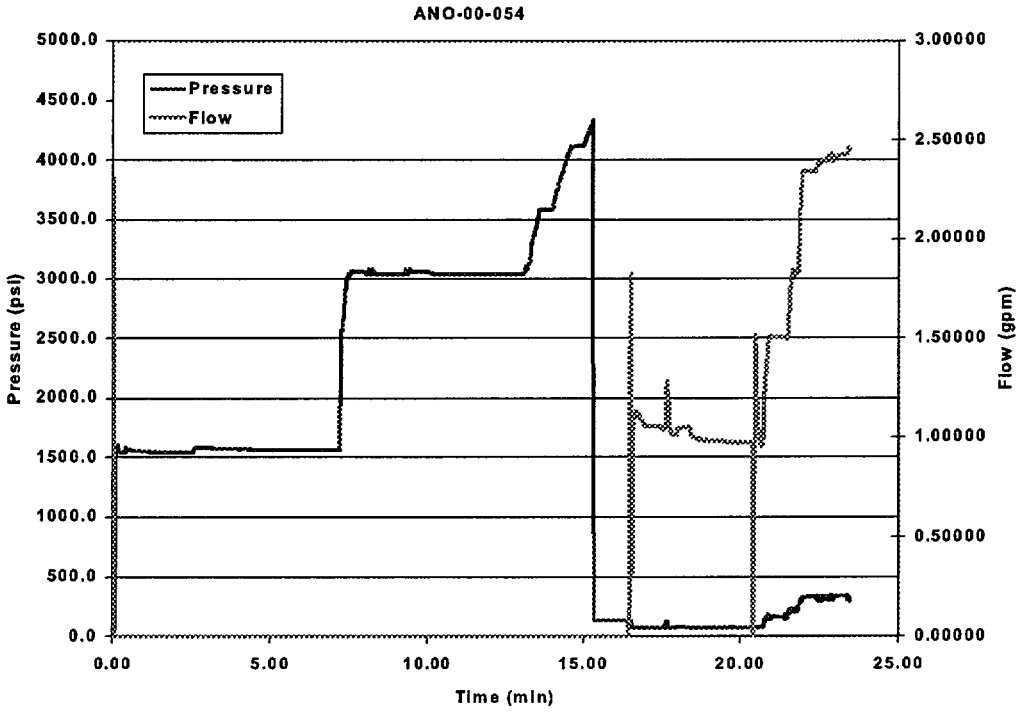
ANO-00-054
Pressure
Flow
5000.0
4500.0
4000.0
3500.0
3000.0
2500.0
2000.0
1500.0
1000.0
500.0
0.0
Pressure (psi)
3.00000
2.50000
2.00000
1.50000
1.00000
0.50000
0.00000
Flow (gpm)
0.00
5.00
10.00
15.00
20.00
25.00
Time (min)

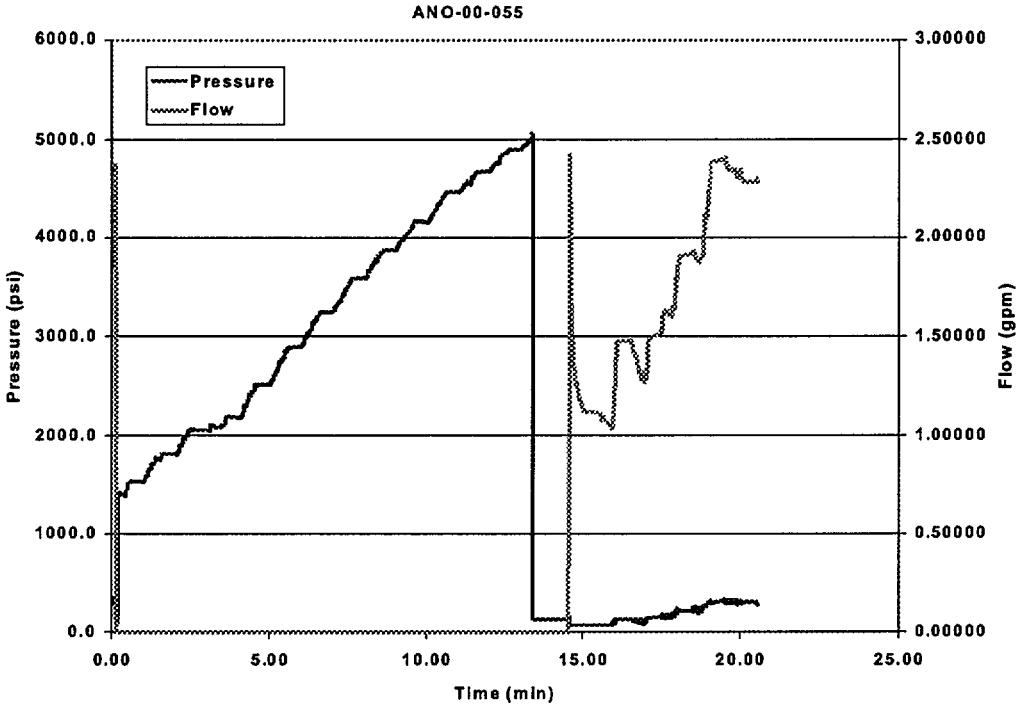
ANO-00-055
Pressure
Flow
6000.0
5000.0
4000.0
3000.0
2000.0
1000.0
0.0
Pressure (psi)
3.00000
2.50000
2.00000
1.50000
1.00000
0.50000
0.00000
Flow (gpm)
0.00
5.00
10.00
15.00
20.00
25.00
Time (min)

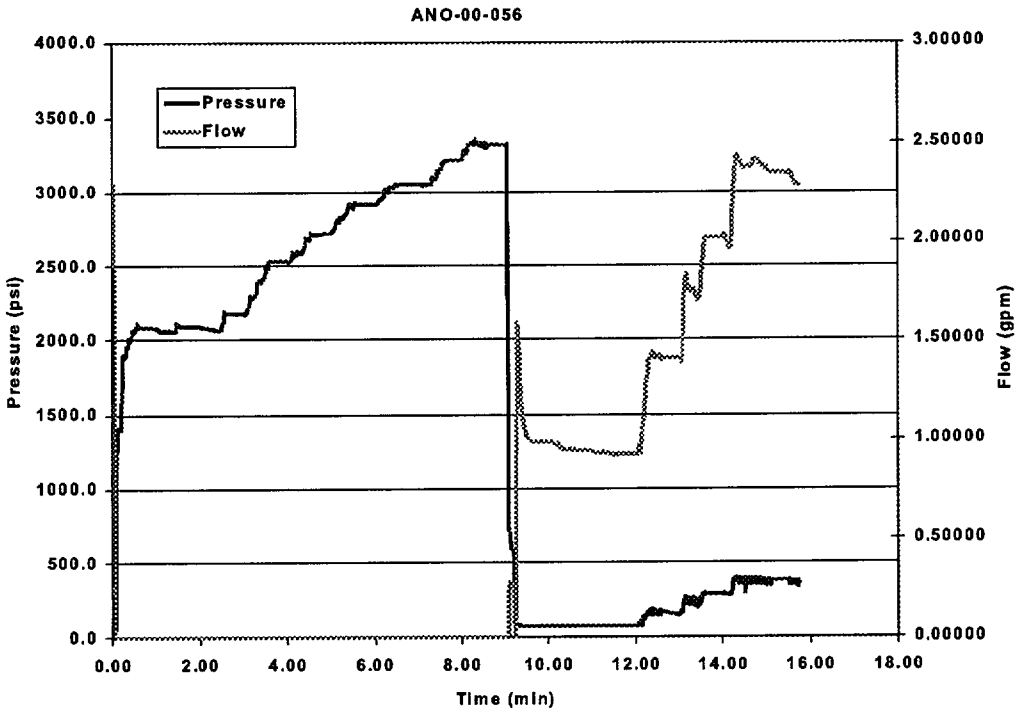
ANO-00-056
Pressure
Flow
Pressure (psi)
Flow (gpm)
Time (min)
4000.0
3500.0
3000.0
2500.0
2000.0
1500.0
1000.0
500.0
0.0
3.00000
2.50000
2.00000
1.50000
1.00000
0.50000
0.00000
0.00
2.00
4.00
6.00
8.00
10.00
12.00
14.00
16.00
18.00

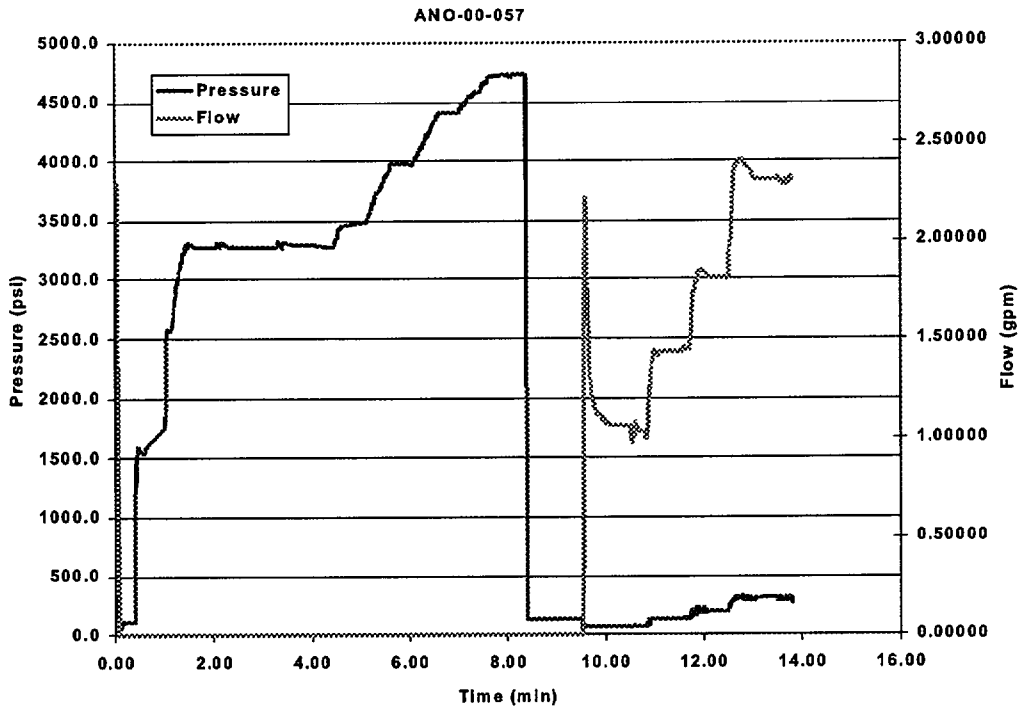
ANO-00-057
Pressure
Flow
Pressure (psi)
Flow (gpm)
Time (min)
5000.0
4500.0
4000.0
3500.0
3000.0
2500.0
2000.0
1500.0
1000.0
500.0
0.0
3.00000
2.50000
2.00000
1.50000
1.00000
0.50000
0.00000
0.00
2.00
4.00
6.00
8.00
10.00
12.00
14.00
16.00

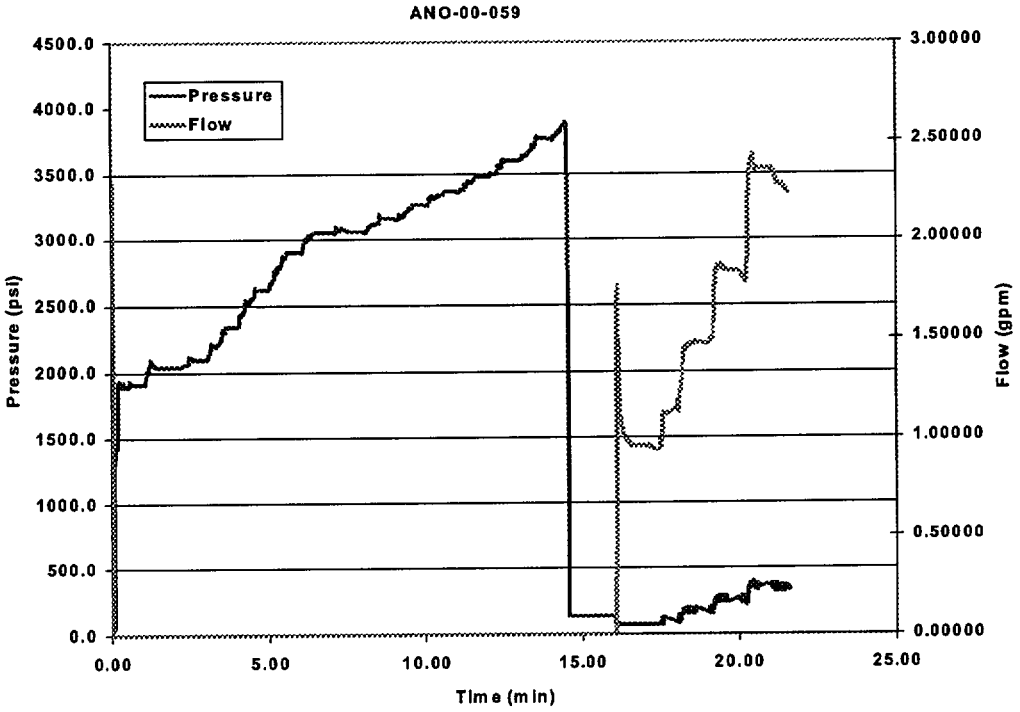
ANO-00-059
Pressure
Flow
4500.0
4000.0
3500.0
3000.0
2500.0
2000.0
1500.0
1000.0
500.0
0.0
Pressure (psi)
3.00000
2.50000
2.00000
1.50000
1.00000
0.50000
0.00000
Flow (gpm)
0.00
5.00
10.00
15.00
20.00
25.00
Time (min)

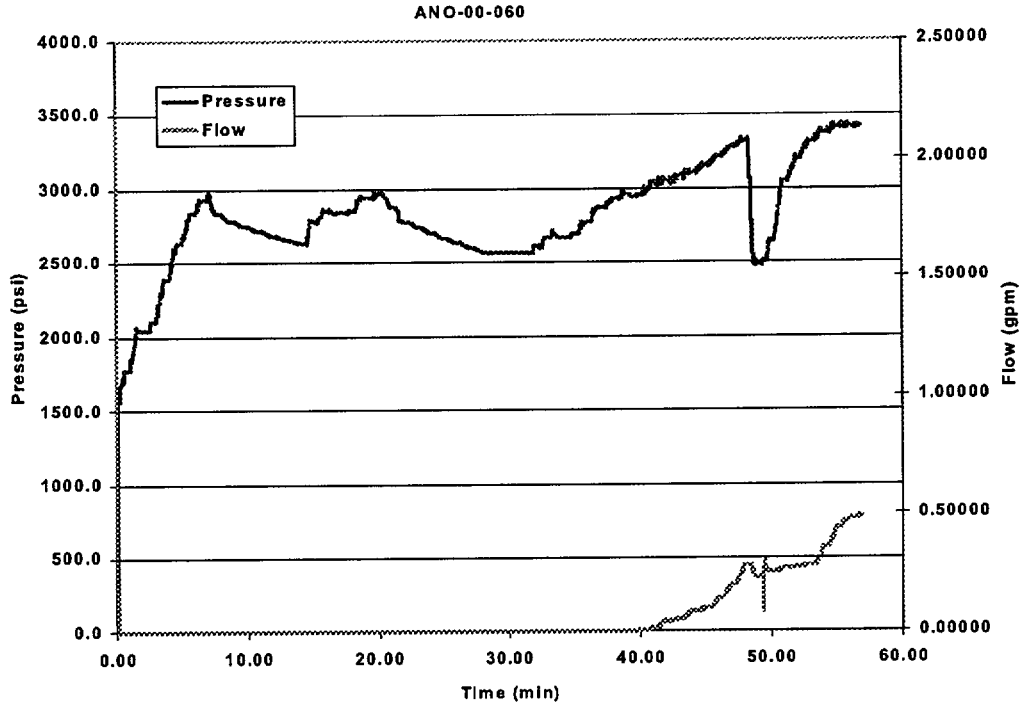
ANO-00-060
Pressure
Flow
4000.0
3500.0
3000.0
2500.0
2000.0
1500.0
1000.0
500.0
0.0
Pressure (psi)
2.50000
2.00000
1.50000
1.00000
0.50000
0.00000
Flow (gpm)
0.00
10.00
20.00
30.00
40.00
50.00
60.00
Time (min)

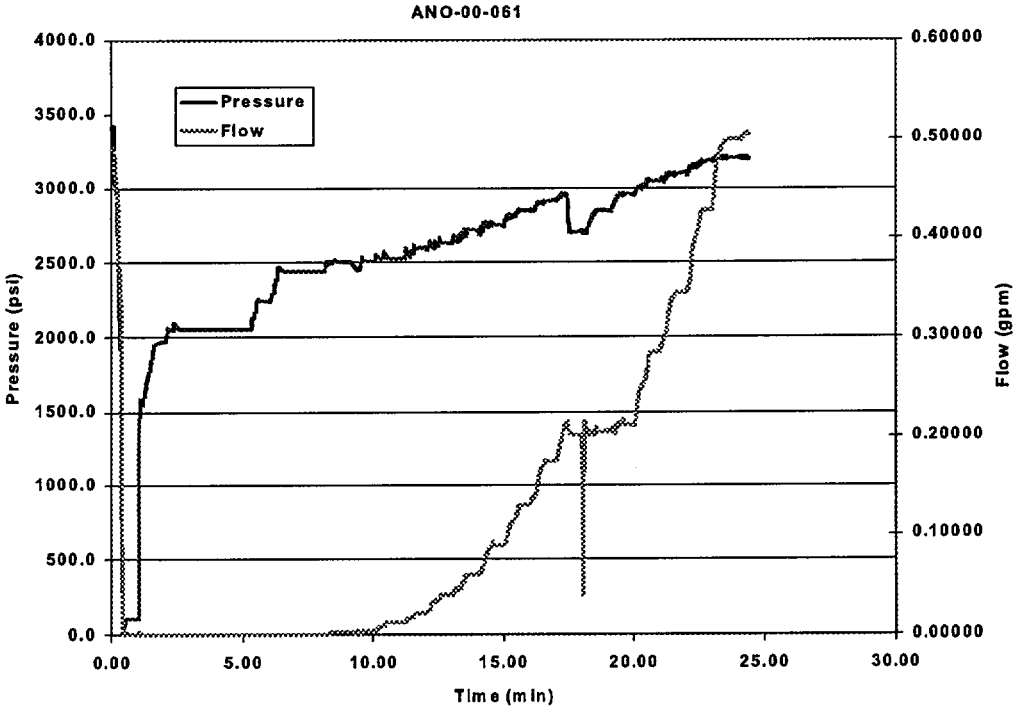
ANO-00-061
Pressure
Flow
Pressure (psi)
Flow (gpm)
Time (min)
4000.0
3500.0
3000.0
2500.0
2000.0
1500.0
1000.0
500.0
0.0
0.60000
0.50000
0.40000
0.30000
0.20000
0.10000
0.00000
0.00
5.00
10.00
15.00
20.00
25.00
30.00

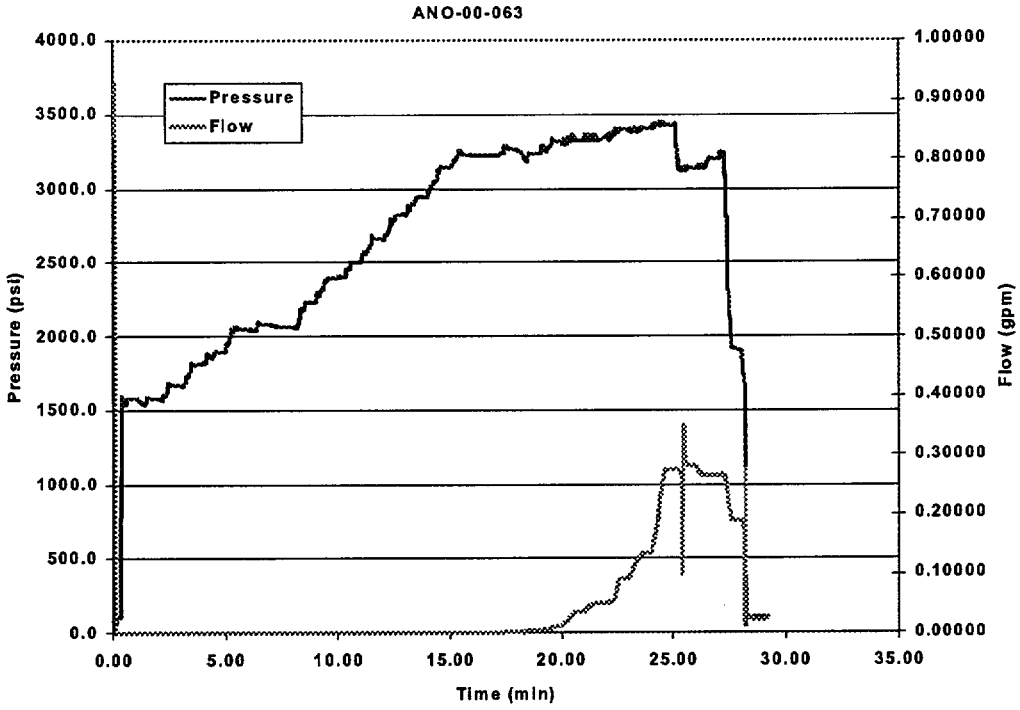
ANO-00-063
Pressure
Flow
Pressure (psi)
Flow (gpm)
Time (min)
4000.0
3500.0
3000.0
2500.0
2000.0
1500.0
1000.0
500.0
0.0
1.00000
0.90000
0.80000
0.70000
0.60000
0.50000
0.40000
0.30000
0.20000
0.10000
0.00000
0.00
5.00
10.00
15.00
20.00
25.00
30.00
35.00

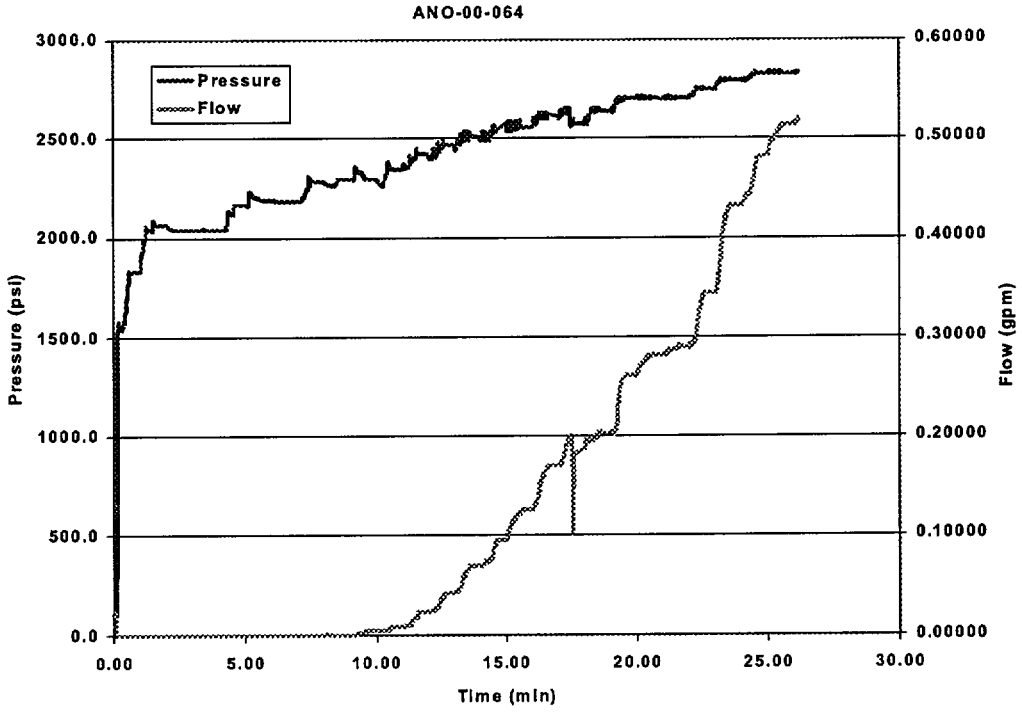
ANO-00-064
Pressure
Flow
Pressure (psi)
Flow (gpm)
Time (min)
3000.0
2500.0
2000.0
1500.0
1000.0
500.0
0.0
0.60000
0.50000
0.40000
0.30000
0.20000
0.10000
0.00000
0.00
5.00
10.00
15.00
20.00
25.00
30.00

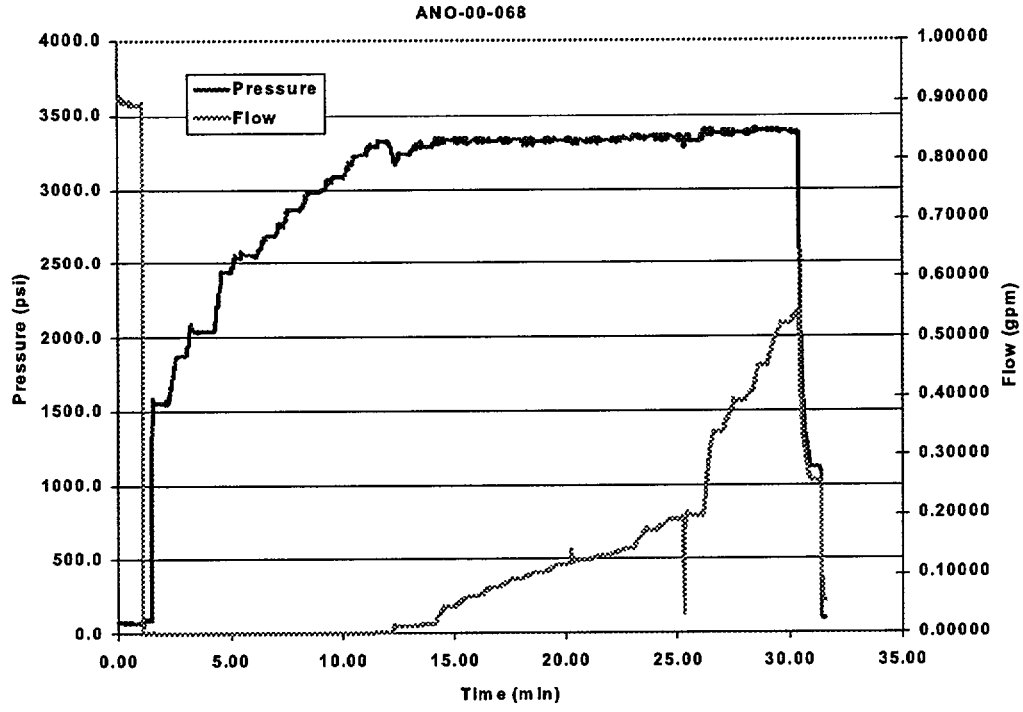
ANO-00-068
Pressure
Flow
Pressure (psi)
Flow (gpm)
Time (min)
4000.0
3500.0
3000.0
2500.0
2000.0
1500.0
1000.0
500.0
0.0
1.00000
0.90000
0.80000
0.70000
0.60000
0.50000
0.40000
0.30000
0.20000
0.10000
0.00000
0.00
5.00
10.00
15.00
20.00
25.00
30.00
35.00

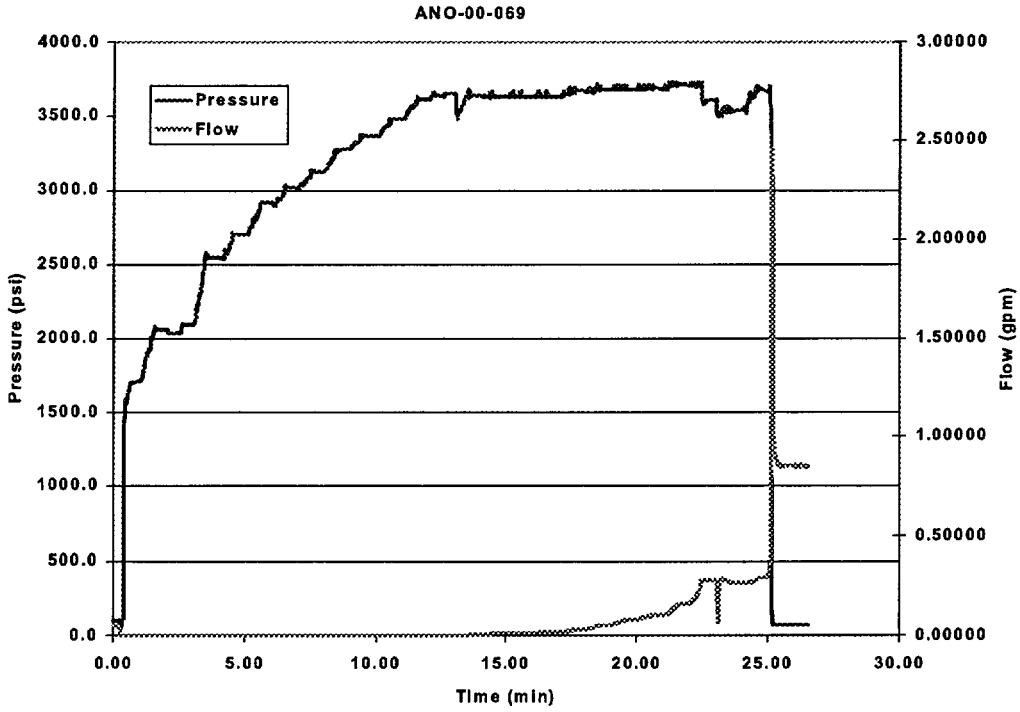
ANO-00-069
Pressure
Flow
4000.0
3500.0
3000.0
2500.0
2000.0
1500.0
1000.0
500.0
0.0
Pressure (psi)
3.00000
2.50000
2.00000
1.50000
1.00000
0.50000
0.00000
Flow (gpm)
0.00
5.00
10.00
15.00
20.00
25.00
30.00
Time (min)

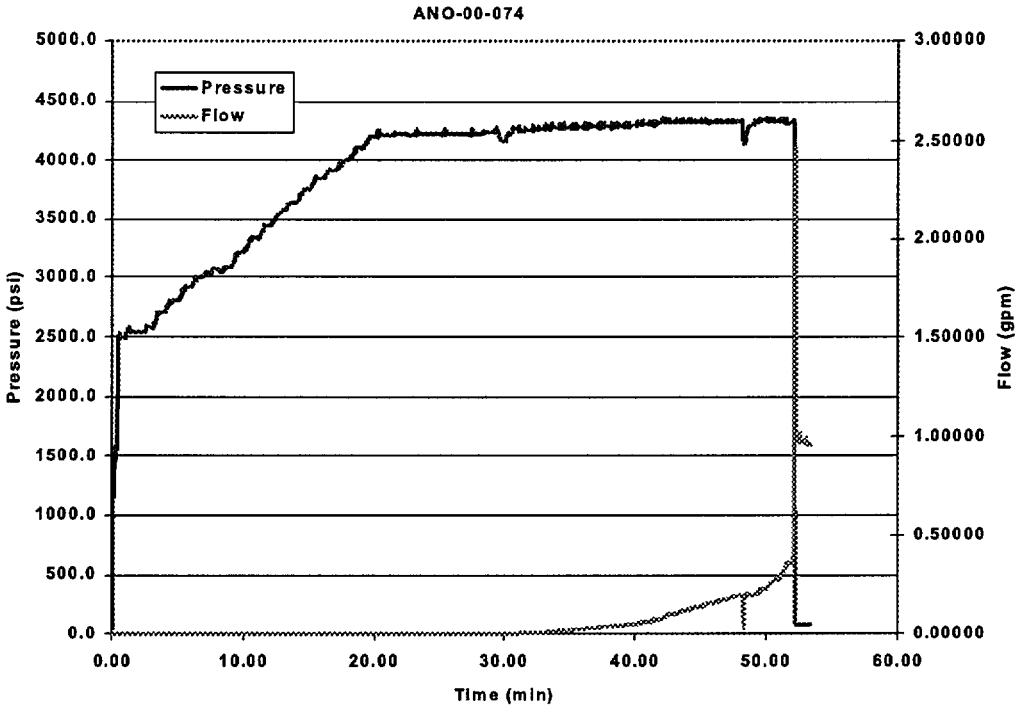
ANO-00-074
Pressure
Flow
5000.0
4500.0
4000.0
3500.0
3000.0
2500.0
2000.0
1500.0
1000.0
500.0
0.0
Pressure (psi)
3.00000
2.50000
2.00000
1.50000
1.00000
0.50000
0.00000
Flow (gpm)
0.00
10.00
20.00
30.00
40.00
50.00
60.00
Time (min)

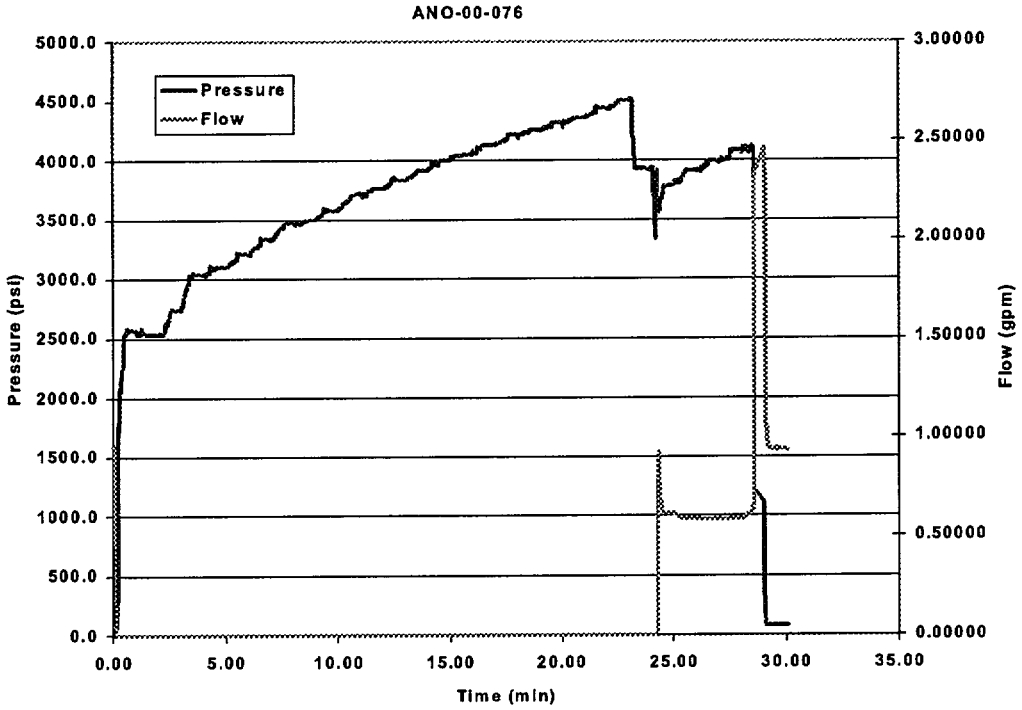
ANO-00-076
Pressure
Flow
Pressure (psi)
Flow (gpm)
Time (min)
5000.0
4500.0
4000.0
3500.0
3000.0
2500.0
2000.0
1500.0
1000.0
500.0
0.0
3.00000
2.50000
2.00000
1.50000
1.00000
0.50000
0.00000
0.00
5.00
10.00
15.00
20.00
25.00
30.00
35.00

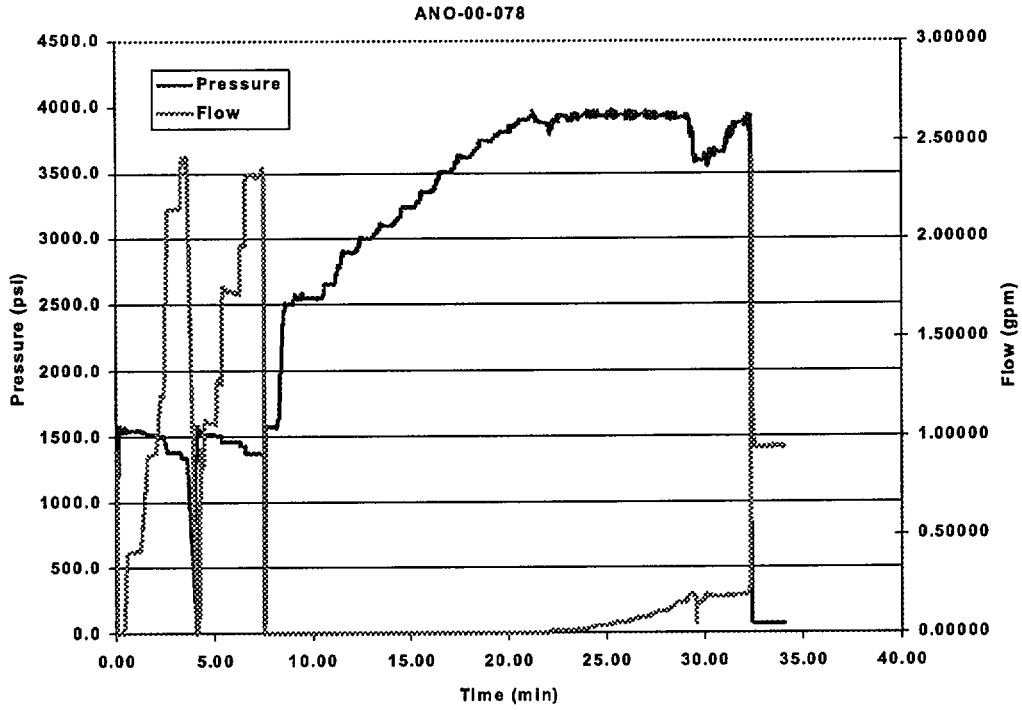
ANO-00-078
Pressure
Flow
Pressure (psi)
Flow (gpm)
Time (min)
4500.0
4000.0
3500.0
3000.0
2500.0
2000.0
1500.0
1000.0
500.0
0.0
3.00000
2.50000
2.00000
1.50000
1.00000
0.50000
0.00000
0.00
5.00
10.00
15.00
20.00
25.00
30.00
35.00
40.00

Westinghouse Pressure and Flow vs Time Plots

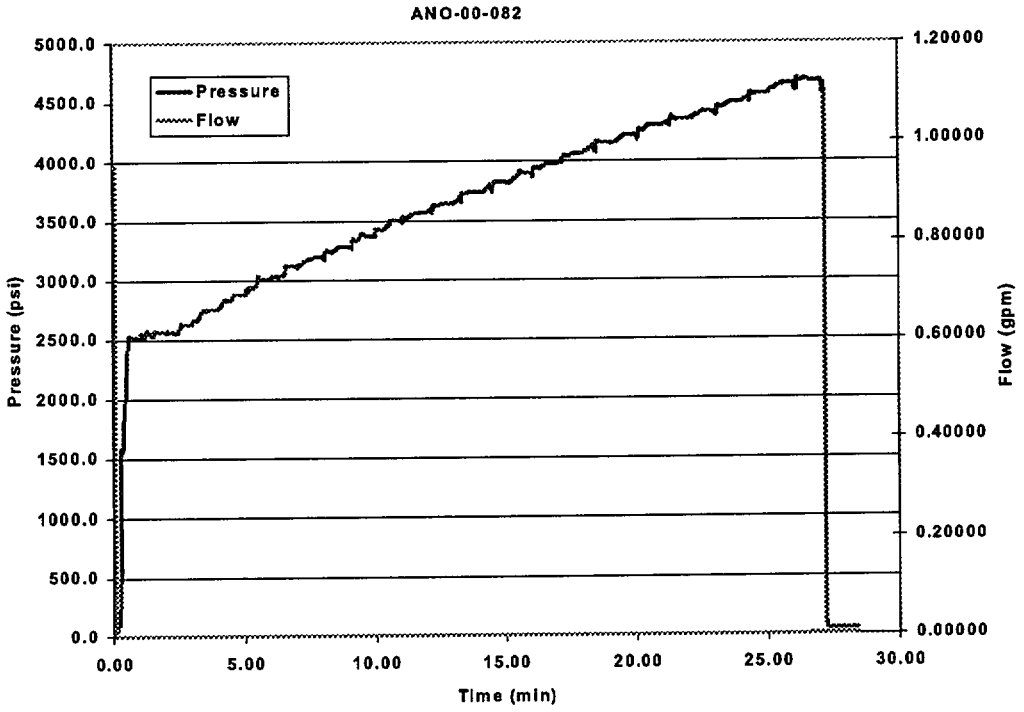

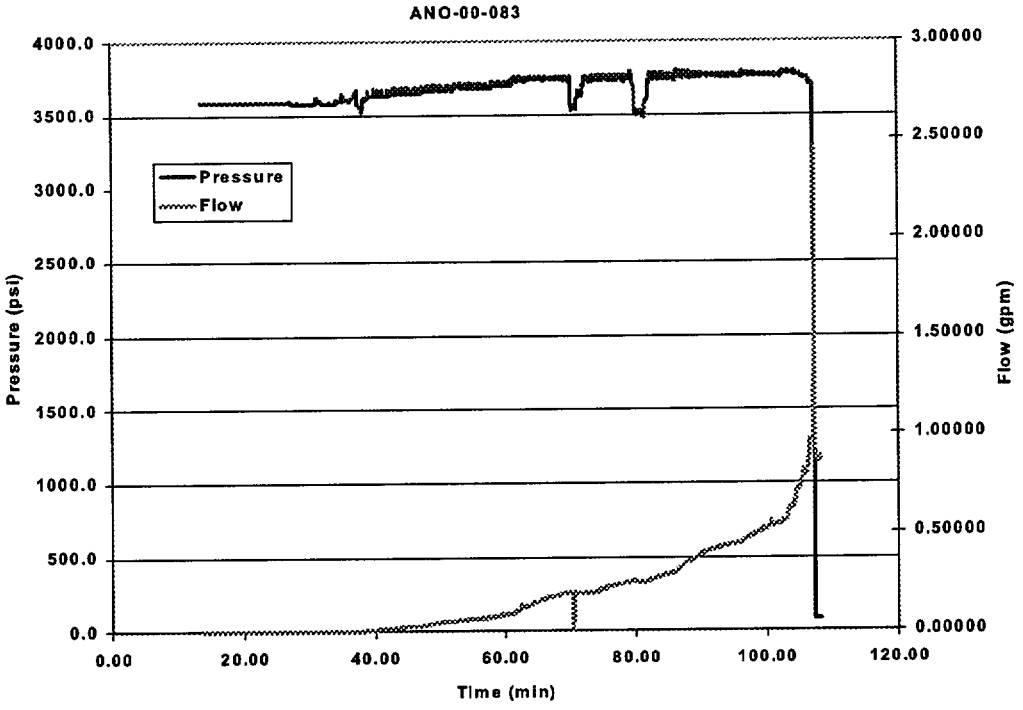

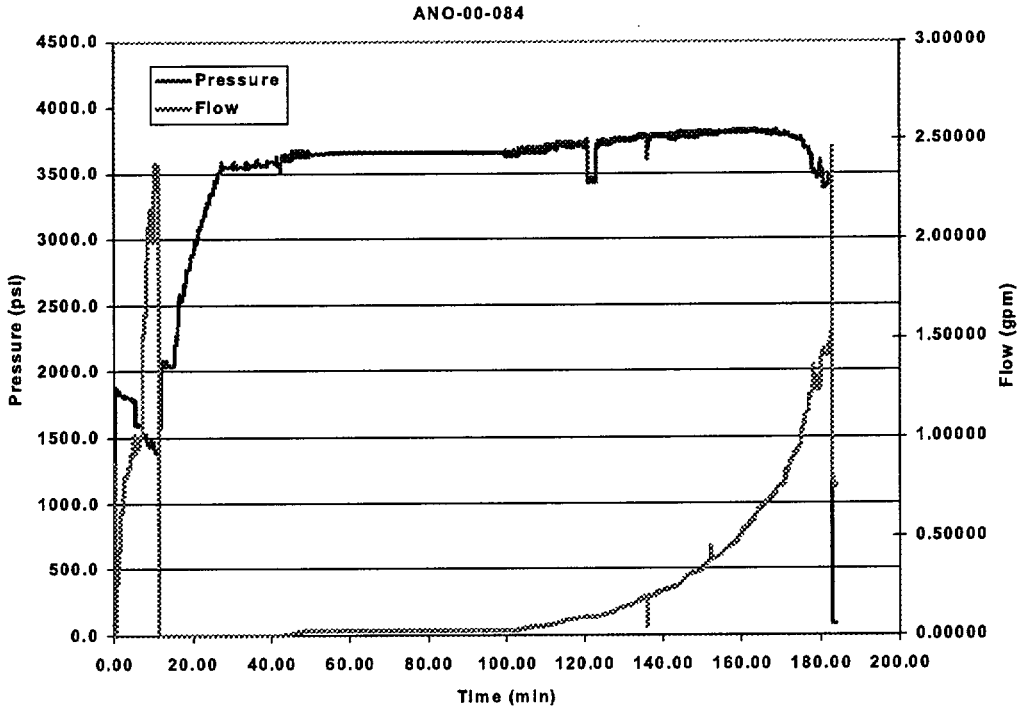
ANO-00-084
Pressure
Flow
Pressure (psi)
Flow (gpm)
Time (min)
4500.0
4000.0
3500.0
3000.0
2500.0
2000.0
1500.0
1000.0
500.0
0.0
3.00000
2.50000
2.00000
1.50000
1.00000
0.50000
0.00000
0.00
20.00
40.00
60.00
80.00
100.00
120.00
140.00
160.00
180.00
200.00

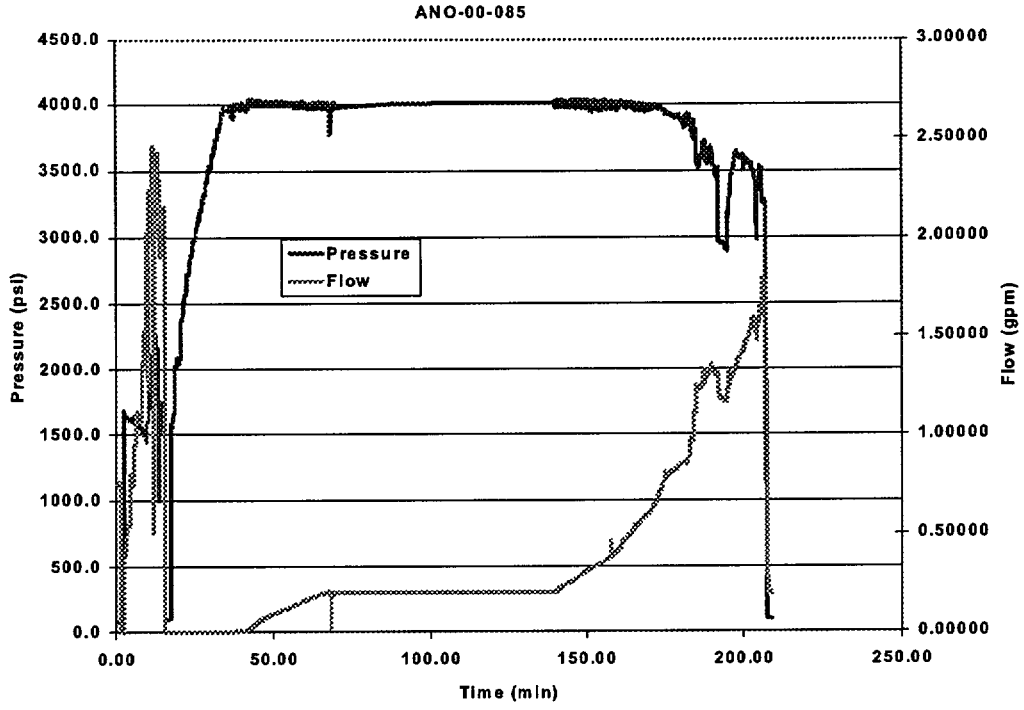
ANO-00-085
Pressure
Flow
Pressure (psi)
Flow (gpm)
Time (min)
4500.0
4000.0
3500.0
3000.0
2500.0
2000.0
1500.0
1000.0
500.0
0.0
3.00000
2.50000
2.00000
1.50000
1.00000
0.50000
0.00000
0.00
50.00
100.00
150.00
200.00
250.00

Westinghouse Pressure and Flow vs Time Plots

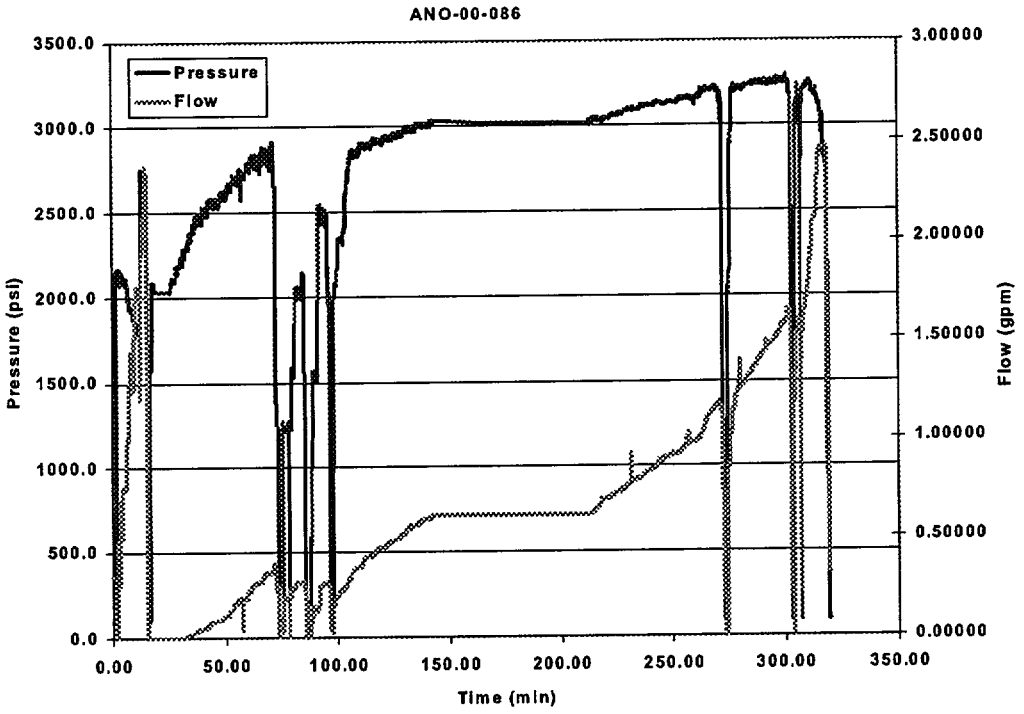

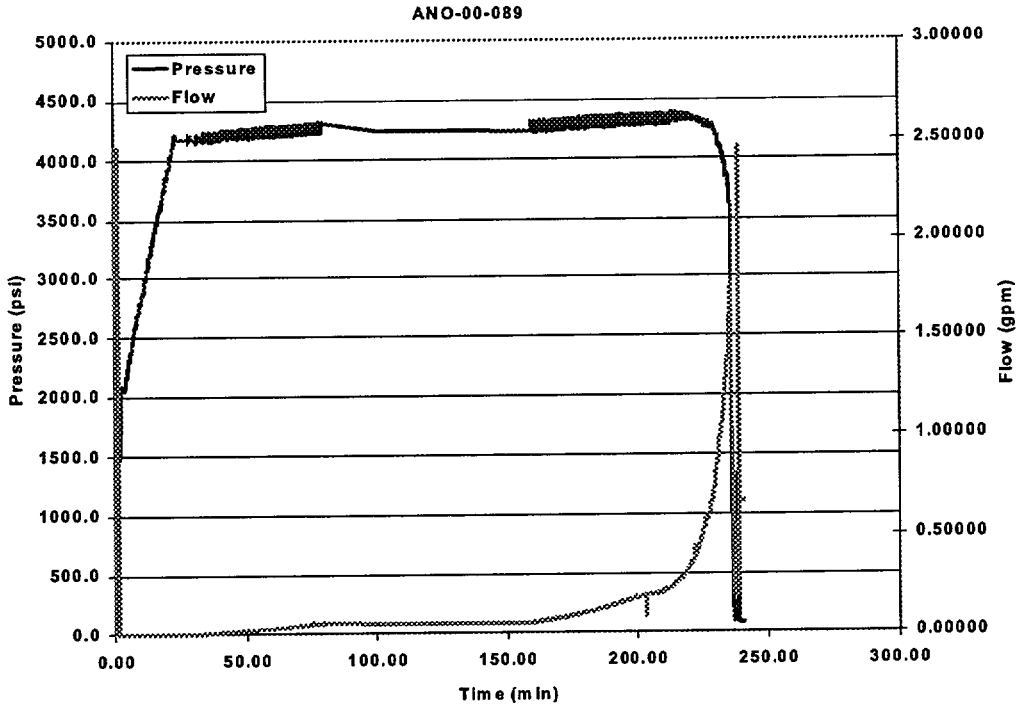

C
SEM MEASURED PROFILES

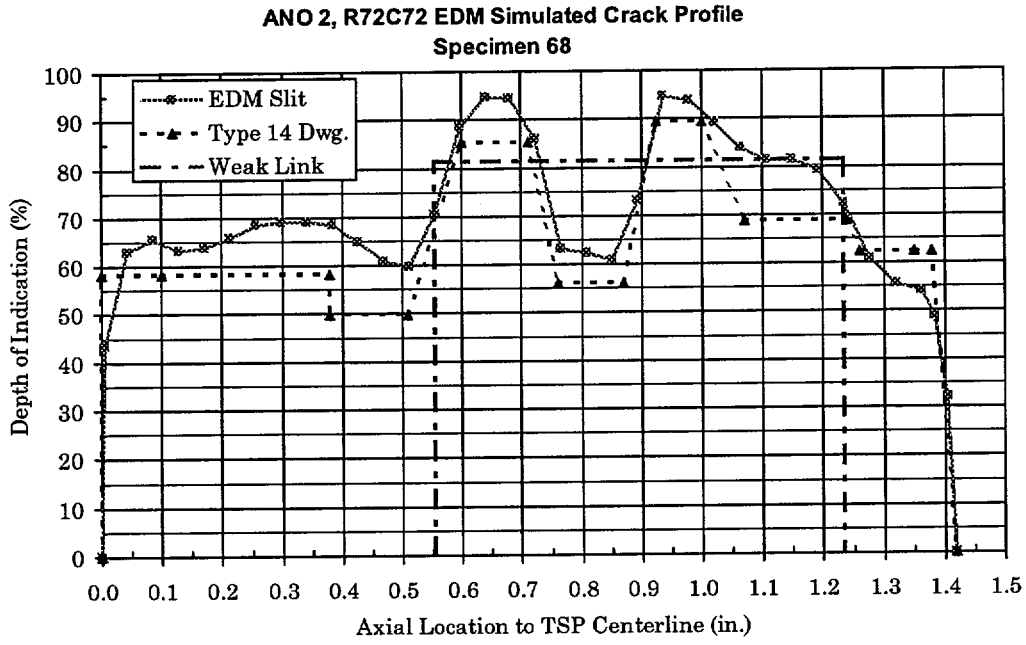
ANO 2, R72C72 EDM Simulated Crack Profile
Specimen 68
EDM Slit
Type 14 Dwg.
Weak Link
Depth of Indication (%)
Axial Location to TSP Centerline (in.)

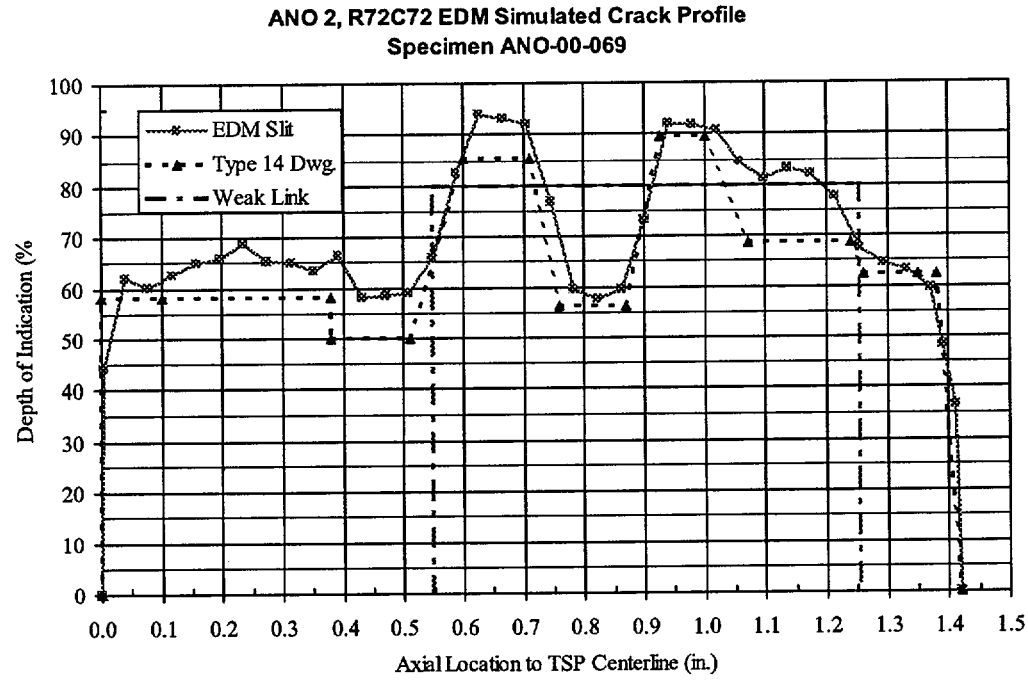
ANO 2, R72C72 EDM Simulated Crack Profile
Specimen ANO-00-069
EDM Slit
Type 14 Dwg.
Weak Link
Depth of Indication (%
Axial Location to TSP Centerline (in.)

ANO 2, R72C72 EDM Simulated Crack Profile
Specimen 70

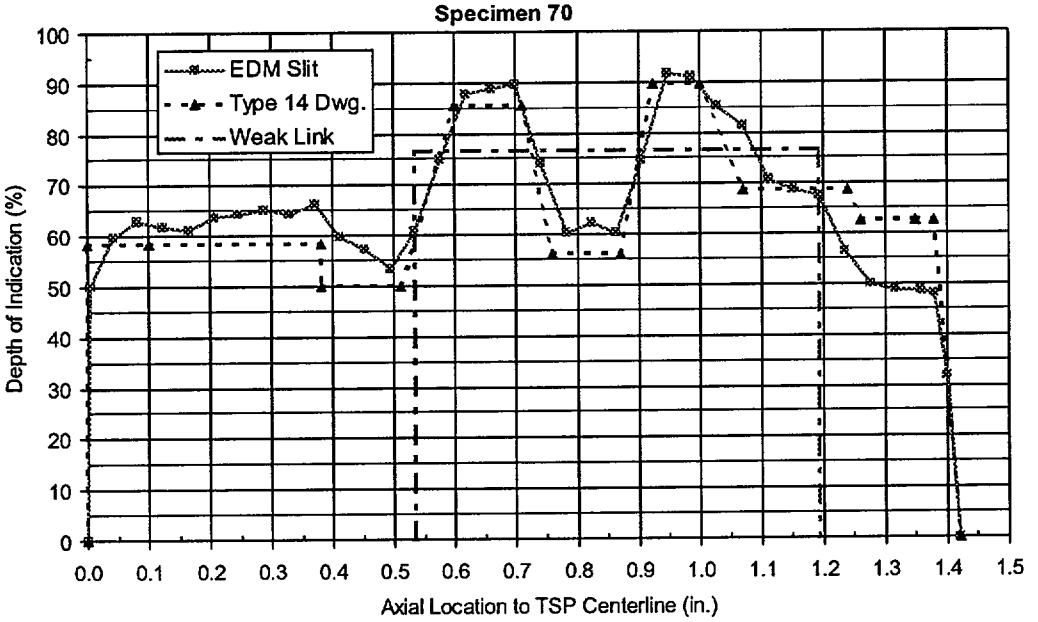

ANO 2, R72C72 EDM Simulated Crack Profile
Specimen 74

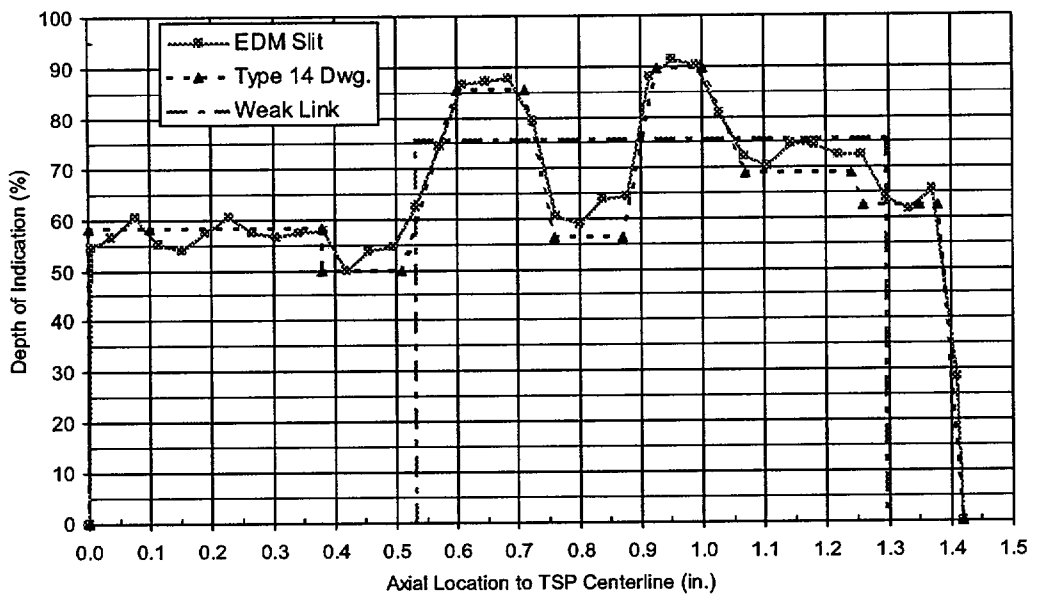

ANO 2, R72C72 EDM Simulated Crack Profile
Specimen 75

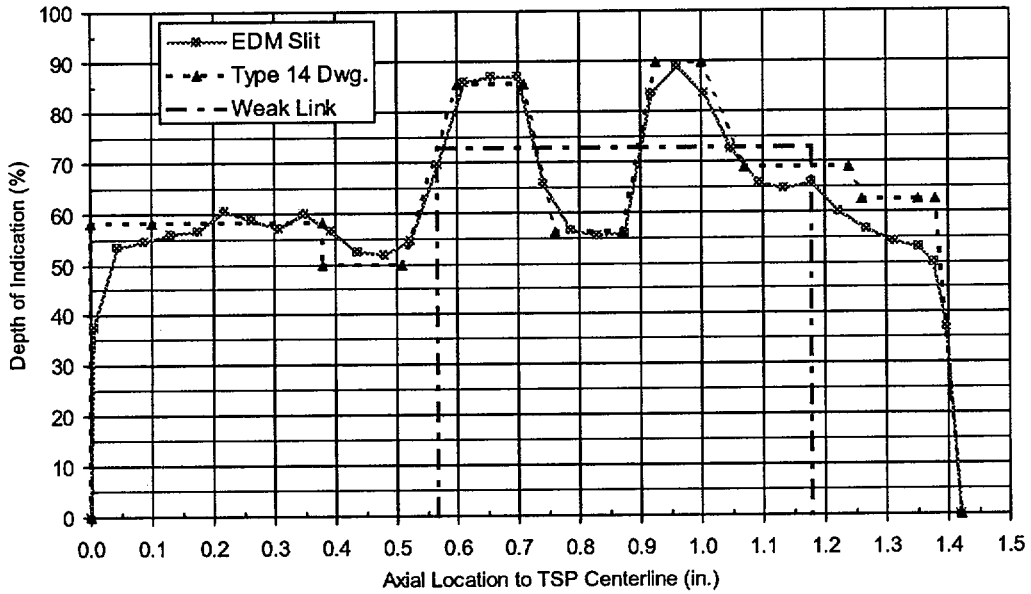

ANO 2, R72C72 EDM Simulated Crack Profile
Specimen Type 76

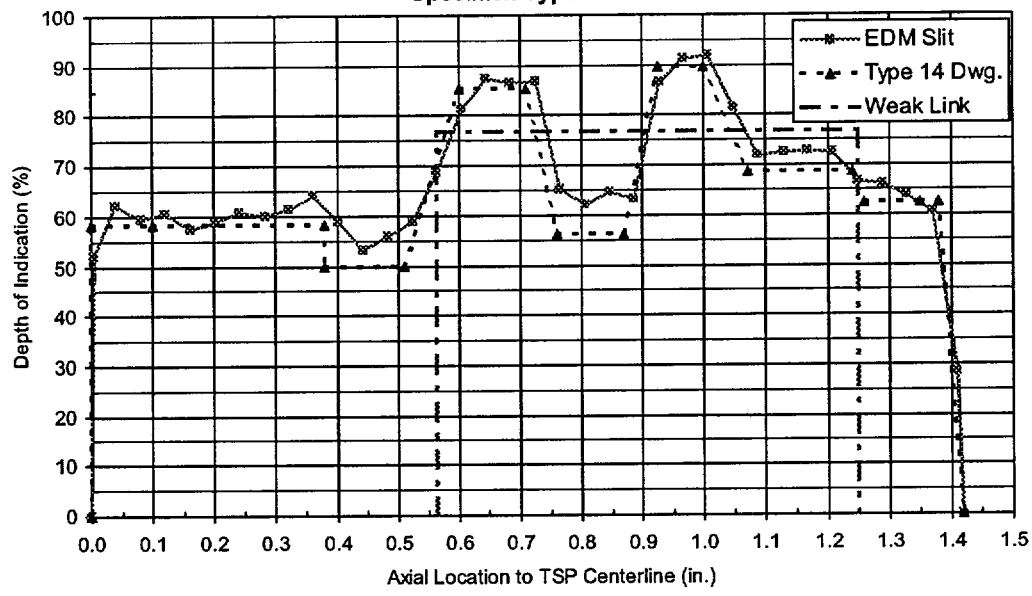

ANO 2, R72C72 EDM Simulated Crack Profile
Specimen Type 76

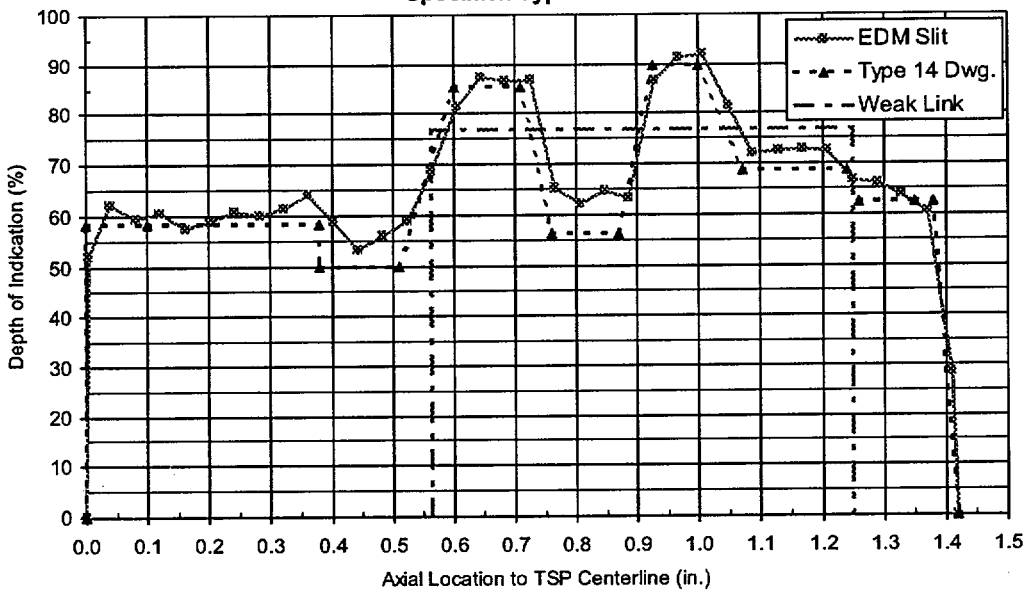

ANO 2, R72C72 EDM Simulated Crack Profile
Specimen 83

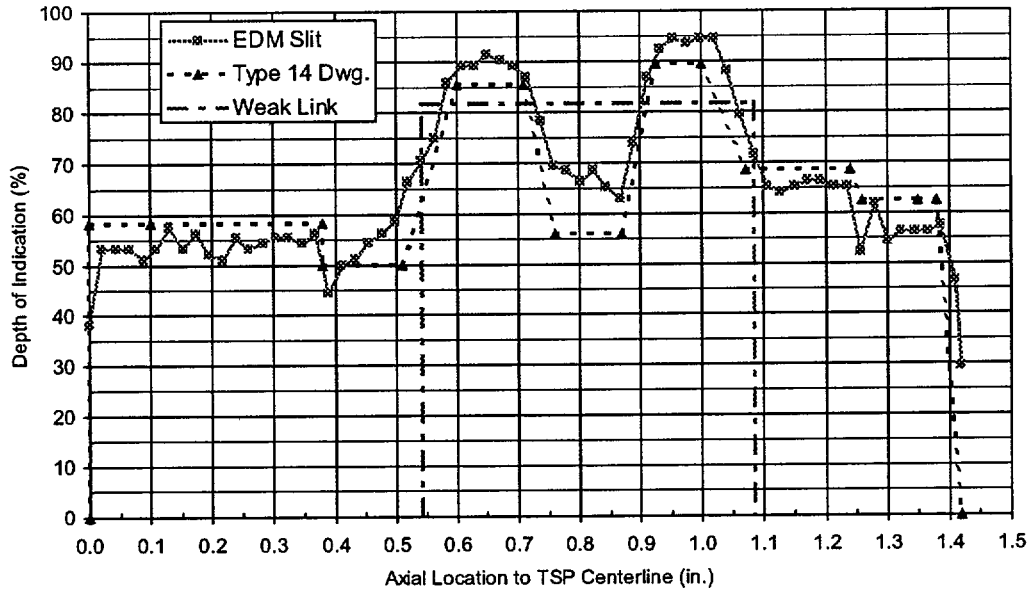

ANO 2, R72C72 EDM Simulated Crack Profile
Specimen 84

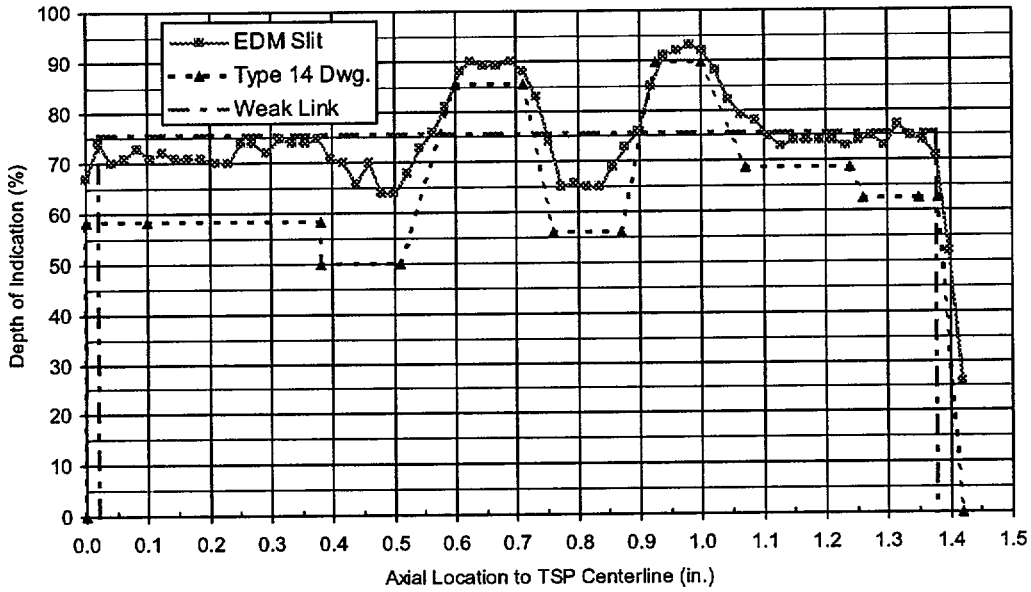

ANO 2, R72C72 EDM Simulated Crack Profile
Specimen 85

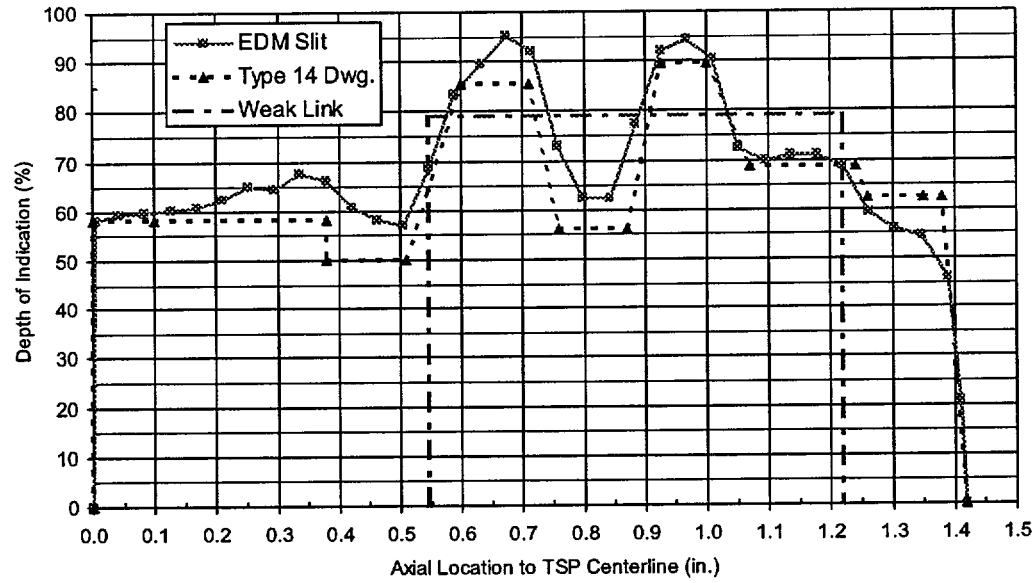

ANO 2, R72C72 EDM Simulated Crack Profile
Specimen 86

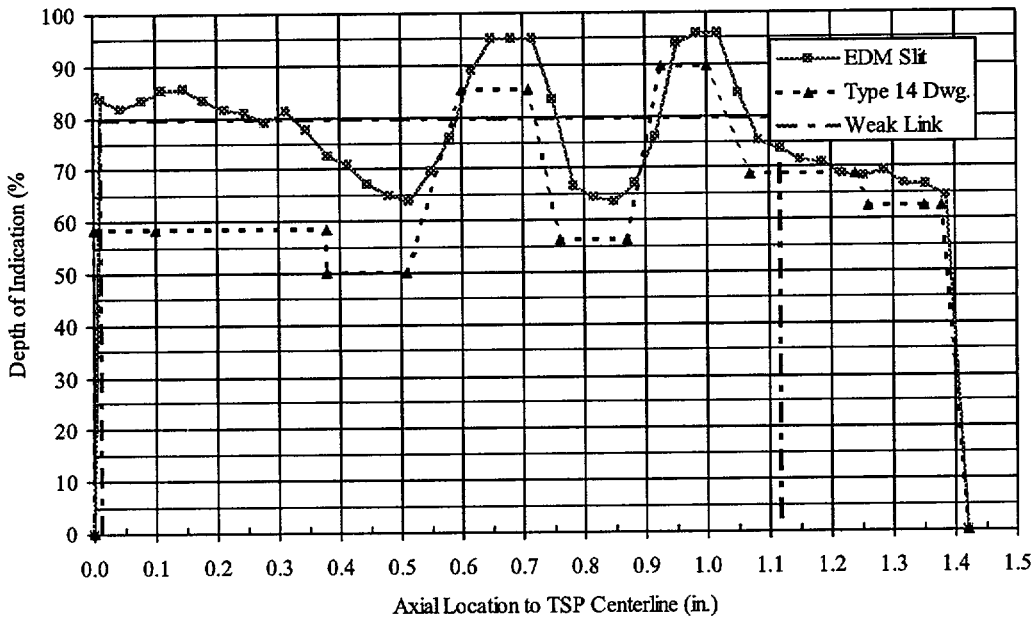

ANO 2, R72C72 EDM Simulated Crack Profile
Specimen 87

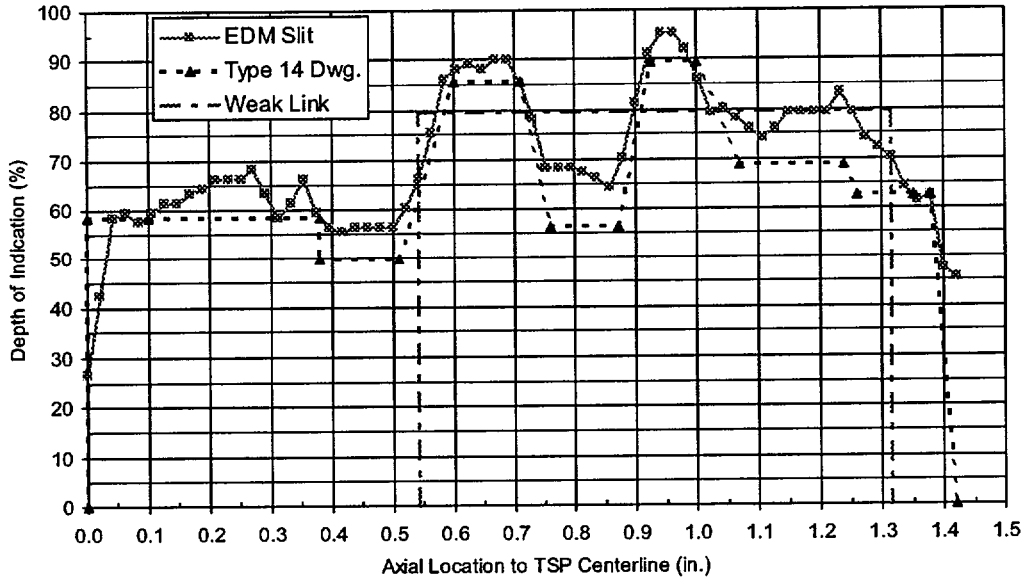

ANO 2, R72C72 EDM Simulated Crack Profile
Specimen Type 88

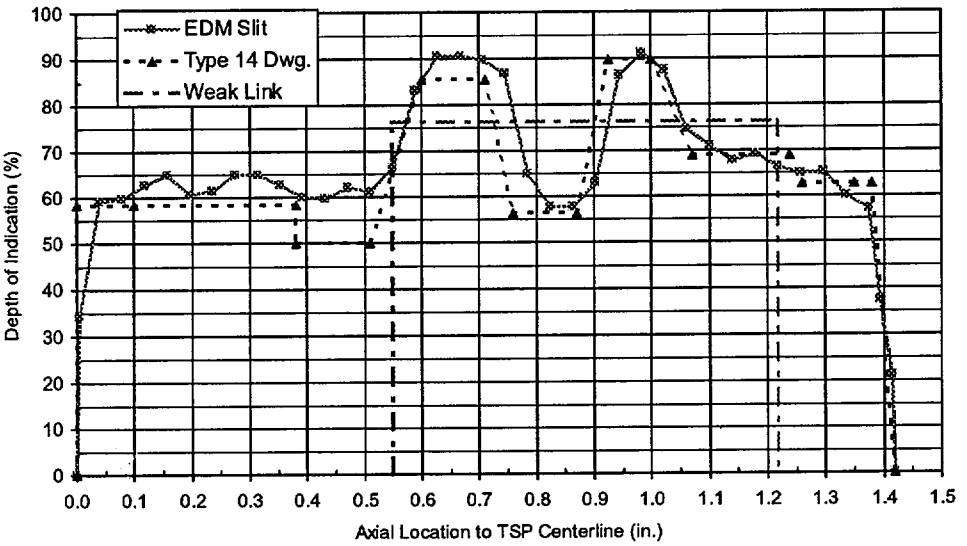

ANO 2, R72C72 EDM Simulated Crack Profile
Specimen Type 89

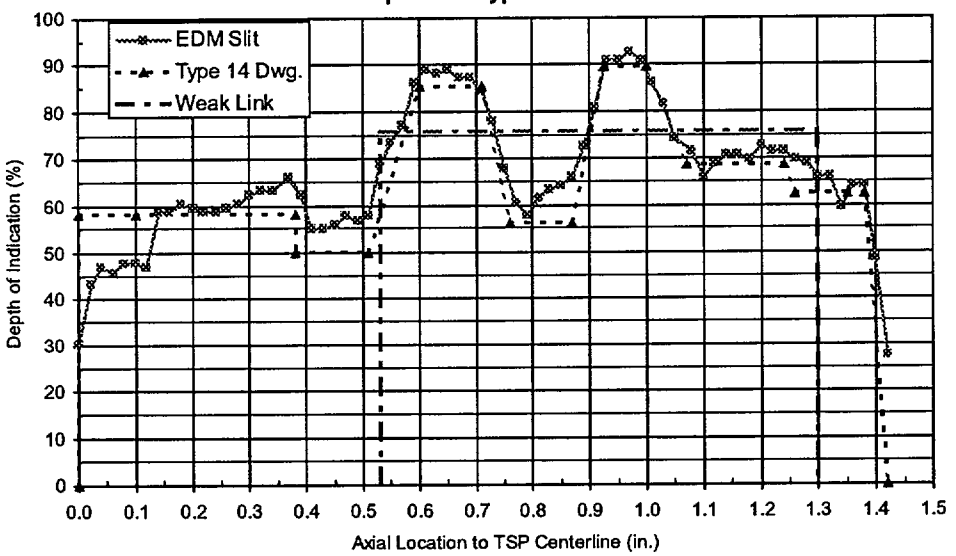

ANO 2, R72C72 EDM Simulated Crack Profile
Specimen 90

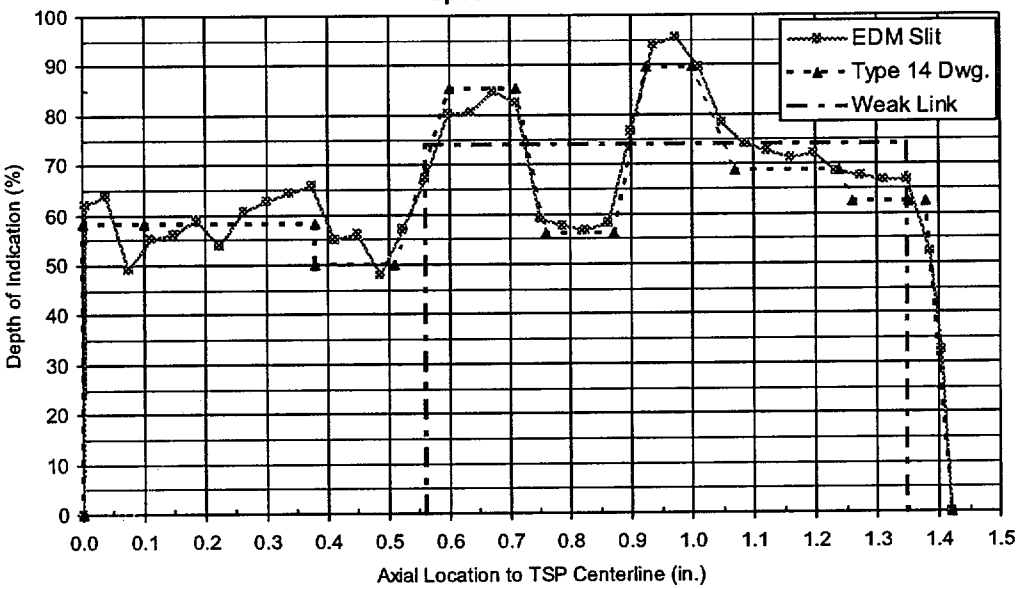

ANO 2, R72C72 EDM Simulated Crack Profile
Specimen 91

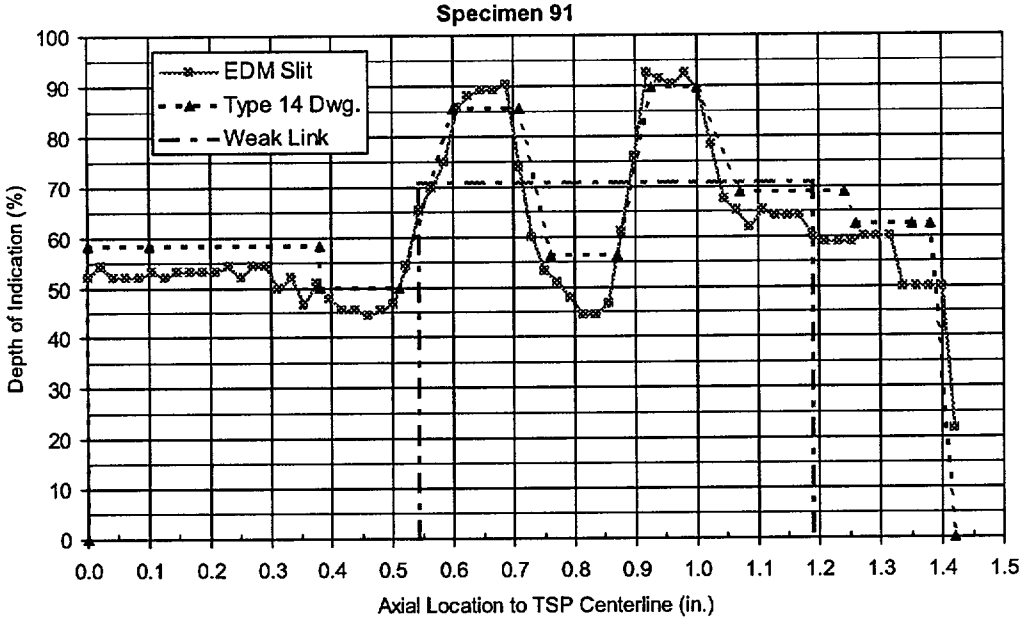

Target:
Nuclear Power

About EPRI

EPRI creates science and technology solutions for the global energy and energy services industry. U.S. electric utilities established the Electric Power Research Institute in 1973 as a nonprofit research consortium for the benefit of utility members, their customers, and society. Now known simply as EPRI, the company provides a wide range of innovative products and services to more than 1000 energy-related organizations in 40 countries. EPRI's multidisciplinary team of scientists and engineers draws on a worldwide network of technical and business expertise to help solve today's toughest energy and environmental problems.

EPRI. Electrify the World

Printed on recycled paper in the United States of America

1001441

EPRI • 3412 Hillview Avenue, Palo Alto, California 94304 • PO Box 10412, Palo Alto, California 94303 • USA
800.313.3774 • 650.855.2121 • askepri@epri.com • www.epri.com